CHEMICAL AND BIOCHEMICAL ASPECTS OF NITROARENE MUTAGENICITY

CHEMICAL AND BIOCHEMICAL ASPECTS OF NITROARENE MUTAGENICITY

By

LENA CATHY ANDREW, B.SC.

A Thesis

Submitted to the School of Graduate Studies

In Partial Fulfillment of the Requirements

For the Degree

Master of Science

McMaster University

MASTER OF SCIENCE (2000) McMaster University

(Chemistry) Hamilton, ON

TITLE: Chemical and Biochemical Aspects of Nitroarene Mutagenicity

AUTHOR: Lena Cathy Andrew, B.Sc. (McMaster University)

SUPERVISOR: Professor B.E. McCarry

NUMBER OF PAGES: xiv, 177

ABSTRACT

Nitroarenes are the nitro-functionalized derivatives of polycyclic aromatic hydrocarbons (PAH) which are found in a variety of environmental matrices, and are potential human carcinogens. The 1997 discovery of a potent mutagen, 3-nitrobenzanthrone, in diesel exhaust has renewed interest in these compounds. Theoretically- and experimentally-determined characteristics of nitroarenes have been explored as predictors of their mutagenic potencies in the Ames reversion assay. In this multifaceted project, the relationships of these parameters and rates of nitroarene metabolism to the mutagenic potencies of 11 nitroarenes in *Salmonella typhimurium* strain YG1021 were explored.

Ab initio calculations at the HF/3-21G level were performed for these molecules. Calculated NO_2 dihedral angles and ε_{LUMO} values were smaller in magnitude than those previously determined by lower quality semi-empirical and STO-3G *ab initio* calculations, and showed poor correlations with nitroarene mutagenicity. Molecular negative electrostatic potential surfaces for the nitroarenes studied possessed two regions which, when placed in a common orientation in 3-dimensional space, suggested specific binding contacts within the active site of the nitroarene-activating enzyme nitroreductase.

An efficient GC-MS method was developed for the analysis of organic extracts from *Salmonella* incubations with nitroarenes in the determination of relative rates of metabolism, and employed a two-stage solid phase extraction sample clean-up scheme. The rates of nitroarene metabolism for six nitroarenes, whose mutagenic potencies ranged over two orders of magnitude, ranged from 450 to 3600 pmol/hr/mL *Salmonella* culture at 25°C and showed a good correlation with mutagenicity.

The results of this work suggest that mutagenic potency is a direct result of intermediate accumulation, and cast serious doubts on the reported correlations between nitroarene physicochemical properties and mutagenic potencies. This study underscores the need for the in-depth examination of the characteristics of nitroarene intermediates as an explanation of nitroarene mutagenic potencies.

ACKNOWLEDGEMENTS

I would first like to thank Dr. Brian McCarry for his patient supervision and guidance - his enthusiasm for research is infectious, and I have learned a lot from working with him. I would also like to thank my esteemed committee members, Dr. Alex Bain and Dr. Paul Berti, for their challenging questions and insight.

Special thanks to my lab mates, past and present (I'm out of the Bat Cave, Spice Girls ☺ !): Suzanne Ackloo, Adrienne Boden-dash-Ruffolo ☺, Lisa Heydorn, Krista Barfoot Kinsie, Laurie Allan and Xiaowen (Wendy) Zhang. Thank you for being the wonderful and caring people that you are! Thank you also to the great people who put a friendly face on the Chemistry Department.

Thank you, Dr. Nick Werstiuk, for your insightful conversations about the wonderful world of theoretical calculations. Thank you Nick Toltl, Aviva Litovitz and Dr. William Leigh, for your laser flash photolysis work on my azides. My thanks also to Dr. Evert Nieboer (Biochemistry) for the use of laboratory space for my bioassays.

Thank you NSERC and the McMaster Department of Chemistry for your financial support, through which this work was made possible.

Lastly, but never leastly, I'd like to say "much love" to my family and friends – thank you for safeguarding my happiness and sanity.

Dad (*mwé ka parlé bau*...I'll settle my tab soon, *oui*...☺),

Mum (*tu-tu* – beautiful you still lives on in each of us...) –

thank you, *pour toute bagaille*.

Without your love, encouragement and genes, I could not have made it.

This thesis is dedicated to you both.

TABLE OF CONTENTS

List of Abbreviations

amu	atomic mass unit
B[a]P	benzo[*a*]pyrene
DCM	dichloromethane
DMSO	dimethylsulfoxide
DNA	deoxyribonucleic acid
DNP	dinitropyrene
EI	electron impact
GC-MS	tandem gas chromatography-mass spectrometry
HF	Hartree-Fock
HOMO	highest occupied molecular orbital
HPLC	high performance liquid chromatography
kDa	kilodalton
LUMO	lowest unoccupied molecular orbital
MW	molecular weight
NA	nitroanthracene
NAN	nitroacenaphthene
NBA	nitrobenzanthrone
NF	nitrofluorene
NFA	nitrofluoranthene
nmol	nanomole
NP	nitropyrene
NR	nitroreductase
PAH	polycyclic aromatic hydrocarbon(s)

pg	picogram
pmol	picomole
rev	revertants
SAR	structure-activity relationship
SCF	self-consistent field
SPE	solid phase extraction
t_R	retention time
µL	microlitre
UV	ultraviolet

LIST OF FIGURES

LIST OF TABLES

1. INTRODUCTION

Polycyclic aromatic hydrocarbons (PAH) and their nitro-functionalized derivatives (or nitroarenes) are found in a variety of environmental matrices, including urban air and combustion emissions. A variety of theoretical and experimental parameters, both physical and biological, have been used in attempts to predict and better understand the characteristics of these compounds that account for their mutagenic activities. The investigation of chemical and biochemical aspects of nitroarene mutagenicity requires a multidisciplinary approach that encompasses a wide range of subject areas, including toxicology, theoretical and analytical chemistry, biochemistry and organic synthesis.

1.1. Polycyclic Aromatic Hydrocarbons and Nitroarenes

The impact of urban air pollution on the environment is of public concern because of its potential negative effects on human health. PAH are a class of compounds that are formed by the incomplete combustion or pyrolysis of organic materials; some members are known or suspected to be human carcinogens [1]. Their principal atmospheric sources in urban areas include fossil fuel usage, vehicular combustion emissions and refuse burning [2]. In some centres, sources such as aluminum smelter emissions [3] and coke oven emissions [2] contribute greatly to the atmospheric burden. The United States Environmental Protection Agency (EPA) has designated several PAH as priority pollutants [4] (Figure 1). On heavily polluted days in Hamilton, ON, the concentrations of individual PAH, such as fluoranthene, pyrene and

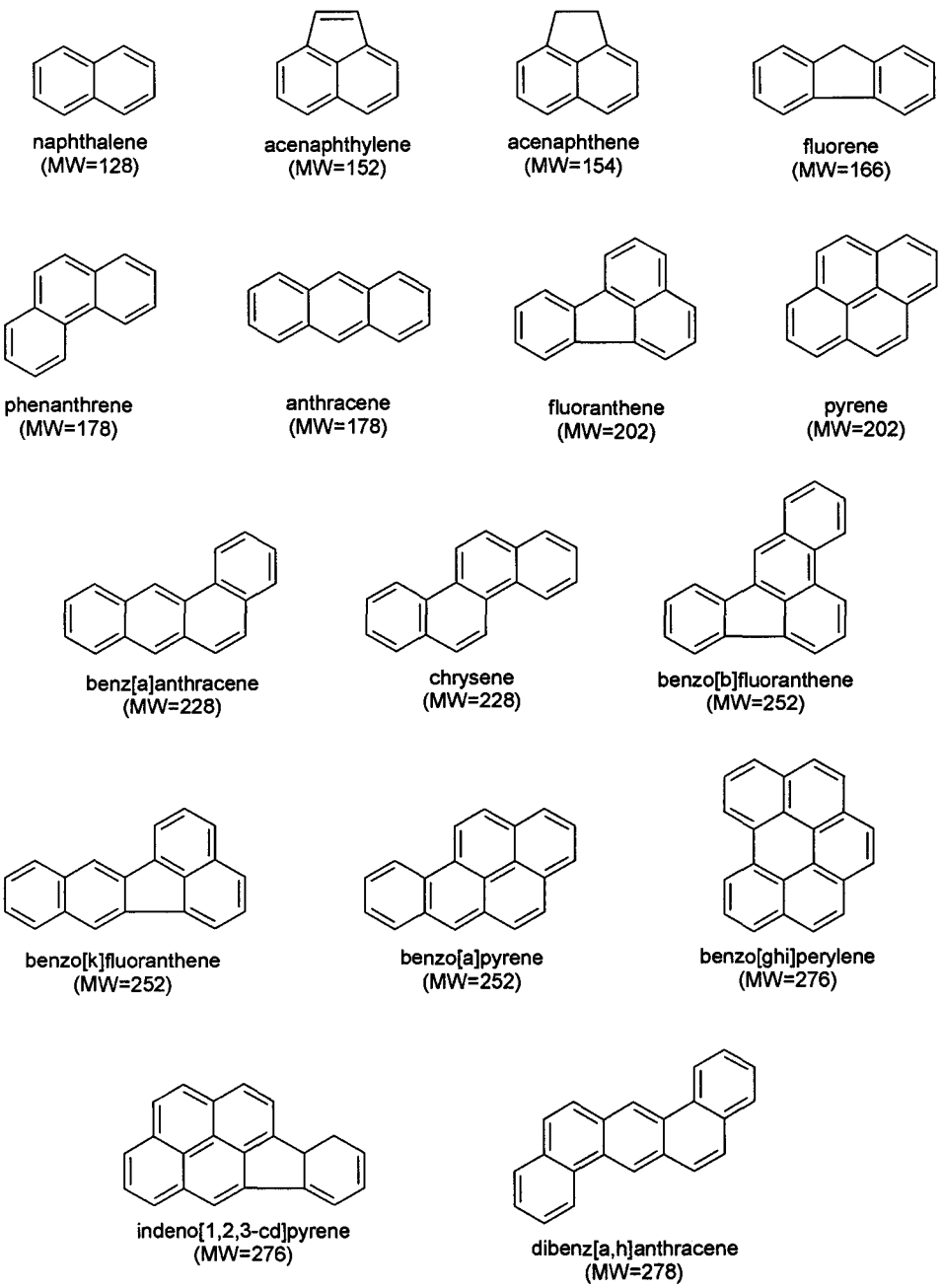

Figure 1. Sixteen PAH identified as priority pollutants by the U.S. EPA [5].

benzanthrone, in air particulate extracts have been found in the 3 to 6 ng/m^3 range [6]. Direct atmospheric releases, industrial inputs, precipitation and run-off via creeks and streams cause the accumulation of PAH in rivers and lakes, primarily in sediments. Fluoranthene and pyrene, for example, were found at concentrations of 80 and 55μg/g in Hamilton Harbour sediment samples that were heavily contaminated by coal tar [7]. These hydrophobic compounds are known to bioaccumulate in the fatty tissues of wildlife living in these environments.

Inhalation serves as the primary exposure route for PAH in humans [8]; these compounds have also been found in cooked food [1]. The average adult inhales 15 to 20m^3 of air daily [9], and it has been estimated that 85% of the carcinogenic PAH in the atmosphere are associated with particles less than 5μm in diameter [10]. Furthermore, it is known that particles less than 2μm in diameter can readily be carried into, and become deposited in, the alveolar regions of the lungs [9]. Thus, lung tissue exposure to PAH can occur through the inhalation of respirable (<10μm diameter) air particulate present in the air [2].

Nitro-functionalized PAH are termed nitroarenes (Figure 2); their levels in urban ambient air are typically in the pg/m^3 range, and their content in diesel particulate falls within the ng/g (ppb) range [11]. Like PAH, the principal atmospheric sources of nitroarenes in urban areas include vehicular exhaust and fossil fuel combustion emissions [2]. Diesel engines use their fuel more efficiently than gasoline engines, making the use of diesel vehicles more attractive economically. However, diesel engines emit more nitrogen oxides (NO_x) and respirable particulate matter [12] than gasoline engines; over 60 nitroarenes have been found in significant amounts in diesel exhaust [13]. Nitroarenes such as 1-NP, 3-NFA and 9-NA, have been known to be diesel exhaust constituents for over 20 years [14].

Nitroarenes are classified as direct-acting mutagens because their biochemical

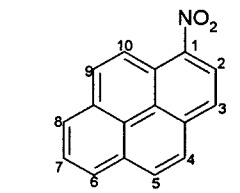

1-nitropyrene (1-NP)
(MW=247)

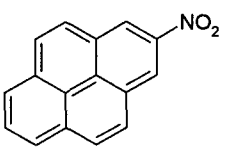

2-nitropyrene (2-NP)
(MW=247)

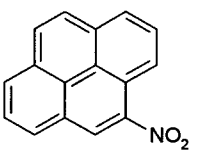

4-nitropyrene (4-NP)
(MW=247)

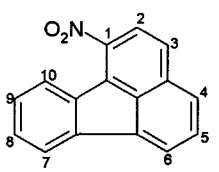

1-nitrofluoranthene (1-NFA)
(MW=247)

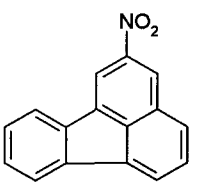

2-nitrofluoranthene (2-NFA)
(MW=247)

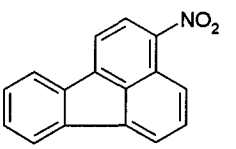

3-nitrofluoranthene (3-NFA)
(MW=247)

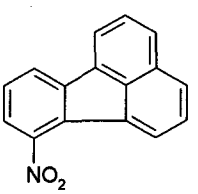

7-nitrofluoranthene (7-NFA)
(MW=247)

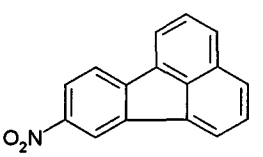

8-nitrofluoranthene (8-NFA)
(MW=247)

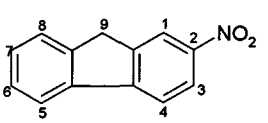

2-nitrofluorene (2-NF)
(MW=211)

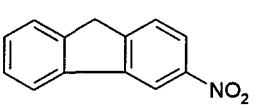

3-nitrofluorene (3-NF)
(MW=211)

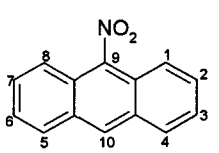

9-nitroanthracene (9-NA)
(MW=223)

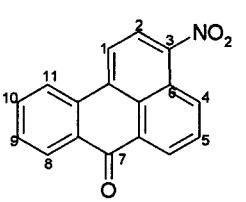

3-nitrobenzanthrone (3-NBA)
(MW=275)

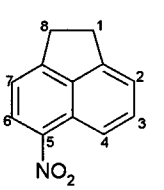

5-nitroacenaphthene (5-NAN)
(MW=199)

Figure 2. Structures of the 13 nitroarenes considered in this study.

conversion to key reactive species that modify DNA and proteins can occur potentially in every cell by a reductive mechanistic pathway. The nitroarene 1-NP accounts for approximately 30% of the observed direct-acting mutagenicity of diesel emission extracts [**15**]; this compound is a useful index of the nitroarene content of diesel emissions since a good correlation has been observed between 1-NP content and the biological properties of diesel emission extracts [**16**]. Nitropyrene is also a fair index of the contribution of vehicular exhaust to urban air pollution [**17**]. Recently, the mononitroarene 3-nitrobenzanthrone (3-NBA) was isolated from diesel exhaust extracts by Enya *et al* and was subsequently shown to be a highly mutagenic substance [**18**].

PAH in the atmosphere undergo chemical reactions with gases in the air such as O_3, NO_x and sulfur oxides (SO_x) to afford functionalized PAH derivatives [**2, 6**]. For example, Arey *et al* demonstrated that the atmospheric nitration of fluoranthene to produce 2-nitrofluoranthene (2-NFA) was the result of initial attack on the fluoranthene nucleus by hydroxyl radicals [**4**], which are derived from ozone (Figure 3). The atmospheric transformation products 2-NFA, 2-nitrodibenzopyranone [**4, 19**] and 2-nitropyrene (2-NP) contribute significantly to the direct acting activity observed in bioassays of air particulate extracts, with 2-NFA accounting for approximately 5% of the direct-acting mutagenicity observed for these extracts [**6, 20**]. Enya *et al* demonstrated that 3-NBA may also be an air transformation product, since it is produced from benzanthrone in the laboratory under artificial atmosphere conditions [**18**]. Nitroarenes emitted into the atmosphere may also be converted to polar quinone and phenol derivatives [**12**]; these oxygenated PAH, as a class, have been observed to contribute a minor percentage (16%) to the overall mutagenicity of air particulate extracts [**17**].

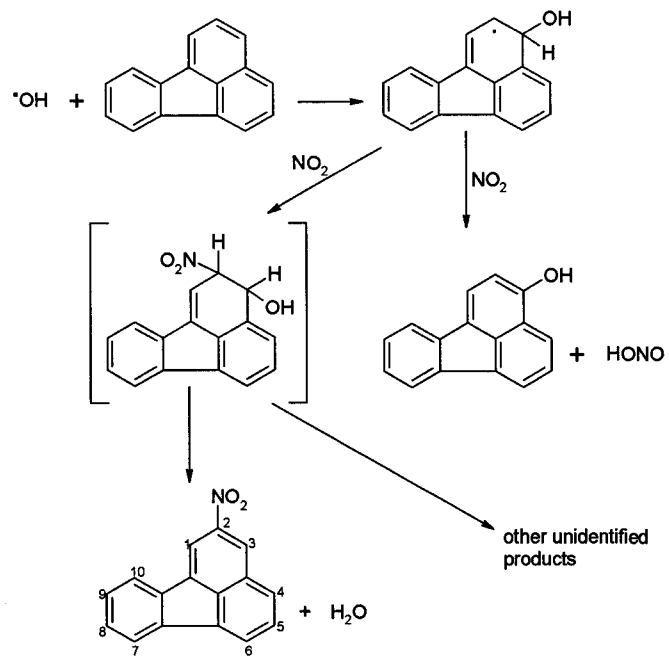

Figure 3. Formation of the atmospheric transformation product 2-nitrofluoranthene. Reproduced from [4].

1.2. Rationale for Study

Several industrial and pollution-derived chemicals, including PAH and nitroarenes, are known to cause alterations in the genetic code, and these mutations can lead to the formation of tumours [**21, 22**]. Chemicals that may be potentially mutagenic or carcinogenic to humans have been studied in both bacterial and animal systems. In short-term mammalian bioassays such as the mouse skin tumour assay and the rat lung implantation assay [**12**], chemical agents are administered to evaluate and characterize their relative carcinogenic potencies. Bacterial bioassays, such as the Ames *Salmonella typhimurium* reversion assay [**23**], are simple, inexpensive assay systems that have been used to study the mutagenicity of single compounds

and of complex mixtures of environmental contaminants. Bacteria possess a high surface area-to-volume ratio compared to mammalian cells in whole organisms, which means that their cell interiors can be highly accessible to exogenous compounds. The speed and low cost of these assays make them attractive models for the study of mutagenesis and the screening of chemical substances and complex mixtures (see Figure 4). The correlation between compounds that are known carcinogens and those that have been found to induce mutations in bacterial assays like the Ames reversion assay, specifically PAH and nitroarenes, is rather high **[25, 26]**. Since it is difficult to extrapolate the high-level exposure data to the effects of relatively low human exposures in the environment **[27]**, an increased understanding of carcinogenic and mutagenic processes occurring within the cell is required in order to better assess risk.

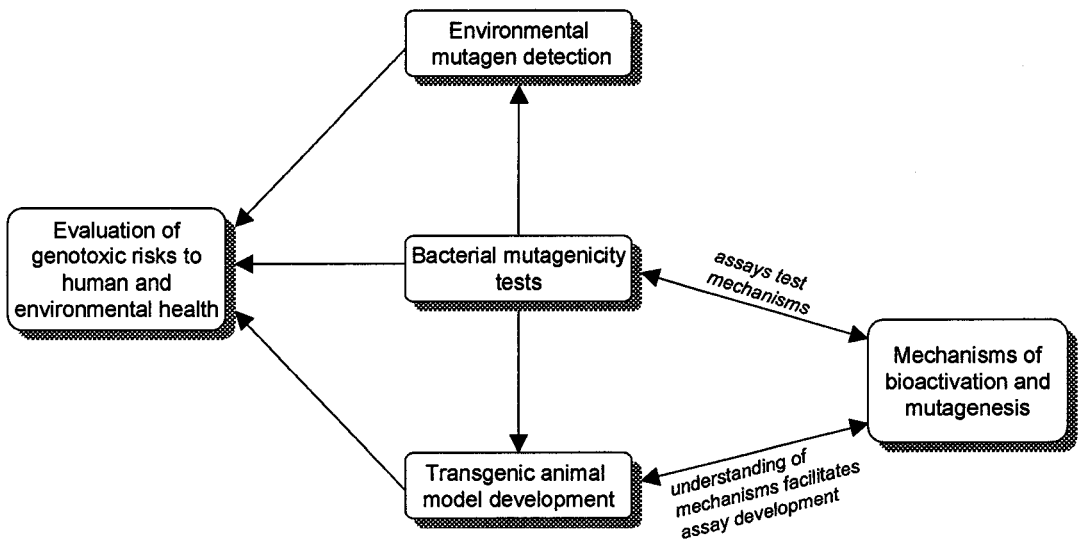

Figure 4. The contribution of engineered bacterial bioassays to the study of environmental mutagenesis. Reproduced from [24].

Previous studies of nitroarene and PAH structure-activity relationships (SAR) postulate that the physicochemical properties of these compounds directly impact the mutagenic and carcinogenic activities observed in biological assays **[28, 29, 30]**. These genome-independent variables include calculated energies of the lowest unoccupied molecular orbital (ε_{LUMO}) and of the highest occupied molecular orbital (ε_{HOMO}), first half-wave reduction potentials ($E_{½}$) and the logarithms of octanol/water partition coefficients (log P or log K_{ow}). These latter parameters are believed to be measures of the ease with which compounds can cross the cell membranes whereupon they are available to become metabolized to the ultimate mutagens within the cell. All conclusions drawn from previous SAR investigations of nitroarenes were based on semi-empirical calculations of molecular orbital energies and geometries. The quality of the results from semi-empirical calculations on large molecules is poorer than would be obtained from higher level calculations such as *ab initio* calculations. In order to examine the correlation between calculated properties and mutagenic potencies of nitroarenes, it is proposed to perform higher level HF/3-21G *ab initio* calculations on a series of nitroarenes.

The mutagenicities of individual nitroarenes vary considerably **[17, 28, 31]**, and it is the aim of this study to investigate some of the properties of isomeric nitroarenes that may contribute to these variations. Dose-response determinations of the mutagenic potencies of nitroarenes using the Ames reversion assay show linear relationships between mutation frequency, which is reflected in colony growth, and doses administered **[17]**. The *Salmonella typhimurium* strain YG1021, which possesses 50 times more nitroreductase (NR) activity than the common strain TA98, shows a significantly enhanced response to nitroarenes compared to this common strain **[32]**.

Little work has been done to investigate relationships between the mutagenic potencies of nitroarenes and their relative rates of metabolism, the generation of electrophilic metabolites

and DNA adduct formation. Intuitively, these latter factors probably have a more direct impact on mutagenic potencies than the physical properties of the nitroarenes themselves, which have been the focus of all prior studies in this area [28, 29, 30]. To date, there has been no systematic investigation of the relationship between mutagenicity and the relative rates of metabolism for a large set of nitroarene compounds, nor has any relationship between relative rates of metabolism and the physicochemical parameters used in SAR investigations been established. It is the goal of this work to investigate these factors. It is hoped that this study will be one of the first in a series that will investigate the physicochemical properties, activities and DNA interactions of nitroarene metabolites as determinants and possible predictors of nitroarene mutagenic potencies.

1.3. Chemical Aspects of Nitroarene Mutagenicity

Two of the first attempts to correlate biological activity with molecular properties were reported by Meyer and Overton, who investigated oil/water partition coefficients as indicators of nervous system drug potencies [28]. Specific biochemical targets and compound classes are well defined in the SAR studies of drug efficacy and toxicology [33]. However, SAR approaches to the investigations of chemical mutagenesis and carcinogenesis, which have been pursued for about 20 years [28, 29, 30], are limited by the fact that non-congeneric mutagenic and carcinogenic compounds have multiple targets and activities.

It was the aim of previous SAR studies not only to use the physical and chemical properties of PAH and nitroarenes to develop predictive models for mutagenicity, but also to develop a better understanding of the factors and mechanisms affecting mutagenesis. Hydrophobicity, expressed as the octanol/water partition coefficient (log P or log K_{ow}), has been

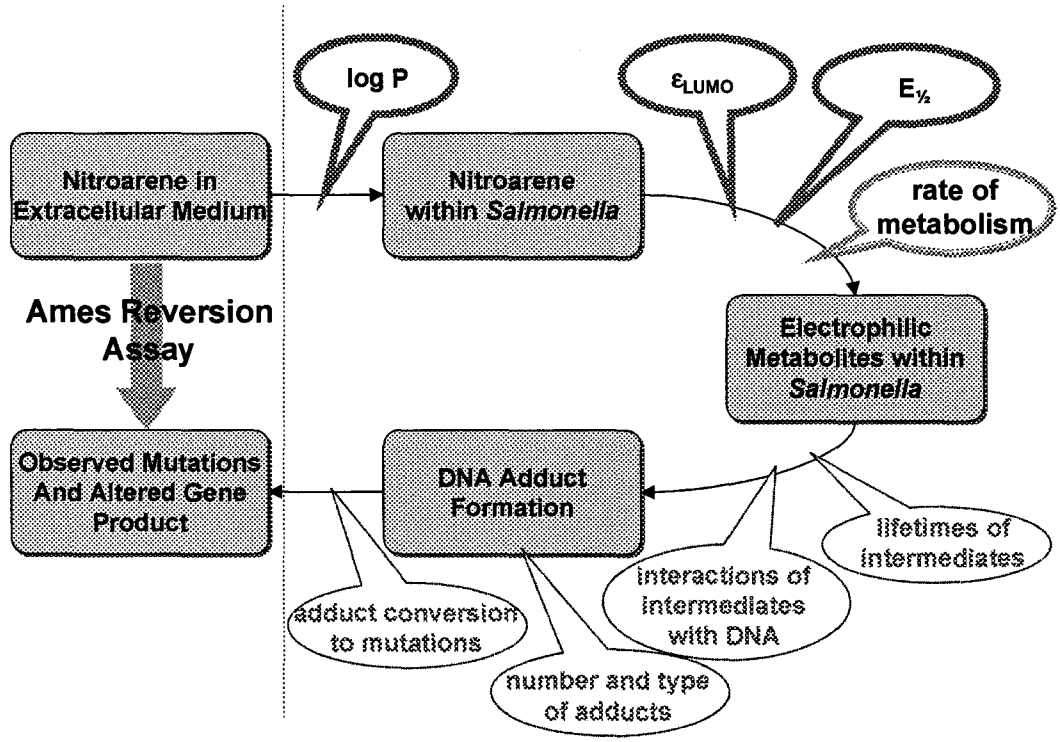

Figure 5. Schematic pathway of nitroarene metabolism and the relationship of experimental and calculated physical parameters to metabolism and the Ames reversion assay.

included as a parameter in SAR investigations of nitroarene mutagenicity for about 10 years **[34, 35]**. The relationship between log P and the rate of substance transport through the cellular material was first reported by Collander **[36]**, and may be an important consideration in the ability of nitroarenes and their metabolites to reach their biochemical targets.

The structural features of nitroarenes that have been proposed to determine nitroarene mutagenicity – i.e., the physical dimensions of the aromatic rings **[25, 28]**, nitro group position and conformation **[37, 38]**, and the ability to stabilize the ultimate genotoxic electrophile through resonance **[37]** – have shown poor relationships with the mutagenic potencies observed in *Salmonella typhimurium* strain TA98. Vance and Levin proposed that a nitro substituent placed

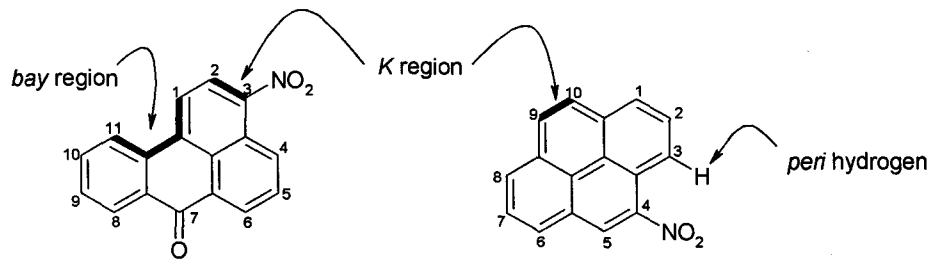

Figure 6. *Peri* hydrogen and *K*-region of 4-nitropyrene and *K*- and *bay* regions of 3-nitrobenzanthrone.

along the long axis of a PAH molecule, such as 3-NFA (Figure 2), would give molecules of a length that would optimize the stability of its intercalation within the major groove of DNA, once tethered to the DNA backbone [**37**]. These structural features are believed to promote 3-NFA genotoxicity by maximizing the base-stacking π interactions between the aromatic ring and the nucleotide bases. The results of semi-empirical calculations were used to propose that the nitro substituents in the *bay*-region of nitroarenes or adjacent to *peri* hydrogens will adopt non-coplanar orientations to minimize steric interference from aromatic ring hydrogens, and that these non-coplanar conformations result in lowered mutagenic potencies [**39**] (see Figure 6). The electron rich *K*-region of the aromatic system, which promotes carcinogenesis by serving as a preferred site for oxidative activation [**2, 40**], may also contribute to the weak mutagenicities observed for nitroarenes like 7-NFA by raising the free energy requirements of nitroreduction.

Previous studies by Maynard *et al* and Klopman *et al* have stipulated that the ease of nitroreduction correlates with nitroarene mutagenic potencies, and is reflected in energetically favourable values of $E_{½}$ and ε_{LUMO} [**39, 41**]. These ε_{LUMO} energies were found to have poor relationships to the mutagenic potencies of nitroreductase-activated nitroarenes [**34, 39, 42**]. In the SAR investigations of Lopez de Compadre *et al*, the activities of nitroarenes and nitrogen-containing heterocycles in *Salmonella typhimurium* strain TA98 were found to decrease

logarithmically with increasing ε_{LUMO} [34]. Similarly, weak trends were observed between the first half-wave reduction potentials ($E_{½}$) for nitroreduction, mutagenicities and nitroreductase activities [25, 41, 43, 44]; these general trends were limited to compounds that were structurally similar [44].

Theoretical Calculations

Electronic configurations are used to describe the geometries and energies of molecules by allocating electrons to specific molecular orbitals (MOs), three-dimensional regions of probability that are described by the wave function ψ. Molecular orbitals can be described as linear combinations of atomic orbitals (LCAOs), with the wavefunction ψ described as the sum of atomic orbitals ϕ_j [45],

$$\psi_i = \Sigma\, c_{ij}\phi_j.$$

The LUMO corresponds to the orbital of lowest energy that can either accept an electron to promote the molecule to an excited or reduced state, or to form an intermolecular bond. Together with the HOMO, the characteristics of these orbitals are frequently considered in discussions of chemical reactivity and structural characteristics.

The Schrödinger equation describes the wavefunction ψ of a molecule using the coordinates of all particles in the molecule and expressions of the electron energy and mutual potential energy between the electrons and atomic nuclei [46]. Because this equation cannot be solved analytically, the Born-Oppenheimer approximation, which fixes the positions of the atomic nuclei, is used to provide a solution based on the electrons only [47]. The positions of these electrons can be represented as vector components within a matrix that can be optimized by semi-empirical or *ab initio* computational methods to yield molecular geometries and energies.

Both *ab initio* and semi-empirical methods optimize the atomic orbitals using Self

Consistent Field theory (SCF), where the repulsive forces of each electron in the molecule are minimized in a static electric field generated by the positions of the nuclei and other electrons [**46**]. The results obtained by high level *ab initio* calculations provide more accurate values for bond lengths, bond angles, dihedral angles and energy values [**47**], but come at a large computational cost since the atomic orbitals are optimized from "first principles". The Born-Oppenheimer approximation of the Schrödinger equation is solved using only fundamental constants and atomic numbers [**47**]; modern *ab initio* methods represent the atomic orbitals using Gaussian function basis sets like 3-21G(*) and 6-31G** [**46**], which are integrated by iteration until an optimal geometry is yielded. Computationally economical alternatives to *ab initio* methods have been developed over the past 30 years. These semi-empirical determinations reproduce the gas phase molecular properties of molecules by solving expressions for ψ that have been simplified by parameterizations representing atomic assumptions [**46**].

Dewar and Thiel's modified neglect of diatomic overlap (MNDO) method [**48**] is an improvement of the neglect of diatomic differential overlap (NDDO) semi-empirical calculation method of Pople *et al* [**49**] and gives an adequate treatment of one- and two-centre repulsion integrals [**46**]. The atomic spectra of 34 molecules were used to assign values for 5 of the 12 atomic parameters for hydrogen, carbon, nitrogen and oxygen [**48**], and while the other seven parameters are derived by the MNDO calculations themselves [**50**]. The MNDO treatment is confined to closed-shell molecules and their valence electrons, and the total energy of the molecule is calculated as the sum of the electronic energies and the repulsions between the cores of adjacent atoms by iterative optimization of the coordinate matrix [**48**].

The limitations of the MNDO method include excessive long-range repulsions [**50**] and underestimation of the stability of sterically crowded molecules [**51**]. This is corrected by the AM1 re-parameterization of this semi-empirical method [**50**]; this revised method makes better

predictions of optimized geometry, particularly that of nitro functional groups which are often incorrectly optimized in a perpendicular conformation by MNDO in molecules like nitrobenzene [50]. Stewart's second re-parameterization of MNDO, PM3, is a significant improvement of the MNDO and AM1 semi-empirical methods since polynitro organic compounds were included in the database of several hundred molecules [52] whose experimentally-determined gas phase properties were used to re-optimize the atomic parameters used for calculation [50]. The PM3 method uses 18 parameters for carbon, nitrogen and oxygen atoms in the molecule, with only 11 assigned for hydrogen since seven parameters involve p orbitals that are absent for this atom [50]. The PM3-calculated molecular enthalpies of formation (ΔH_f) for 26 organic nitro compounds had an average error of 5.2 kcal/mol compared to observed values [52]. This error is three times lower than the average error observed for AM1 (15.7 kcal/mol) and almost eight times lower than the average error calculated for MNDO (39.6 kcal/mol) [52]. Although the optimized geometries yielded by PM3 are generally within 2% of the values observed from *ab initio* calculations and X-ray crystal structures for small molecules [50], predicted geometries are still prone to error. This is reflected by the virtually non-existent rotational energy barriers calculated for formamide [54], and inherently unreliable ΔH° values [51].

1.4. Mutagenesis, the Ames Reversion Assay and Nitroarene Metabolism

The propensity of chemical agents to induce cancer has been studied for decades. In 1918, Yamagiwa and Ichikawa showed that the application of coal tar to rabbit ears induced carcinoma [54]. Benzo[*a*]pyrene (B[*a*]P) was found to be the major carcinogenic constituent of coal tar in 1938 by Kenneway [55]. B[*a*]P and other PAH have been shown to induce point mutations in mouse lymphoma cells and to cause *in vitro* cell transformation in human fibroblasts [15]. Industrial workers coming in contact with benzanthrone were shown to suffer from

photocontact dermatitis upon exposure to light [**56**].

Mutagenesis is defined as the alteration of DNA resulting in heritable traits [**57**], and is one of the first events in carcinogenesis, the initiation of cancerous growth. Mutagenesis is promoted by genotoxicity, which is the ability of a chemical agent to covalently modify DNA. The correlation between mutagenicity and the degree of DNA adduct formation has been established by Beland and Howard [**58, 59, 60**]. Quantitative determinations of DNA adduct formation from exposures to PAH and nitroarenes can be accomplished by high performance liquid chromatographic analysis [**60**] and by the ^{32}P-postlabelling assay method developed by Randerath and Gupta [**61, 62**].

The Ames reversion assay is a simple system that uses the bacterium *Salmonella typhimurium* to determine the mutagenic potencies of chemical agents like nitroarenes. These prokaryotic cells do not possess a membrane-bound nucleus; thus, the genetic material is directly exposed to genotoxins or genotoxic metabolites given that they cross the cell membrane. Bacteria possess cell walls for added protection against their environment, and Gram negative bacteria, like *Salmonella typhimurium*, have more porous cell walls that do not retain the crystal violet stain used to classify this feature [**63**]. In wild-type *Salmonella typhimurium*, the biosynthesis of the essential amino acid L-histidine is under *his* operon control [**64**], with the enzymes required for this biosynthesis produced only when L-histidine is not present in the growth medium. An engineered mutation (*hisD3052*), when introduced into the $(GC)_4$ repeat region of the *hisD* gene in *Salmonella typhimurium* strains interrupts the expression of the enzyme histidinol dehydrogenase; this nicotinamide adenine dinucleotide (NAD)-dependent enzyme catalyzes the conversion of L-histidinol to L-histidine [**64**]. In the Ames reversion assay, incubation with nitroarenes can restore the bacteria's ability to synthesize histidine by inducing a frameshift mutation that reestablishes the reading frame of the *hisD* gene. These frameshift

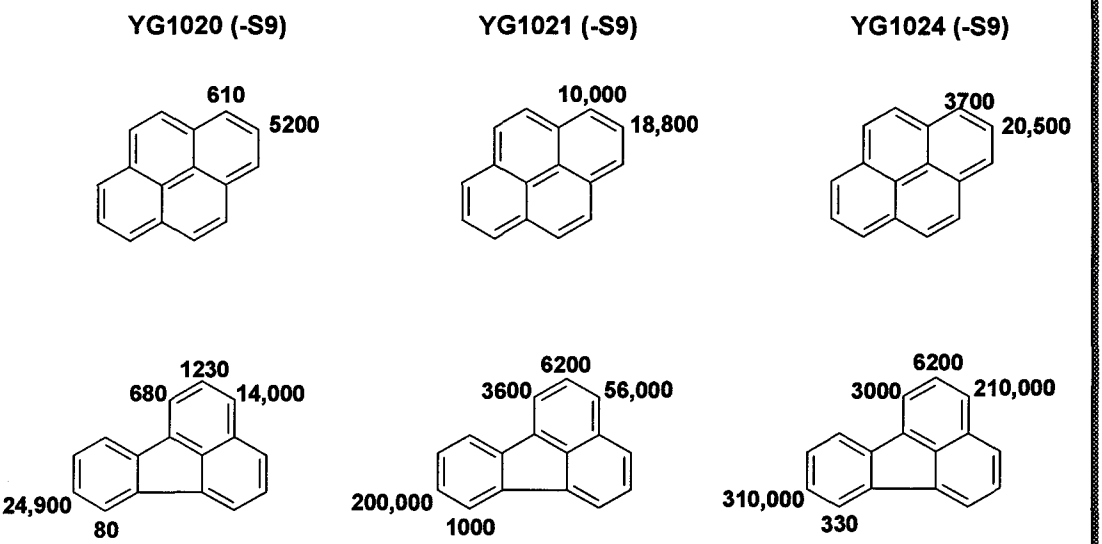

Figure 7. Comparative mutagenicities of nitropyrenes and nitrofluoranthenes in three *Salmonella typhimurium* strains. Data from [17].
Numbers represent the mutagenic potency of nitroarene isomers in units of revertants per nanomole.

mutations show a dose response dependence [**17, 65**], which is reflected in the number of bacterial colonies that grow on histidine-free agar medium (see Figure 7).

DNA adducts can result in the expressions of different types of mutations; the most common mutations are base-pair substitutions [**66**], which preserve the reading frame of DNA, and frameshift mutations. Base-pair substitution mutations are detected by TA100-type strains of *Salmonella typhimurium*. Frameshift mutations are detected by TA98-type strains of *Salmonella typhimurium*. The Ames reversion assay has been shown to be 80 to 90% accurate in the prediction of carcinogenicity from the mutagenicity observed for a wide range of genotoxic compounds [**2**]. Within a chemical class of compounds, such PAH and nitroarenes, the order of potencies in the Ames reversion assay often mirrors the potencies as carcinogens [**2, 57**].

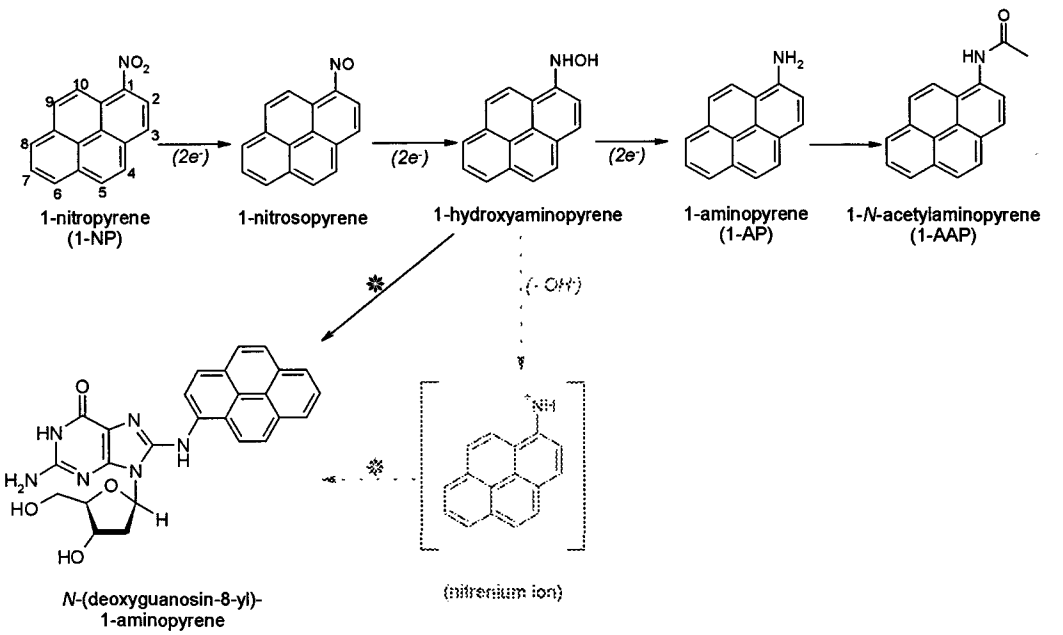

Figure 8. Derivatives of 1-nitropyrene and C8-deoxyguanosine adduct. I.
Stepwise reduction, acetylation and adduct formation in *Salmonella typhimurium*.
✲ Intermediates form adducts in double-stranded DNA, and are isolated by enzymatic hydrolysis and dephosphorylation of the resulting nucleotides.

The TA98 strain of *Salmonella typhimurium* possesses a full complement of three nitroreductase enzymes, with the major component being the "classical" nitroreductase (NR) [**25, 32**]. Classical NR of *Salmonella typhimurium* is an enzyme of 217 amino acid residues, with a mass of approximately 24kDa [**67**] and a 1-NP activity in TA98 of 10pmol/min/mg protein [**68**]. The classical NR gene has been cloned into plasmid pBR322 that was used to transform strain TA98 into an NR-overproducing strain called YG1021 [**32**]. *Salmonella typhimurium* strain YG1021 shows an increased response to nitroarenes compared to strain TA98 [**32**]. As shown in Figure 8, NR catalyzes sequential two-electron reductions of nitroarenes through the nitroso- and *N*-hydroxylarylamine intermediates to afford arylamines.

The enzymes in humans that can metabolize nitroarenes reductively under anaerobic conditions include NADPH-cytochrome P450 oxidoreductase, cytosolic xanthine oxidase, NADH-

quinone oxidoreductase (formerly known as diphtheria toxin diaphorase), and aldehyde oxidase [69]. These microsomal and mitochondrial oxygen-sensitive nitroreductases [70] catalyze the one electron reduction of nitroarenes to the nitro radical anion. However, in the presence of oxygen, the nitroarene is regenerated through a futile redox cycle in which superoxide is produced [68].

Nitroreduction serves to activate nitroarenes compounds to intermediate species that can modify DNA directly to afford DNA adducts that result in frameshift mutations. The first chemical intermediate produced by the nitroreduction of 1-NP in *Salmonella typhimurium*, 1-nitrosopyrene, was found to be 50 times more mutagenic in TA98 than 1-NP [71]. The nitroreduction of nitroarenes also generates *N*-hydroxylarylamine intermediates which have been shown by Kadlubar, Beland and Howard to react directly with DNA under slightly acidic conditions [59, 72, 73]; it has been postulated that *N*-hydroxylamines react to form highly electrophilic nitrenium ions that serve as the ultimate genotoxins [21]. The rate and ease of nitroarene reduction is rationalized to be related to the efficiency of *N*-hydroxylarylamine production and the extent of DNA adduct formation since the latter is correlated to mutagenic potency [58, 60].

The formation of conjugated metabolites is used to make exogenic compounds like PAH and nitroarenes less toxic and more water-soluble for elimination. Acetylation is a major arylamine metabolism route in mammalian systems [74, 75], and arylamines, the products of the reduction of nitroarenes, can be acetylated to form *N*-acetylarylamines in mammals and in cellcultures. The enzyme acetyl CoA:aromatic amine *N*-acetyltransferase functions as an *O*- and *N*-acetyltransferase in *Salmonella typhimurium* – several nitroarenes, including 3-NFA [20], 2-NP [75], 3-NBA [18], nitrophenanthrenes [76] and 1,8-dinitropyrene (1,8-DNP) [65] require acetylation of their arylamines to fully express their mutagenic potencies. The increased stabilities and lifetimes of the ultimate genotoxin nitrenium ions produced from *N*- and *O*-acetylated arylhydroxylamine derivatives (see Figure 9), in comparison to the nitrenium ions produced from

N-hydroxylarylamines, further promotes the mutagenicity of nitroarenes and is typified by the mutagenicity and carcinogenicity of 2-*N*-acetylaminofluorene (2-AAF) [77].

Like acetylation, oxidation is a process used by organisms to detoxify exogenic compounds. The mixed-function oxidoreductase cytochrome P450 is a membrane-bound protein that can metabolize a wide variety of organic compounds [78, 79]. The isozymes CYP1A1, CYP1A2 and CYP3A4 are responsible for the metabolism of PAH and nitroarenes in humans [78]. Liver homogenate prepared from rats treated with the polychlorinated biphenyl mixture Aroclor 1254 contain elevated levels of cytochrome P450 enzymes [23]. The 9000x*g* supernatant of this homogenate, called S9 mix, is co-incubated with *Salmonella typhimurium* in the version of the Ames reversion assay that is used to determine the mutagenic potencies of oxidatively-derived metabolites [23]. Both nitroarenes and PAH undergo oxidative metabolism via arene epoxides (see Figure 9). A number of the ring-oxidized products derived from 4-nitropyrene are shown in Figure 10. The bacterial mutagenicities of some ring-oxidized products of nitroarenes are of a similar magnitude as the original nitroarenes [25], demonstrating that the metabolism of these compounds in mammalian systems yields mutagenic metabolites.

Additive as well as synergistic effects have been observed in the mutagenic responses of simple mixtures of nitroarenes [81]. Binary mixtures of 1-NP and 3-nitrobenzo[a]pyrene are shown to have bacterial and mammalian mutagenic potency, as well as synergistic mutagenicity in *Salmonella typhimurium* [82]. Since nitroarenes and PAH are not encountered in isolation in the environment, investigations of the modulatory effects of PAH on nitroarene mutagenicity in bacteria [83] attempt to address the effect of complex environmental mixtures on exposure and mutagenicity.

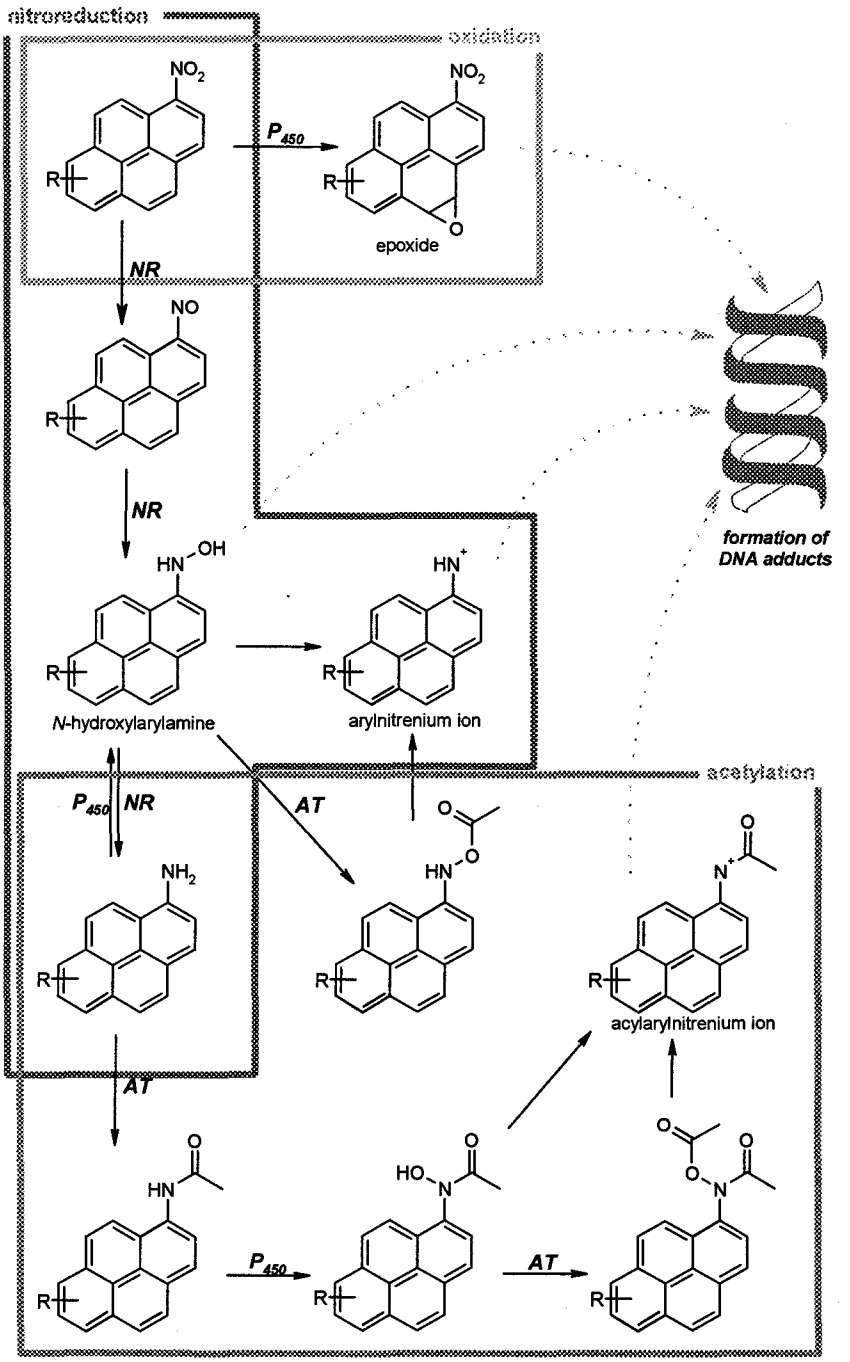

Figure 9. Pathways for 1-nitropyrene metabolite activation in *Salmonella typhimurium*. Adapted from [80].

R=H or OH. Boxes indicate major metabolic routes. Enzymes are indicated in italics. *AT:* Acetyltransferase. *NR:* Nitroreductase. P_{450}: Cytochrome P450.

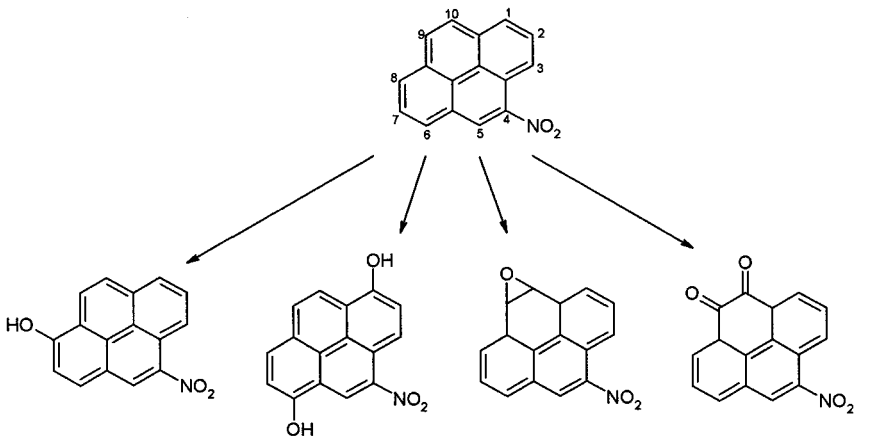

Figure 10. Oxidative metabolism of 4-nitropyrene in the rat [25].

1.5. Use of Gas Chromatography-Mass Spectrometry in Metabolism Studies

In previous studies of the metabolism of mutagenic nitroarenes, radiolabelled forms of the nitroarenes were incubated with bacterial- and eukaryotic cell culture suspensions. Organic extracts were prepared and analyzed by high performance liquid chromatography (HPLC), with absorbance and/or fluorescence detection together with liquid scintillation counting as the off-line detector **[20, 65, 84]**. The principle problem with this approach is the need to synthesize each nitroarene in radiolabelled form – in some cases, this task is not trivial.

Capillary gas chromatography (GC) is inherently more efficient than HPLC due to the significantly lower viscosity of a gaseous mobile phase compared to a liquid one. Modern GC capillary columns have between 100 000 and 300 000 theoretical plates, at least one order of magnitude greater than the number of theoretical plates of typical HPLC columns **[85]**. The detection limits achieved by tandem GC-MS lie in the range of HPLC with fluorescence detection and about two orders of magnitude more sensitive than HPLC methods using diode array detection **[86, 87]**. Capillary GC-MS is routinely used in the isolation and identification of

compounds in complex environmental matrices, such as extracts of tobacco and marijuana smoke condensates [**88**], air particulate extracts [**17**] and aquatic sediments [**7**].

Biological matrices have also been analyzed using MS detection in tandem with GC and capillary electrochromatography in studies of PAH metabolites from rat liver tissue and nitroarene DNA adducts [**85, 89**]. Variable degrees of nitroarene reduction to arylamines within the ion source at the GC-MS interface can contribute errors in nitroarene quantitation [**15, 90**] since the molecular ion of the arylamine has the same m/z value as the nitroarene fragment ion $[M\text{-}NO]^{+}$ [**14**]. This error can be minimized by the use of internal standards and dry sample conditions, which reduces hydrogen radical generation from the presence of water in the ion source.

The electron affinity of the nitro group makes the formation of anions by electron capture favourable and enables the MS detection of nitroarenes in negative ion mode, making this method highly sensitive [**15, 89**]. Nitroarenes are also amenable to electron impact (EI) ionization to afford radical cations that fragment either by direct bond cleavage or through bond rearrangements to generate characteristic fragment ions. The ions produced from nitroarenes by EI include the molecular ion, M^{+}, and the fragments $[M\text{-}NO]^{+}$ (-30 mass units), $[M\text{-}NO_2]^{+}$ (-46 mass units), $[M\text{-}CNO_2]^{+}$ (-58 mass units), $[M\text{-}HNO_2]^{+}$ (-47 mass units), and $[M\text{-}H_2NO_2]^{+}$ (-48 mass units) [**13**]. In nitroarene EI spectra, the ion abundance of the rearrangement ion $[M\text{-}NO]^{+}$ tends to be greater than the abundance of the direct bond cleavage product $[M\text{-}NO_2]^{+}$ due to the higher resonance stabilization that occurs in the respective product ions, $[Ar\text{-}O]^{+}$ and Ar^{+}, respectively [**91**]. The sensitivity of GC-MS analyses precludes the use of radioisotopes and permits incubations to be performed at concentrations of nitroarene that are in the middle of the dose-response data normal used for the Ames reversion assay. Thus, the metabolism in the Ames reversion assay and kinetics experiments can be conducted under identical conditions.

1.6. Syntheses of Nitroarenes, Their Metabolites and Arylazides

In the laboratory, quantitative mononitration of PAH has been accomplished by treatment of PAH with concentrated or fuming HNO_3 in an organic solvent like acetic anhydride [**92, 93, 94**], or by reaction with $NaNO_3$ in trifluoroacetic acid [**43**]. Reactive PAH such as pyrene require only a slight excess of the nitrating agent. The nitrofluoranthene isomers that are produced under these conditions are similar to the profile of isomers found in the analysis of diesel exhaust extracts [**95**], with 3- and 8-NFA being the major products. The isomer profiles obtained from the N_2O_5 nitration of PAH in gaseous or adsorbed forms are very different from the products of electrophilic nitrations [**96**]. For example, 2-nitrofluoranthene (2-NFA) is formed in very low (<1%) yield by the direct nitration of fluoranthene with HNO_3, however, 2-NFA is the major product obtained in the nitration with N_2O_5 [**96**].

The study of nitroarenes and their metabolites requires facile syntheses of various derivatives that can serve as authentic chromatographic and mass spectral standards (Figure 11). The nitrosoarene isomers tend to be stable but rather reactive while the *N*-hydroxylarylamine intermediates are generally unstable, precluding their isolation and characterization from cells. The syntheses of these metabolic intermediates provide adequate quantities for chemical characterization, genotoxicity assays and chromatographic analyses. Nitrosoarenes can be synthesized from the corresponding arylamines by their treatment with Caro's acid, a mixture of potassium persulfate ($K_2S_2O_5$) and sulfuric acid (H_2SO_4) [**97**]. In addition to nitrosoarenes, *N*-hydroxylarylamines can be produced on the laboratory scale by the *meta*-chloroperbenzoic acid (mCPBA) oxidation of arylamines [**98, 99**] and by the ascorbic acid reduction of nitrosoarenes [**100**]. Nitroarenes are also reported to produce *N*-hydroxylarylamines in the Pd/C catalyzed reduction by phosphinic acid in a two-phase THF/water system [**101**].

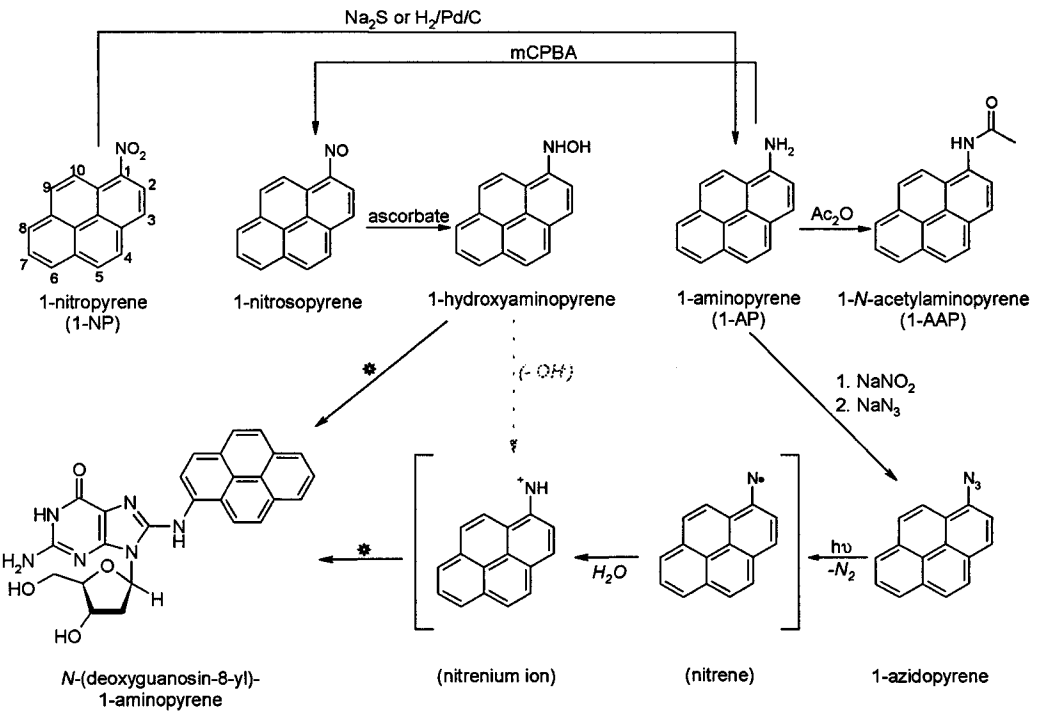

Figure 11. Derivatives of 1-nitropyrene and C8-deoxyguanosine adduct. II.
Synthetic routes to metabolite standards and adduct generation *in situ.*
✱ Intermediates form adducts in double-stranded DNA, and are isolated by enzymatic hydrolysis and dephosphorylation of the resulting nucleotides.

The nucleotide deoxyguanosine is the common site of covalent modification within DNA by electrophilic nitroarene metabolites. For example, the DNA adducts produced from 2-NF are the 3-(deoxyguanosin-N2-yl)- and *N*-(deoxyguanosin-8-yl)-type adducts of the arylamine and *N*-acetylarylamine **[102, 103]** (see Figure 11). The only *in situ* adduct produced from the treatment of 1-nitrosopyrene with ascorbate in the presence of double-stranded DNA is *N*-(deoxyguanosin-8-yl)-1-aminopyrene **[102, 104]**. Humphries *et al* recently postulated that the mechanism of DNA adduct formation at the weakly nucleophilic C8-position of deoxyguanosine involves initial electrophilic attack by the nitrenium ion at the purinyl N7 position, with ylide intermediate rearrangement to yield the observed C8 adduct **[105]** (Figure 12).

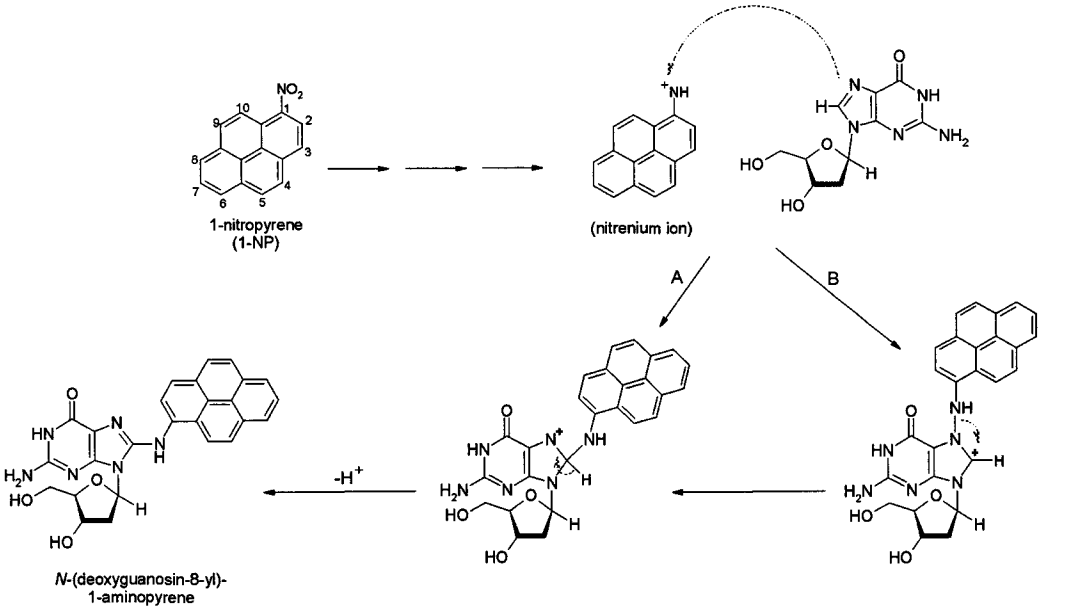

Figure 12. Mechanisms of deoxyguanosine adduct formation from 1-nitropyrene.
A. Initial electrophilic attack at C8. **B.** Proposed initial electrophilic attack at N7, adapted from [**105**].

The hydrogenation of nitroarenes over platinum (Pt) or carbon-doped palladium (Pd/C) catalysts is the most common method used to produce their arylamines [**106**] (see Figure 11). The arylamine derivatives of the nitroarenes can also be easily produced on the laboratory scale by Zinin reduction, where divalent sulfur (polysulfides) acts as the reducing agent [**107**]:

$$2ArNO_2 + 6S^{2-} + 6H^+ \rightarrow 2ArNH_2 + 3S_2O_3^{2-} + H_2O.$$

The rate-determining step is attack on the nitro group by the sulfide ion; the less hindered nitro group in dinitro compounds is reduced preferentially [**107**]. The reducing agents lithium aluminum hydride ($LiAlH_4$) and lithium borohydride ($LiBH_4$) are not suited for the reduction of nitroarenes to arylamines, however, as they form azoxy and azo derivatives [**107**]. As shown in Figure 11, *N*-acetylarylamine standards can be synthesized by treatment of the corresponding arylamine with acetic anhydride.

Arylazides are produced by arylamine diazotization with sodium nitrite ($NaNO_2$) in aqueous medium to generate the diazonium salt, followed by the nucleophilic addition of the azide

ion (N_3^-) to generate the arylazide [**108**]. The photolysis of these photolabile compounds yields singlet nitrenes and the lifetimes of various nitrene species have been reported [**109, 110**]. Water acts as proton donor in aqueous solution to generate the weakly acidic nitrenium ion from the short-lived nitrene species [**111, 112**]; these nitrenium ions are equivalent to the species produced by the formal loss of the hydroxyl group from the *N*-hydroxylarylamine intermediates of nitroarenes (see Figure 11). Arylazides have been used for the photoaffinity labelling of enzymes [**110**], and Andrews, Wild and McClelland *et al* have demonstrated that arylazide photolysis in the presence of calf thymus DNA generates *in situ* the same DNA adducts isolated from incubations of *Salmonella typhimurium* with nitroarenes [**65, 111, 112**]. The differing mutagenicities observed for 1-azidopyrene, 6-azidochrysene and 2-azidofluorene were observed to correlate with the short-lived photolysis product mutagenicity and the mutagenicity of the corresponding nitroarenes in *Salmonella typhimurium* strain TA98 [**112**]. The rate of formation and the reactivity of arylnitrenium ions, and the lifetime of arylnitrenes determined by laser flash photolysis [**111**] are indications of ultimate genotoxin generation and, potentially, the mutagenic potencies of nitroarenes.

1.7. Objectives

Previous studies have used theoretical and experimental parameters in attempts to predict the characteristics of nitroarenes that account for their mutagenicities. The overall goal of this project was to investigate some of these factors for a set of nitroarenes whose range of activities was comparable to those previously examined in larger SAR studies. The specific objectives of this research were:

1. to perform *ab initio* calculations at the HF/3-21G level for 13 nitroarenes,
2. to develop an analytical method for the determination of relative rates of metabolism of

nitroarenes in *Salmonella typhimurium* strain YG1021,

3. to ascertain whether a relationship exists between the mutagenic potency of 13 nitroarenes and their relative rates of reductive metabolism by YG1021 cultures,
4. to examine the possible correlations between the biological activities of 13 nitroarenes – relative rates of metabolism and mutagenic potency, and their physicochemical parameters – half-wave reduction potential ($E_{½}$), calculated hydrophobicity (log P) and calculated quantum mechanical values (ε_{LUMO}, ε_{HOMO} and ΔH_f), and
5. to examine nitrene generation by the novel compound 3-azidobenzanthrone using laser flash photolysis.

2. RESULTS AND DISCUSSION

In this investigation of the chemical and biochemical aspects of nitroarene mutagenicity, a set of 13 nitroarenes was selected for its large range of mutagenic potencies. The semi-empirical calculations performed on the structures of these compounds were compared to the results of previous studies and assessed for quality by comparison to *ab initio* calculations performed in this work. The values obtained from these calculations were used to critically evaluate the relationships of theoretical and experimental properties of these nitroarenes to their mutagenic potencies, and to investigate whether these factors could account for the range of mutagenicities observed.

Very little research has been done on characteristics of nitroarene intermediates that may explain the mutagenicities observed in the Ames reversion assay. Intuitively, processes that transpire closer to the mutagenic event have a greater impact on the nitroarene mutagenic potency observed. To date, there has been no systematic investigation of the relationship between mutagenicity and the relative rates of metabolism for a large set of compounds. An efficient analytical method was devised in this project in order for this property to be explored and evaluated for relationships to the structure and activity of nitroarenes.

2.1. Molecular Modelling

Before comparisons between previous SAR results and this work could be made, it was important to know whether the computer system and package used for MNDO and PM3 semi-empirical calculations in this study would yield similar results to those reported in the literature for

some nitroarenes. One objective of this thesis was to look at some values claimed by previous investigators to be important determinants of mutagenicity – namely ε_{LUMO} and NO_2 dihedral angles **[34, 37, 38]**. The HF/3-21G basis set was selected for *ab initio* calculations in this work as an improvement to the quality of the theoretical data generated. This level of *ab initio* calculations is lower in quality to the 6-31G** level; however, the latter calculations would have required an estimated week of more for each structure, well above the time available for this project. The results of these calculations could then be compared to previously reported *ab initio* STO-3G values **[39]** and to the semi-empirical calculation results of this study. Although HF/3-21G is a lower level of *ab initio* theory, its structural and energetic results are better than those yielded by both semi-empirical and the now obsolete STO-3G *ab initio* level calculations **[47]**, and could strengthen any structure activity relationships that exist.

2.1.1. Semi-Empirical Calculations using MNDO and PM3

Previous studies have concluded that ε_{LUMO} is a quantitative determinant of mutagenic potency **[39, 41]**, and as a result this parameter has been included frequently in the SAR of nitroarenes **[34, 35]**. It was a goal of this work to re-evaluate results of MNDO and PM3 semi-empirical calculations and their potential use as determinants of nitroarene mutagenicity. In addition to comparing ε_{LUMO} values, this study would examine other properties, particularly molecular energies, nitroarene geometries and charge distributions, and their correlation with mutagenicities and rates of metabolism.

MNDO and PM3 calculations were undertaken on a personal computer equipped with a 133 MHz processor, without using X-ray crystal structure coordinates as starting points for the molecular energy minimizations. The first PM3 calculations were performed with no restrictions

on the NO_2 dihedral angle relative to the aromatic plane, and afforded calculated dihedral angles for all 13 nitroarenes to be predicted as 0°, a seemingly default value. From MNDO calculations, the dihedral angle was zero degrees, except for 1-, 3- and 7-NFA, whose NO_2 groups were predicted to be perpendicular to the ring plane. This perpendicular NO_2 group orientation was also reported by Loew *et al* for these nitrofluoranthenes **[42]**.

Bond lengths between the ring carbon and the NO_2 group nitrogen ranged from 1.492 (1-NFA, PM3) to 1.515 Å (9-NA, MNDO). All nitro group geometries were calculated to be planar. Calculations were repeated for 1-NP, 4-NP, 1-NFA, 3-NFA, 7-NFA, 5-NAN, 3-NBA, and 9-NA (see Figure 2), whose structures possess a *peri* hydrogen, using a preset dihedral angle of 48°. This angle corresponds to the dihedral angle found in the x-ray crystal structure of 1,5-dinitronaphthalene **[39]** and is used as a model for the steric hindrance in these nitroarenes. This second set of calculations for these nitroarenes converged to different energy minimized structures than previously obtained, yielding NO_2 dihedral angles ranging from 46° (5-NAN and 3-NFA, PM3) to 66° (9-NA, MNDO). A third calculation using a restrained dihedral angle of 90° was performed for 9-nitroanthracene, and both the PM3 and MNDO calculations converged to structures with NO_2 dihedral angles of 90°.

Stewart has commented that there is no simple test that indicates when the global rather than local minimum has been reached **[50]**, and it is understandable why previous investigators have used X-ray crystal structure coordinates as starting points for their calculations. Since it was found that the semi-empirically calculated structures were dependent on the starting conformation of the molecule, the values associated with the nitroarene structures derived from restricted dihedral angles of 48° were used for the nitroarenes possessing *peri* hydrogens in this study (Table 1). In the case of 9-nitroanthracene, the structure with an NO_2 dihedral angle of 90° was used since it was the conformation of lowest calculated energy. This was the only nitroarene for which X-ray crystal structures existed, and two separate reports had shown dihedral angles of

Compound	NO_2 Dihedral Angle*	
	PM3	MNDO
9-Nitroanthracene	90	90
3-Nitrobenzanthrone	49	58
1-Nitropyrene	49	53
4-Nitropyrene	49	53
7-Nitrofluoranthene	50	58
1-Nitrofluoranthene	49	58
5-Nitroacenaphthene	46	56
3-Nitrofluoranthene	46	56
2-Nitrofluoranthene	0	0
2-Nitrofluorene	0	0
2-Nitropyrene	0	0
3-Nitrofluorene	0	0
8-Nitrofluoranthene	0	0

Table 1. Dihedral angles of the NO_2 group calculated in this study. I. Semi-empirical results.
* Relative to aromatic ring plane.

both 45° [113] and 90° [114] for this molecule. Since this work cannot explicitly determine whether the global minima for all structures was obtained, in addition to the theoretical limitations of semi-empirical calculations, conclusions drawn from these calculations should be viewed cautiously.

The energy differences between the nitroarene structures obtained by the first and NO_2 dihedral angle-restricted sets of calculations ranged from +1.2 kcal/mol (3-NFA, MNDO) to -13.7 kcal/mol (9-NA, MNDO), and generally indicated that a more stable structure was obtained from the NO_2 dihedral angle-restricted calculations. However, these energy differences do not indicate that the calculation result is the global minimum structure, and a better structure may be accessible by a calculation that displays different properties, including the NO_2 dihedral angle. Jung *et al* found that 3-NFA had a minimum energy with an NO_2 conformation of 52°, and possessed a 12 kcal/mol rotational barrier to give a 90° NO_2 group conformation by MNDO calculation [115]. These rotational barriers, which are often overestimated by PM3 and MNDO [47], can be easily overcome in biological systems through molecular binding to proteins and/or enzymes. Koshland's induced-fit mechanism [116] states that the binding of a substrate to the enzyme active site provides a change in environment that facilitates the conformational change of its functional group. This raises the question of the importance of NO_2 group conformation to mutagenic potency.

Heats of formation for the nitrofluoranthenes ranged from +88.7 to +90.0 kcal/mol (MNDO) and +70.4 to +73.8 kcal/mol (PM3). For the nitropyrenes, heats of formation were lower and ranged from +77.2 to 78.9 kcal/mol (MNDO) and +54.9 to +58.9 kcal/mol (PM3). Binding energies for the isomeric 247 molecular weight nitropyrenes and nitrofluoranthenes (see Figure 2) were slightly larger for the fully aromatic nitropyrene series than the non-alternant nitrofluoranthene one, and ranged from –3345 to –3358 kcal/mol in the MNDO calculations and –3361 to –3380 kcal/mol in the PM3 calculations. The compounds 2-NP, 2-NFA and 8-NFA had

larger binding energy values compared to their isomers; these values may indicate increased stability due to the absence of steric interaction between a *peri* hydrogen or *pseudo*-bay region adjacent to the NO_2 group.

Molecular orbital energies that were obtained by MNDO calculations were similar to the results of Lopez de Compadre *et al* [**34**]. A general trend that was observed in the calculations was the apparent larger repulsive forces present in MNDO-derived structures compared to the same molecules whose structures were calculated using PM3. This was reflected in larger dihedral angles and smaller band gaps ($\Delta\varepsilon = \varepsilon_{LUMO}-\varepsilon_{HOMO}$) in MNDO versus PM3 calculations (see Table 2). Stewart's construction of the PM3 basis set parameters used experimental values from compounds with large differences between MNDO-calculated and experimental values, and polynitro organics [**50**], which make this semi-empirical method better suited to calculating the structures of nitroarenes.

In this study, LUMO and HOMO distributions were looked at qualitatively, particularly since their energies are frequently used as indices of mutagenic potency in structure-activity investigations [**34,117**]. Both PM3 and MNDO calculations for the compounds 2-NP and 9-NA showed no LUMO surface area over the NO_2 group, the supposed site of reduction. This is also a reflection of limitations of semi-empirical calculations, since it is most logical for the promotion of an electron to a formally electropositive region, namely the nitrogen atom of the nitro group, to be the least energetically expensive, and most probable. If it is assumed that initial reduction of the NO_2 group requires placement of an electron in the vicinity of the electropositive nitrogen or the oxygens of the NO_2 group, the semi-empirical LUMO energy values for 2-NP and 9-NA are invalid in the SAR discussions of these structures.

Nitroarene structures that were derived in this study using semi-empirical calculations,

Compound	ε_{LUMO} (in eV) PM3	MNDO	MNDO[◆]	Band Gap[*] (in eV) PM3	MNDO
3-Nitrofluorene	-1.165	-1.275	------	8.251	7.936
5-Nitroacenaphthene	-1.295	-1.275	-1.218	7.985	7.944
2-Nitrofluorene	-1.376	-1.436	-1.529	8.166	7.874
2-Nitropyrene	-1.507	-1.453	-1.49	7.254	7.134
7-Nitrofluoranthene	-1.524	-1.458	-1.388	7.672	7.493
2-Nitrofluoranthene	-1.688	-1.633	------	7.578	7.398
9-Nitroanthracene	-1.739	-1.509	-1.673	7.217	7.209
4-Nitropyrene	-1.685	-1.560	-1.575	7.101	7.032
8-Nitrofluoranthene	-1.720	-1.663	-1.594	7.497	7.327
1-Nitropyrene	-1.767	-1.653	-1.670	7.090	6.985
1-Nitrofluoranthene	-1.727	-1.625	-1.584	7.516	7.365
3-Nitrofluoranthene	-1.791	-1.665	-1.634	7.499	7.366
3-Nitrobenzanthrone	-2.037	-1.836	------	7.382	7.392

Table 2. LUMO energies and band gap values calculated in this study. I. Semi-empirical results.

[*] Band gap = $\Delta\varepsilon = \varepsilon_{LUMO} - \varepsilon_{HOMO}$.

[◆] Determined by Lopez de Compadre *et al* [**34**].

without the use of a starting x-ray crystal structure, were similar to those obtained by previous investigators. As well, calculated non-coplanar conformations of the NO_2 group were observed for nitroarenes possessing a *peri* hydrogen, but only when the NO_2 dihedral angles were restricted to 48° prior to geometry optimization. It was concluded that the optimized geometries and associated energies derived from semi-empirical calculations were of questionable quality.

2.1.2. *Ab Initio* Calculations using 3-21G Basis Set

The geometry-optimized structures of nitroarenes were derived using HF/3-21G level *ab initio* calculations in this study. The purpose of using this level of theory was to obtain better theoretical data about the structure of these compounds, which can be compared to the results of lower level calculations that have been performed previously. *Ab initio* calculations have been virtually ignored in the study of nitroarene mutagenicity because of the computational cost required for these calculations, and specifically because of the findings of Maynard *et al* in 1986, where STO-3G *ab initio* calculations were shown to display similar trends as PM3 calculations **[39]**.

Calculations using the HF/3-21G basis set, a lower level *ab initio* method presenting a higher level of theory than both semi-empirical and STO-3G basis set calculations, yield more reliable results than these latter calculations and were performed for two initial purposes. First, to compare and evaluate the quantitative and qualitative results of semi-empirical output to *ab initio* results. Secondly, to investigate other output that is yielded from the calculations, including dipole moments, bond angles and electrostatic potentials, as possible indices of biological activity. The comparison of these HF/3-21G calculation results to the lower level STO-3G *ab initio* outcomes of Maynard *et al* **[39]** may indicate that the relative gains in theoretical information are worth the initial computational investment.

Initially, single point calculations of the nitroarenes were attempted using the geometries optimized by PM3 calculations. This approach was found to be inappropriate; for example, the calculated structure of the aromatic ring of 3-NBA was found to have a slightly concave shape by this method, as opposed to a planar ring. It was observed that each *ab initio* geometry optimization calculation required approximately 3 to 4 days to complete on the Octane workstation. It is estimated that this time could have been shortened to 1 day if the workstation's resources were not shared, since calculations were performed using approximately 20% of the Octane's resources. In contrast, the Spartan program on the same workstation completed PM3 calculations of 2-nitropyrene and 3-nitrofluoranthene within seconds. This large increase in time illustrates one of the deterrents of attempting *ab initio* calculations for larger molecules.

Semi-empirical and *ab initio* calculations showed marked differences in surface map outputs and dihedral angles of the NO_2 group. Figure 13 shows the striking difference in dihedral angle of the NO_2 group for 3-nitrofluoranthene, where the *ab initio* calculation shows a coplanar conformation (zero dihedral angle) in contrast to the result of the PM3 calculation using Spartan (46° dihedral angle). In the same figure, the PM3 calculation result for 2-NP was found to have no LUMO surface on the nitro group, which was not the case with the HF/3-21G result. As discussed in the previous section, the absence of LUMO surface about the nitro group in both PM3 and MNDO calculations calls these calculations into question since it is logical that some region of probability for electron promotion lies about the formally electropositive nitrogen atom. With this reasoning, the HF/3-21G basis set calculation results are intuitively of higher quality than the semi-empirical results.

The HF/3-21G geometry optimization calculations also yielded planar nitro groups and O-N-O bond angles ranging from 123° to 125°. Nitro group torsional angles were zero for 7 of the 13 nitroarenes whose structures were calculated, including 3-NFA and 5-NAN, whose structures possess *peri* hydrogens which have been rationalized to lead to non-coplanar

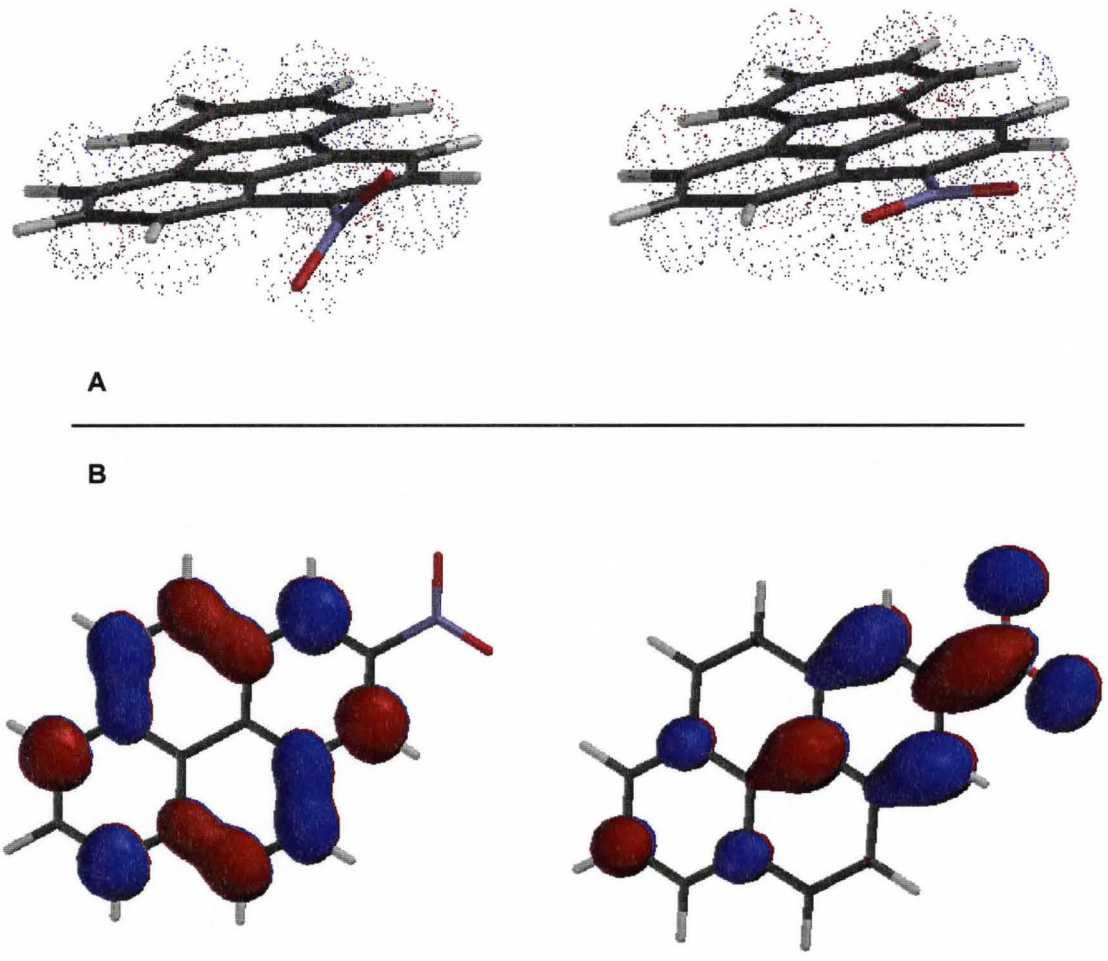

Figure 13. Comparison of the results of PM3 and HF/3-21G calculations.
A. Dihedral angles and LUMO surface maps of 3-NFA calculated by PM3 (left) and HF/3-21G (right).
B. LUMO surface maps of 2-NP calculated by PM3 (left) and HF/3-21G (right).

Compound	NO_2 Dihedral Angle*		
	3-21G	PM3	MNDO
9-Nitroanthracene	45	90	90
3-Nitrobenzanthrone	19	49	58
1-Nitropyrene	17	49	53
4-Nitropyrene	16	49	53
7-Nitrofluoranthene	13	50	58
1-Nitrofluoranthene	12	49	58
5-Nitroacenaphthene	0	46	56
3-Nitrofluoranthene	0	46	56
2-Nitrofluoranthene	0	0	0
2-Nitrofluorene	0	0	0
2-Nitropyrene	0	0	0
3-Nitrofluorene	0	0	0
8-Nitrofluoranthene	0	0	0

Table 3. Dihedral angles of the NO_2 group calculated in this study. II. *Ab initio* and semi-empirical results.
* Relative to aromatic ring plane.

conformers (see Table 3). Non-zero NO_2 torsion angles ranged from 12° (1-NFA) to 45° (9-NA) and were much smaller than those derived from semi-empirical calculations. Vibrational frequencies were calculated for the 14 nitroarenes and all showed 6 values equal to zero, which corresponded to the three translational and three rotational degrees of freedom which do not change the molecular electronic energy [47] – the largest absolute values of these vibrations was $4x10^{-5}$ cm^{-1} (see Appendix 2). Also, repeated calculations using a restricted NO_2 dihedral angle of 48° for 3-nitrofluoranthene and 48° and 90° for 9-nitroanthracene yielded the same optimized structure as the unrestricted calculation. However, further modelling of the nitroarene structures by this method would be required to ascertain whether true global minima were obtained.

Compound	ε_{LUMO} 3-21G	ε_{LUMO} STO-3G*
2-Nitrofluorene	0.0366 au 0.997 eV	0.162 au 4.41 eV
7-Nitrofluoranthene	0.0322 au 0.876 eV	0.148 au 4.02 eV
8-Nitrofluoranthene	0.0230 au 0.626 eV	0.133 au 3.62 eV
1-Nitrofluoranthene	0.0146 au 0.397 eV	0.128 au 3.48 eV
3-Nitrofluoranthene	0.0118 au 0.321 eV	0.132 au 3.59 eV

Table 4. ε_{LUMO} values determined by *ab initio* calculations.
* Determined by Maynard *et al* [39].

In the PM3 calculations, 90 electrons were considered in the case of the nitroarenes isomers with a molecular weight of 247Da, while 128 electrons were considered in the HF/3-21G *ab initio* calculations. The inclusion of the 38 core electrons in the *ab initio* calculations resulted in different electronic distributions and molecular orbitals for the nitroarenes. This partly explains the increased total calculated energies that ranged from –923 a.u. (3-nitrobenzanthrone) to -660 a.u. (5-nitroacenaphthene). ε_{LUMO} values ranged from –0.0003740 a.u. (3-nitrobenzanthrone) to 0.04538 a.u. (3-nitrofluorene) (-0.01018 to 1.235 eV) and were of significantly lower magnitude than those values calculated by semi-empirical methods and the STO-3G results of Maynard *et al* **[39]** (Table 3). ε_{HOMO} values ranged from –0.3207 a.u. (2-nitrofluorene) to –0.2867 a.u. (2-nitropyrene) (-8.726 to –7.801eV). Band gap ($\Delta\varepsilon$) values ranged from 0.3090 a.u. (1-NP) to 0.3614 a.u. (3-NF) (8.408 to 9.834 eV) (see Table 4). These lower energy ε_{LUMO} and ε_{HOMO} values, and larger $\Delta\varepsilon$ values, suggest that the structures obtained by HF/3-21G calculations have less diffuse molecular orbitals **[47]**, which translate to lowered electronic repulsions and more stable predicted molecules than by previously employed methods.

The NO_2 group conformation from the x-ray crystal structure of 1,5-dinitronaphthalene was used to estimate the non-coplanarity of the NO_2 group in the presence of a *peri* hydrogen in 1-NFA, 3-NFA, 7-NFA and 1-NP in the work of Maynard *et al* **[39]**. The dihedral angles obtained by HF/3-21G *ab initio* calculations for 7 of the 13 nitroarenes were zero; the non-zero values were of lower magnitude than those obtained by semi-empirical methods (Table 1). This difference can be attributed to the higher quality basis set afforded by HF/3-21G. PM3 and MNDO calculations inherently overestimate the instability of sterically crowded molecules and yield unreliable ΔH° values and dihedral angles **[51]**. STO-3G calculations are limited by unreliable dipole moment calculations and overestimated bond lengths **[51]**, which may explain the higher steric interference between the *peri* hydrogen and the NO_2 moiety that is reflected in larger NO_2 dihedral angles and higher energy ε_{LUMO} values.

Compound	ε_{LUMO} (in eV)			Band Gap* (in eV)		
	3-21G	PM3	MNDO	3-21G	PM3	MNDO
3-Nitrofluorene	1.235	-1.165	-1.275	9.835	8.251	7.936
5-Nitroacenaphthene	1.000	-1.295	-1.275	9.414	7.985	7.944
2-Nitrofluorene	0.9969	-1.376	-1.436	9.723	8.166	7.874
2-Nitropyrene	0.9774	-1.507	-1.453	8.789	7.254	7.134
7-Nitrofluoranthene	0.8761	-1.524	-1.458	9.226	7.672	7.493
2-Nitrofluoranthene	0.6961	-1.688	-1.633	9.193	7.578	7.398
9-Nitroanthracene	0.6944	-1.739	-1.509	8.591	7.217	7.209
4-Nitropyrene	0.6749	-1.685	-1.560	8.477	7.101	7.032
8-Nitrofluoranthene	0.6259	-1.720	-1.663	9.061	7.497	7.327
1-Nitropyrene	0.4955	-1.767	-1.653	8.408	7.090	6.985
1-Nitrofluoranthene	0.3962	-1.727	-1.625	8.815	7.516	7.365
3-Nitrofluoranthene	0.3210	-1.791	-1.665	8.810	7.499	7.366
3-Nitrobenzanthrone	-0.01018	-2.037	-1.836	8.654	7.382	7.392

Table 5. LUMO energies and band gap values calculated in this study. II. *Ab initio* and semi-empirical results.
* Band gap = $\Delta\varepsilon = \varepsilon_{LUMO} - \varepsilon_{HOMO}$

The relatively small HF/3-21G basis set was selected for *ab initio* calculations because its size made the geometry optimization of molecules like nitroarenes, which possess 20 or more heavy atoms, tenable. In spite of its good accuracy, the HF/3-21G basis set is limited because of the omission of electron-electron interactions (electron correlation) in the SCF calculations, which

limits the accuracy of the calculated energies and the validity of using ε_{LUMO} values as indices of electron affinity [**47**]. Furthermore, modelling nitroarene structures in the gas phase may have its own limits, since these calculated values are used to explain nitroarene characteristics in solution.

Log P values calculated by the Ghose-Crippen method [**118**] within the Spartan package differed from those obtained by Lopez de Compadre *et al* [**34**], and ranged from 3.80 for the nitrofluorenes to 4.38 for the 8 members of the nitrofluoranthene and nitropyrene series (Table 6). Dipole moments (μ) ranged from 4.39 Debye for the difunctionalized 3-nitrobenzanthrone molecule to 6.52 Debye for 8-nitrofluoranthene. Mulliken atomic charges on the nitrogen atom ranged from 0.12 to 0.19, and ranged from 0.27 to 0.38 for the *ortho* carbon. Natural atomic charges on the nitrogen atom were essentially equal (0.49 to 0.51 range) and on the *ortho* carbon, ranged from 0.06 to 0.12. Higher quality atomic charges are yielded by the calculation of electrostatic potentials [**51**] and were found to range from 0.87 (3-nitrofluorene) to 1.02 (9-nitroanthracene) for nitrogen, and –0.39 (9-NA) to –0.05 (2-NP) for the *ortho* carbon.

Molecular electrostatic potential surfaces were also calculated for the nitroarenes. This aspect of nitroarene structures has never been investigated. The electrostatic potential, defined as the net electric potential field felt by a point near the static charge distribution of a molecule or atom [**47**], has been shown to be reliable descriptor of molecular reactivity and is used in drug design [**119**]. For the nitroarenes, negative electrostatic potential surfaces were large in the vicinity of the NO_2 group as expected, but were also present in localized portions of the aromatic ring as shown in Figure 14 and Appendix 1. These localizations on the aromatic ring displayed π orbital character, and as shown in Figure 14, the overlay of nitroarene electrostatic potential surfaces with a common orientation of the nitroarene molecule in 3D space displays two regions of electrostatic potential. This was observed with overlays of nitroarenes possessing both high and low mutagenic potencies, and suggests a common binding contact within the cleft of

Compound	log P	
1-Nitropyrene	4.38	4.69 *
2-Nitropyrene	4.38	4.69 *
4-Nitropyrene	4.38	4.69 *
1-Nitrofluoranthene	4.38	4.69 *
2-Nitrofluoranthene	4.38	4.69 *
3-Nitrofluoranthene	4.38	4.69 *
7-Nitrofluoranthene	4.38	4.69 *
8-Nitrofluoranthene	4.38	4.69 *
9-Nitroanthracene	4.06	4.78 *
3-Nitrobenzanthrone	3.92	------
2-Nitrofluorene	3.80	3.37 *
3-Nitrofluorene	3.80	3.37 *
5-Nitroacenaphthene	3.54	3.85 *

Table 6. Calculated hydrophobicities of nitroarenes.
* Determined by Lopez de Compadre *et al* [34]

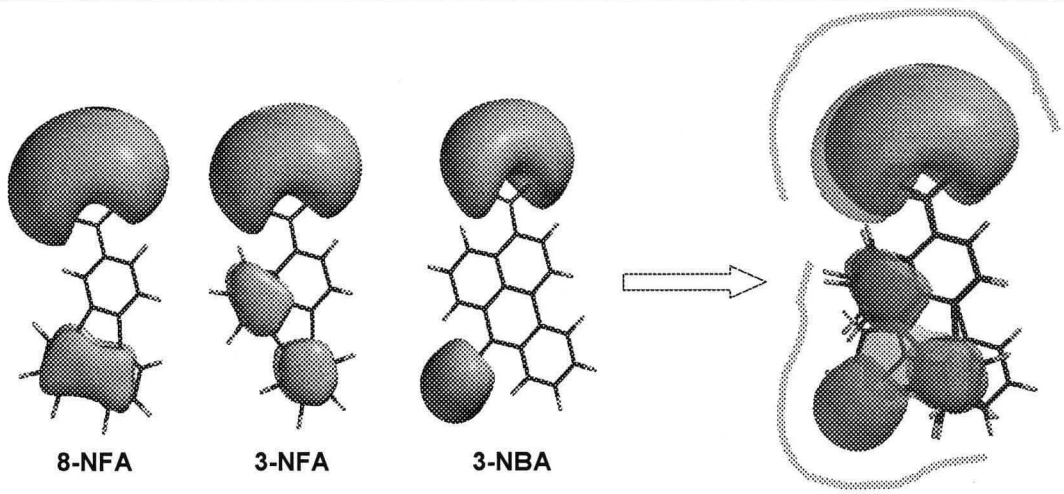

Figure 14. Electrostatic surface map overlays of selected nitroarenes and the suggested electropositive region of the nitroreductase binding site.

nitroreductase.

This study is not only the first to report nitroarene structures determined by HF/3-21G *ab initio* calculations – the electrostatic potential surface maps of these molecules as potential indicators of nitroarene affinity for nitroreductase were also investigated. The molecular orbital energies calculated by this *ab initio* method were more reliable than those obtained by MNDO and PM3, since positive ε_{LUMO} values, signifying the endergonic process of electron promotion and/or reduction, and more stable molecular structures, were obtained.

Although HF/3-21G *ab initio* calculations yielded better results than semi-empirical and STO-3G calculations, the use of nitroarene structures to predict mutagenic potency is questionable. The addition of an electron to form the nitro anion radical species would undoubtedly alter the electronic distribution within the molecule, and would affect the calculated energies and nitro group conformations that would be observed. It is most relevant to place the effort of high-level calculations in a context where differences in molecular structure have a direct,

as opposed to indirect, effect on biological activity. The differences in the structures and energetics of nitroarenes may be more related to their affinity for the active site of the nitroreductase enzyme, rather than the propensity of their activated metabolites to form adducts with DNA and induce mutations.

2.2. Mutagenicity of Nitroarenes and Relative Rates of Metabolism

Large SAR studies have used mutagenic potency data from a variety of sources; the variability of this data from lab to lab may introduce errors. In this work, it was desired to have mutagenicity data spanning a wide range of mutagenic potencies determined by one laboratory. Furthermore, it was important that the relative rates of nitroarene metabolism be determined using the same reducing system used to determine the mutagenicity data, namely the same strain of bacteria, operator and conditions of determination. The mutagenic potencies and the relative rates of metabolism would be determined using *Salmonella typhimurium* strain YG1021, a strain containing extra copies of the nitroreductase gene.

Another goal of this work was to develop an analytical method that could be used to determine relative rates of reductive metabolism of a range of nitroarenes that would avoid the need to have each compound available in a radiolabelled form. Gas chromatographic analysis was selected over liquid chromatographic methods because of the higher resolution of GC methods and because of the ready availability of instrumentation for GC-MS analysis. The approach was to determine the relative rates of metabolism for 13 nitroarenes whose structures had been modelled by theoretical calculations, and whose mutagenic potencies had been determined in this laboratory, and then to use this data to investigate possible structure activity relationships.

2.2.1. Mutagenic Potencies of Nitroarenes

Mutagenic potencies are usually determined for purified substances such as nitroarenes, although in the real world these compounds would only be minor constituents of complex mixtures in the environment. Compounds like the nitropyrenes and nitrofluoranthenes are found in the environment at trace levels in matrices such as air particulate [2], diesel particulate extracts [11] and aquatic sediments [7]. These isomers with a molecular weight of 247 Da show a large range of mutagenic potencies, particularly the nitrofluoranthenes whose potencies range over nearly 4 orders of magnitude in *Salmonella typhimurium* strains TA98 and YG1021 **[17, 34, 65, 116]**. Because of the wide range of potencies and the sensitivity of the Ames reversion assay, the purity of the nitroarene isomers is of tantamount importance. For example, when a 1% abundance of the highly mutagenic compound 1,8-dinitropyrene (1,8-DNP) was present in a sample of 1-nitropyrene, it was shown that over 80% of the activity observed in TA98 was due to this 1% contaminant **[13]**.

Mutagenic potencies were determined for 11 of the 13 nitroarenes selected for this study; a sample of 4-NP was not available, and the sample of 3-NF was found to be impure by GC analysis. Mutagenic potencies were found by linear regression analysis of counts from duplicate plates (see Table 7). As previously encountered in this laboratory, a 72-hour growth period was used for proper development of plates. The r^2 values for the linear regression analyses of these dose-responses averaged 0.92 at the 95% confidence interval, and ranged from 0.83 (3-NBA) to 0.99 (2-NP) (see Figure 15 and Appendix 3). Dose-responses for the standard 1,8-DNP showed very good consistency of day-to-day results of the assay. The isomeric 247 Da molecular weight nitropyrenes and nitrofluoranthenes showed mutagenic potencies ranging over 2 orders of magnitude, with 7-NFA having a mutagenicity of 1000 rev/nmol and 8-NFA having a mutagenic potency of 140 000 rev/nmol. These mutagenic potencies are the result of reduction of the nitro group, although some of these mutagenicities may be further augmented by acetylation, as

Compound	Mutagenic Potency (revertants/nmol)
8-Nitrofluoranthene	140000
3-Nitrobenzanthrone	110000
3-Nitrofluoranthene	33000
2-Nitropyrene	13000
1-Nitropyrene	9700
2-Nitrofluoranthene	7800
1-Nitrofluoranthene	1300
7-Nitrofluoranthene	1000
2-Nitrofluorene	870
5-Nitroacenaphthene	170
9-Nitroanthracene	170

Table 7. Mutagenic potencies for 11 nitroarenes in *Salmonella typhimurium* strain YG1021.

demonstrated for 3-NBA by Enya *et al* [18] and 3-NFA by Ball *et al* [20].

The mutagenic potencies found in this study were used to set a dose for the metabolism experiments to ensure that these experiments were carried out at a dose below the toxicity for these bacteria. For the nitroarenes with activities ranging from 170 to 140 000 rev/nmol, the dose of 450 pmol nitroarene per 2mL *Salmonella* culture was selected for the metabolism experiments.

Dose (ng)	Revertants per plate
0	25
0	41
3.96	247
3.96	256
7.93	427
7.93	401
11.9	576
11.9	641
15.9	924
15.9	905
19.8	1033
19.8	1108
Revertants/nmol	13000 ± 3.4%
r^2 (95%)	0.99

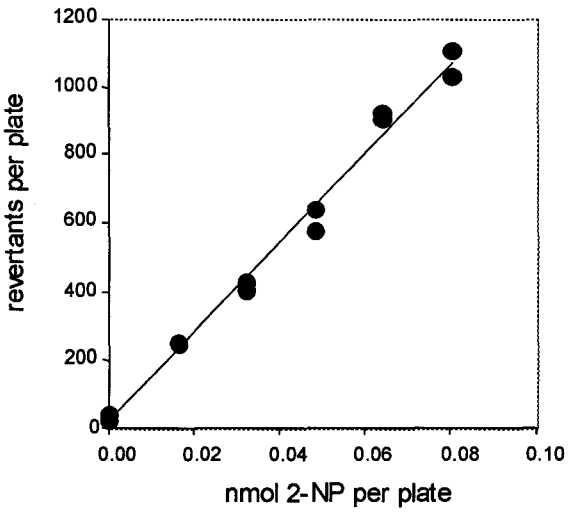

Figure 15. Dose response data for 2-nitropyrene in *Salmonella typhimurium* strain YG1021.
O = Point not included in linear regression analysis

This dose is within the linear response range of all nitroarenes examined in this study.

2.2.2. Metabolism Method Development

Before the relative rates of reductive metabolism could be determined, an efficient and reliable analytical method needed to be developed. Several issues needed to be addressed during the development of this method. First, the bioassay methodology, including dosing of the *Salmonella typhimurium* cultures, scale of the experiments and extraction procedure needed to be tailored to the GC-MS method. Secondly, the analytical methodology, namely the clean up of the extracts prior to analysis, the selection of internal standards, GC column selection, temperature program optimization, the determination of recoveries and quantitation would need to be explored. Due to time constraints, the rates of metabolism were determined for 6 of the

available 11 nitroarenes, where the range of mutagenicities spanned two orders of magnitude. The compounds examined were 2-NFA, 3-NFA, 8-NFA, 1-NP, 2-NP and 3-NBA (see Figure 2).

Previous metabolism experiments have been performed using radiolabelled nitroarenes and reversed-phase LC analyses of organic extracts of *Salmonella* growth medium. Fractions were collected and analyzed using liquid scintillation counting. This method had the advantage that all radiolabelled products are easily detected, free from analytical interferences. However, the requirement to prepare and purify each substrate in radiolabelled form is both costly and time-consuming. This approach was the used by Andrews to examine the metabolism of 1,8-DNP **[65]** and by Ball *et al* to determine rates of metabolism of 2-NFA and 3-NFA in *Salmonella typhimurium* strain TA98 **[20]**. An alternate method is based on the quantitation of arylamine metabolite peaks by liquid chromatography with fluorescence detection; the rate of production of 1-aminopyrene was used to determine the rate of 1-NP metabolism **[83]**. This method is sensitive and selective, but only allows the monitoring of fluorescent compounds; nitroarenes have extremely low fluorescence quantum yields. The potential advantages of tandem gas chromatography-mass spectrometry over these methods include increased chromatographic resolution, mass spectrometric detection and confirmation of the structure of nitroarenes and metabolites, and the ability to use unlabelled nitroarenes as substrates.

Determining Nitroarene Dose for Metabolism Studies

In the Ames bioassay, toxicity effects are observed as a decreasing number of revertants at higher plate doses due to cell death. It was important to select a dose that could be used to assay all nitroarenes, yet remain within the linear range of response of the assay. The amount of nitroarene that met this criterion was 0.450 nmol per 2mL culture, corresponding to 0.0225 nmol/plate or 5.6 ng/plate (nitropyrenes and nitrofluoranthenes) in the Ames bioassay. For 8-NFA, this dose would result in 3150 ± 310 revertants per plate, near or at the upper limit of

linearity for this assay. All other compounds would give numbers of revertants less than this value.

Extraction Method

Ball *et al* used 2:1 ethyl acetate/acetone as the extraction solvent for *Salmonella* experiments [**20**]. This solvent was thought to quench the cellular reactions since acetone is fully miscible with the aqueous phase and would disrupt the *Salmonella typhimurium* culture system. Ball *et al* found that >95% of radioactivity was extracted into the organic phase at all time points in their determinations of the metabolism of 2-NFA and 3-NFA; furthermore, no time-related trends in the ability to extract metabolites were observed [**20**]. Centrifugation was not used in this method since loss of nitroarene by partitioning within the lipid component of the cell pellet was considered a possibility. Unlike the recoveries reported by Ball *et al*, Pothuluri *et al* used ethyl acetate extraction followed by centrifugation in their liquid chromatographic method, and achieved an extraction efficiency of 78% by scintillation counting [**120**].

Recovery and Internal Standard Selection

In this study, recoveries were assessed using 1-nitropyrene-d_9 (1-NP-d_9) as an extraction standard. The term extraction standard is used since the addition of this deuterated nitroarene to the cell culture would occur at the end of the incubation and just prior to solvent extraction. Since it was not added at the start of the incubation, 1-NP-d_9 does not function as a true recovery standard. It cannot assess processes occurring during the experiment, prior to extraction, that may account for variability, such as partitioning within lipid materials. This deuterated compound was used to assess recovery for several reasons. It possessed a similar hydrophobicity to the nitroarenes studied and was expected to behave similarly in its partitioning within the cellular material, clean up properties and chromatographic retention compared to other

nitroarenes. The chromatographic behaviour on a GC column showed that it eluted within a nitroarene standard chromatogram (see Figure 18). Its fragmentation and degree of reduction in the ion source could be used as an indication of similar processes occurring with other nitroarenes.

To determine the amounts of a nitroarene in an extract at each time point in a metabolism experiment, internal standards were required for quantitation. In other studies, radiolabelled substrates have been commonly used as both recovery and internal standards; Ball used ^{3}H-labelled 2-NFA to both assess extraction efficiency and identify chromatographic peaks in the determination of the rates of metabolism of 2-NFA and 3-NFA [**20**]. Although this method is excellent for the assessment of recoveries, the competitive metabolism between the ^{3}H-labelled nitroarene standard and other nitroarenes is of concern, and is not discussed in that previous work.

PAH have hydrophobicities similar to the nitroarenes and do not undergo any known reduction metabolism. PAH seemed to be ideal candidates for use as recovery standards in metabolism experiments. However, PAH have been shown to modify the mutagenic potencies of nitroarenes [**83**] and therefore may affect the rates of metabolism of nitroarenes. Lee *et al* showed that naphthalene and chrysene had minimal inhibitory effects on nitroarene mutagenic potency in *Salmonella typhimurium* [**83**]. Thus, chrysene has the potential to be an ideal recovery standard for this method because of its size, retention time and inertness in *Salmonella typhimurium* strain YG1021, but was not investigated for the following reasons:

1. the lower polarity of this PAH relative to a nitroarene may result in losses during the clean-up of the organic extract; Modica *et al* observed that using the weak solvent 100% cyclohexane effectively eluted PAH in alumina column chromatographic clean-ups of organic extracts of rat tissues [**121**],

2. the lack of activity modulation by chrysene on 1-NP activity may not hold true for other nitroarenes, several PAH have shown dose-dependent synergistic mutagenicity with co-incubation of nitroarenes in *Salmonella typhimurium* [**83**], and
3. the amount of testing and checking needed to ensure that chrysene would be useful as a recovery standard seemed too onerous for the potential value of the method.

Two PAH, chrysene and perylene, were selected for use as internal standards in the quantitation of extracted nitroarenes because of their intermediate molecular weights relative to the nitroarenes and their retention times in GC-MS analyses, which come before and after the nitroarenes in this study (see Figure 18). These PAH were shown to have similar analytical responses in the GC-MS methods used in this study.

Development of a Clean-Up Method

A suitable clean up method needed to be developed for the preparation of extract samples prior to GC-MS analysis in order to remove aliphatic and polar contaminants from cellular material, yet still retain the analytes of interest. Solid phase extraction (SPE) is a method used in this laboratory for the clean up of extracts from a wide range of environmental samples, and has been shown to have excellent sample recoveries [**122**]. A neutral alumina SPE cartridge was used since alumina is a milder sorbent, and because some nitroarenes are believed to be reduced on silica [**65**]. Two potential sources of nitroarene loss during sample preparation include photochemical degradation and adsorption onto glass, as reported by White for 6-nitrobenzo[a]pyrene [**15**]. All experiments were conducted under yellow light to minimize photochemical losses. In addition, all glassware was washed with dichloromethane (DCM) to elute any adsorbed nitroarenes.

The first clean-up method that was examined had serious drawbacks. A 2mL aliquot of

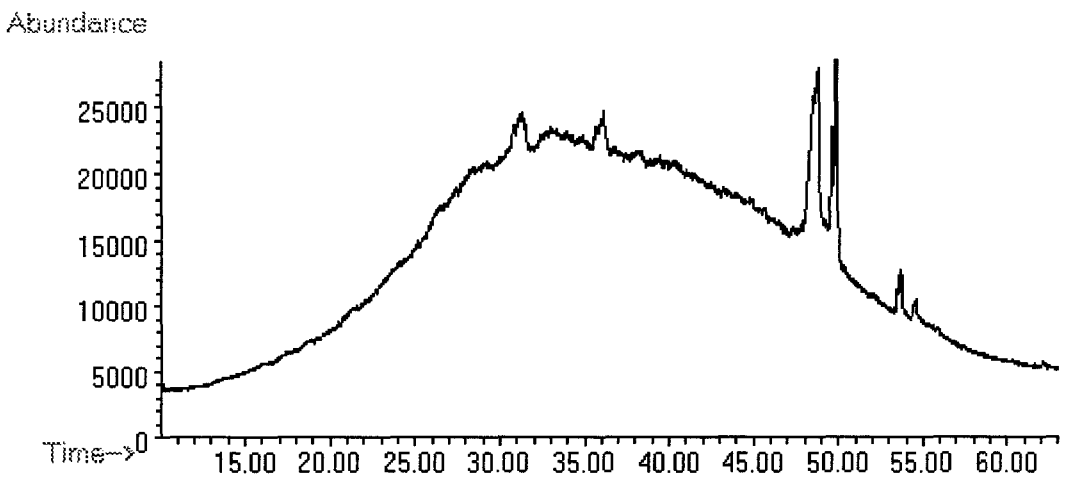

Figure 16. First attempt at analysis of an SPE-cleaned extract from an incubation of *Salmonella typhimurium* strain YG1021 spiked with 3-nitrofluoranthene.

Salmonella typhimurium culture was extracted as per the method of Ball *et al* **[20]** and the residue was taken up in DCM and applied to an alumina SPE cartridge. The cartridge was eluted with additional DCM and the load and wash were retained and evaporated to dryness prior to analysis by GC-MS with toluene as solvent. The resulting chromatogram, shown in Figure 16, showed that the sample contained large amounts of aliphatic interferences which completely overwhelmed the 3-NFA spike that had been added to the extract.

The method used in this laboratory to remove aliphatic impurities from environmental samples is Sephadex LH20 chromatography **[17, 122]**. This method, while highly effective, is slow and is unsuited to metabolism studies where 5 to 6 time points needed to be analyzed in duplicate for each nitroarene. A simple and effective alternative to the Sephadex LH20 clean-up step needed to be found.

The polarity difference between aliphatics, triglycerides and aromatics suggested a two-

step elution method could be applied to an SPE cartridge. It was hypothesized that hexane elution of an SPE cartridge would elute aliphatics, triglycerides and other non-polar compounds while retaining the aromatics, and subsequent elution with DCM would elute the aromatics. The residue from the ethyl acetate/acetone extraction was taken up in hexane, applied to the alumina SPE cartridge and eluted sequentially with hexane followed by DCM. The GC-MS chromatogram of the DCM eluent showed no trace of aliphatic contamination. However, as the reproducibility of the method was assessed, it was noted that some sample recoveries were poor. It was rationalized that hexane may be a poor solvent for the dissolution of all components of the crude extract, whereas DCM was an excellent solvent.

The crude extract was treated with 200μL DCM and vigorously mixed to dissolve the residue whereupon 5mL of hexane was added slowly with mild agitation to afford a solution that had a composition of approximately 4% DCM/hexane. This solution was loaded onto the alumina SPE cartridge and the cartridge was eluted with additional hexane prior to elution with DCM. This two-stage SPE method was shown to be both efficient and effective as a clean-up step, as seen in the overlay of chromatograms from the metabolism experiments for 8-NFA (see Figure 19).

The incubations for the experiments were performed on the same day with the same stock of culture in an attempt to reduce the variability of the results. The sensitivity of GC-MS analysis allowed the experiments to be carried out on a 2mL scale, since metabolites were not isolated for structural characterization. As with the Ames reversion assay, late log phase growth (12 hours) *Salmonella typhimurium* YG1021 culture was used. Kranendonk *et al* studied phase I enzymes like nitroreductase in *Salmonella typhimurium* and found that significant differences in enzyme profiles existed between cultures in different growth phases **[123]**; this other potential source of variation was minimized by performing all experiments on the same day. Unlike the Ames reversion assay, culture growth was carried out at 37°C, followed by the performance of relative rate of metabolism experiments at 25°C. Earlier trials at 37°C showed an extremely

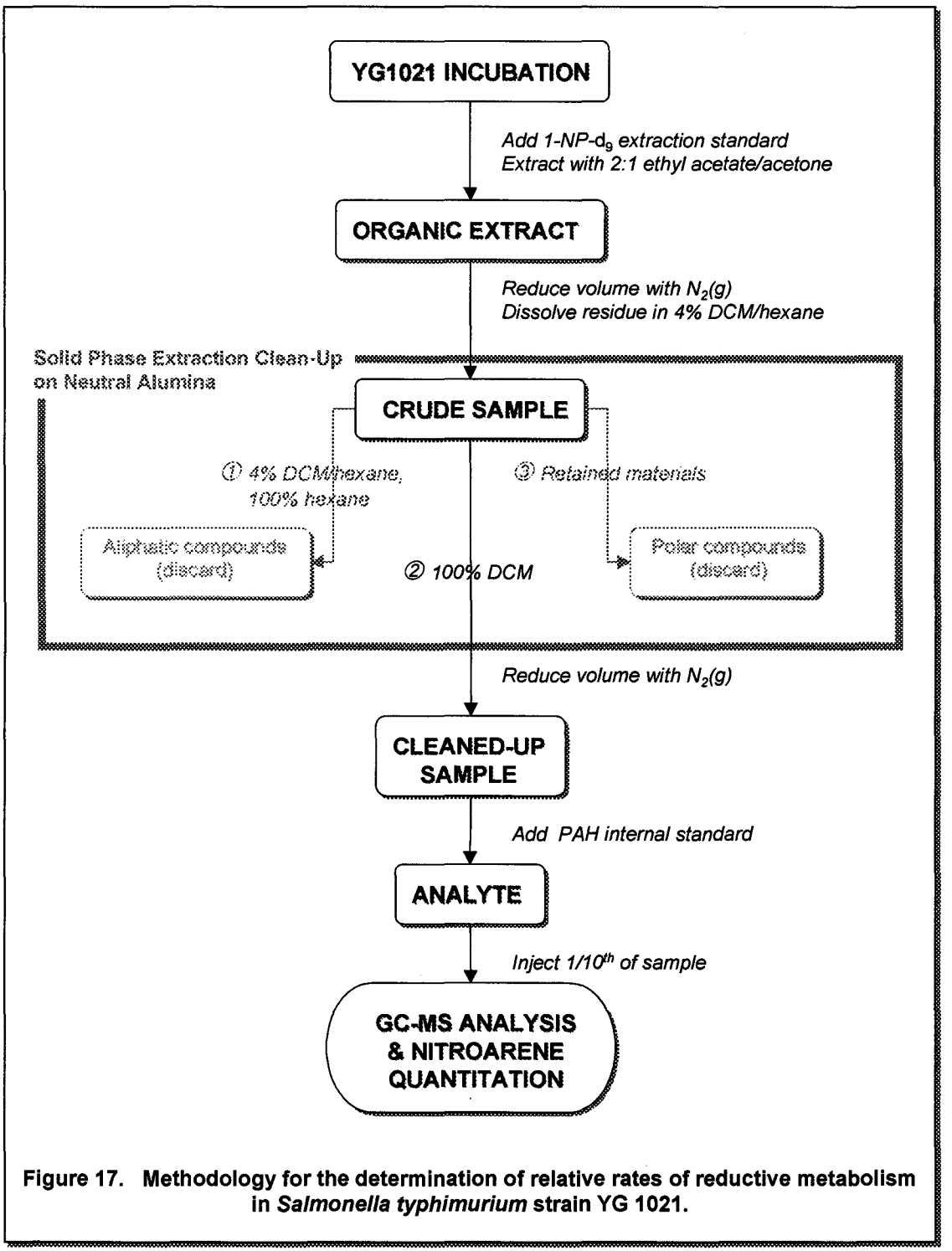

Figure 17. Methodology for the determination of relative rates of reductive metabolism in *Salmonella typhimurium* strain YG 1021.

rapid loss of 3-NFA (>99% metabolised after 10 minutes), and the introduction of errors in time, the independent variable, was a concern. In particular, compounds like 3-NBA and 8-NFA whose higher mutagenicities were expected to result in faster relative rates of metabolism to have higher independent time variable errors if experiments were run at 37°C.

GC-MS Method Development

Legzdins had shown previously that a capillary GC column with a 50% phenyl methyl silicone stationary phase (DB17ht) was well suited for the analysis of nitroarenes [17]. The temperature program used by Legzdins was altered significantly to suit the purposes of this project. The details of this temperature program can be found in the Experimental section. All seven nitrofluoranthenes and nitropyrenes are resolved using the DB-17 column, with a 95% valley observed between the two closest peaks, 7-NFA (t_R = 14.69 min)and 2-NFA (t_R = 14.79 min) (Figure 18). The retention times of 1-nitropyrene (t_R = 16.14 min) and 1-nitropyrene-d_9 (t_R = 16.08 min) resulted in a separation of peaks with a 50% valley; however, these peaks are easily resolved because they have different masses. The quantitation standards chrysene and perylene possess retention times that bracket the nitroarenes with the exception of 3-nitrobenzanthrone which elutes at 19.18 minutes using method B. The overall times of these GC programs were 21 and 23 minutes, so samples could be injected every 25 minutes.

Detection limits for the nitroarenes using methods A and B (see Experimental section) were estimated by using serial dilutions of a nitroarene standard containing 20μM nitroarene, 5μM PAH calibration standards and 10μM extraction standard 1-nitropyrene-d_9, and plotting the resulting signal-to-noise ratios against concentration. The detection limits were defined to be the concentrations found to correspond to a signal-to-noise ratio of 3:1. The detection limits listed in Table 6 agree with detection limits observed for PAH and nitroarenes by other investigators using

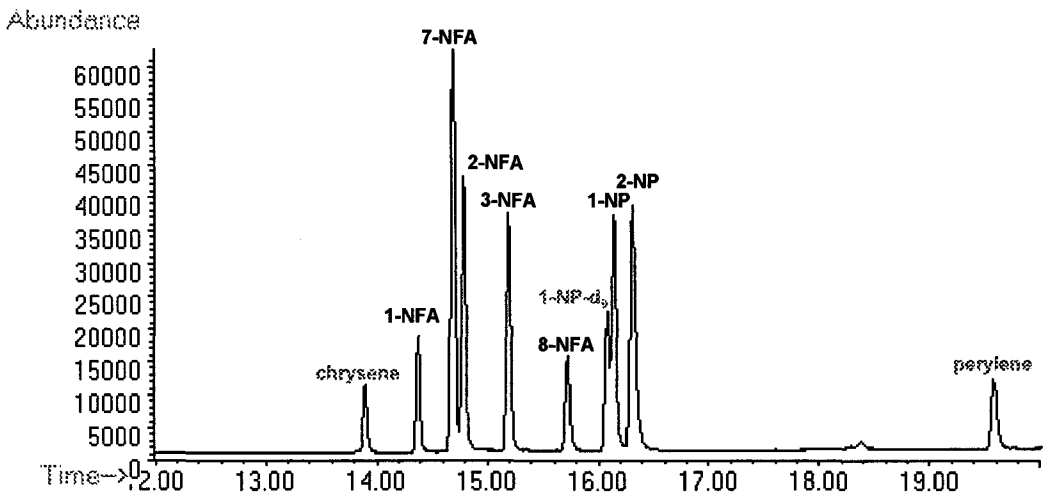

Figure 18. GC-MS chromatogram of a nitroarene standard analyzed by method A.

similar instrumentation [**65, 123**].

No nitroarene reduction upon injection was observed at an initial column temperature of 80°C; at higher temperatures, however, some reduction was observed. The variability in the ratios of [M] to [M-30] ions was high, and was observed in some analyses run on the same day. Nitroarene reduction to the amine occurs at the gas chromatogram-mass spectrometer interface within the ion source; the [M-30] ion corresponds to both the [M-NO] rearrangement fragment of the nitroarene, as well as the molecular ion of the arylamine reduction product [**9, 15, 90**].

Given that reduction of the nitro group may occur at varying degrees between analyses, it was imperative to use the sum of fragment ion peak areas to ensure more accurate quantitation of the nitroarenes. These fragment ions were selected based on the most abundant ion fragments observed for the EI spectra of the nitroarenes and the arylamines (see Experimental

section). The peak ratios within standards run intermittently during the analyses of the extracts were used to estimate the response factors of the internal standards compared with the extraction standard (1-nitropyrene-d_9) and the nitroarenes. Recoveries were determined by calculating the response factor based on the ratio of amounts of PAH and 1-nitropyrene-d_9 injected (1:5) and the ratio of their chromatogram peak areas from analysis of a standard. This response factor was used to determine the amount of extraction standard present in each sample; the quantitation of nitroarenes present in each sample recovered by extraction was accomplished in a similar

Compound	Molecular Weight	Detection Limit (pg) Method A	Method B
Chrysene	228	8	6
1-Nitrofluoranthene	247	60	—
2-Nitrofluoranthene	247	28	—
3-Nitrofluoranthene	247	35	—
7-Nitrofluoranthene	247	16	—
8-Nitrofluoranthene	247	56	—
1-Nitropyrene	247	38	—
2-Nitropyrene	247	22	—
Perylene	252	13	8
1-Nitropyrene-d_9	256	45	32
3-Nitrobenzanthrone	275	—	59

Table 8. Detection limits of nitroarenes using GC-MS selected ion monitoring methods.

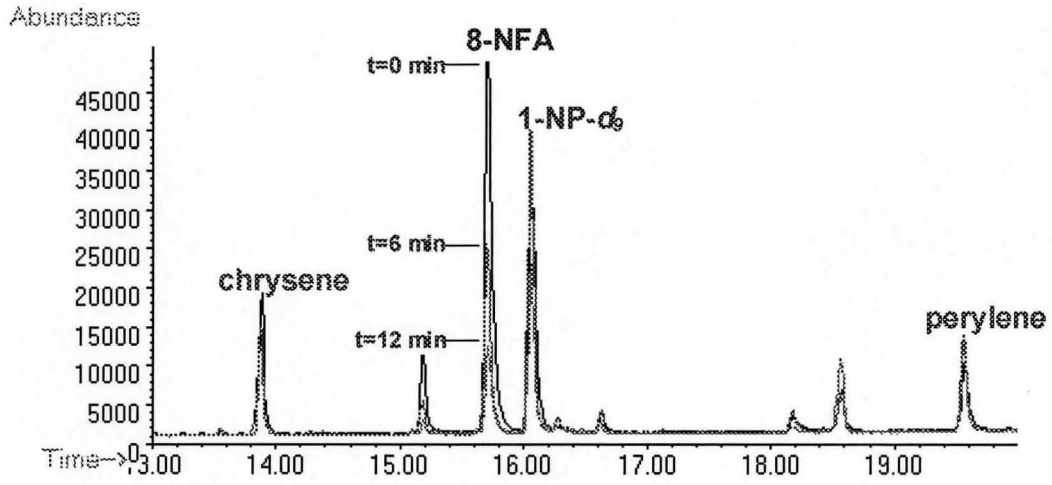

Figure 19. Overlay of GC-MS chromatograms used to determine the relative rate of metabolism of 8-nitrofluoranthene.

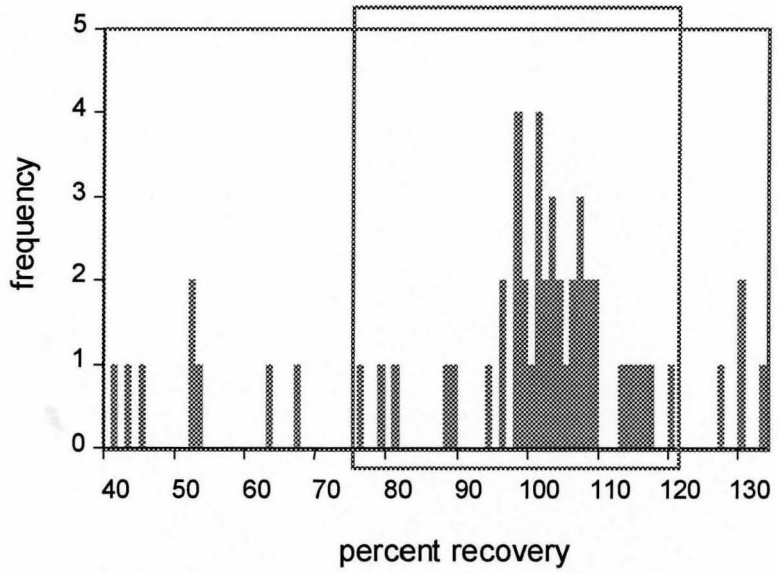

Figure 20. Extraction recoveries observed for relative rate of metabolism experiments.
Boxed region indicates samples with extraction recoveries suitable for analysis.

fashion.

The sample recoveries for this analytical method were 97±22% S.D. and ranged from 41 to 132%. As shown in Figure 20, 88% of the samples had extraction recoveries ranging from 76 to 121% and were deemed suitable for inclusion in the metabolism studies. None of these recoveries was used to scale the nitroarene quantities calculated from the experiments. The amount of each nitroarene found in each extract was estimated to have an error of 20%; this estimate was based on the average error for 8 sets of duplicate analyses.

2.2.3. Nitroarene Metabolism in *Salmonella typhimurium* YG1021

Although it was the goal to determine the relative rates of metabolism for 11 nitroarenes, data were determined for only 6 of these nitroarenes whose mutagenicities ranged over 2 orders of magnitude in YG1021. It was found that the relative rates of reductive metabolism did not vary significantly for four of these compounds: 2-NFA, 8-NFA, 1-NP and 2-NFA.

The rate data for all 6 nitroarenes spanned at least 2.5 half lives (Appendix 4). First order (lnA vs t) plots were constructed and used to derive first order initial rates and half-lives for the nitroarenes in the *Salmonella typhimurium* incubations, and showed good linearity with r^2 values averaging 0.93 at the 95% confidence level. The equation $v_o = k_A[A]$ was used to give initial rate values that showed the same qualitative trend of higher relative rates of reductive metabolism for compounds of increasing mutagenicities. As shown in Table 9, 3-NBA had over two times the initial rate of loss in the YG1021 culture than 3-NFA, and the rates of loss of the other 4 nitroarenes, 1-NP, 2-NP, 2-NFA and 8-NFA were essentially identical. However, since the dose used in the 8-NFA metabolism experiments would result in plate counts near or at the upper limit of linearity in the Ames reversion assay, the rate of 8-NFA reductive metabolism determined in

this study was suspected to be reduced due to toxicity.

Ball *et al* determined that the rate of 3-aminofluoranthene production was 27 times the rate of 2-aminofluoranthene production in TA98, yet the mutagenic potency of 3-NFA was only 7 times that of 2-NFA [**20**]. Ball *et al* concluded that the mutagenicity of 2-NFA was lower than that of 3-NFA due to its lower affinity for nitroreductase [**20**]. In this study, the rate of 3-NFA loss was only 3 times the rate of 2-nitrofluoranthene loss in YG1021, and the ratio of mutagenic potencies for these two compounds was 4:1.

The rates determined in this work are not directly comparable to the rates determined by Ball *et al* [**20**] and Andrews [**65**] since these latter experiments were conducted 37^{o}C, used a

Compound	Rate (pmol/hr/mL culture)	Half-life (min)
3-NBA	3600	2.60
3-NFA	1390	6.73
2-NP	497	18.8
1-NP	493	18.9
2-NFA	450	20.8
8-NFA	446	21.0

Table 9. Rates of reductive metabolism and half-lives of nitroarenes in *Salmonella typhimurium* strain YG1021 culture.

different *Salmonella typhimurium* strain and used different nitroarene concentrations. The ratio of rates of metabolism to mutagenic potency were higher than those observed by Ball *et al*, and ranged from 17:1 for 2-NFA to 31:1 for 3-NBA. Keeping in mind the limited set of nitroarenes used in this study, it is believed that the higher relative rates of 3-NBA and 3-NFA metabolism result in higher accumulations of reactive intermediates available to form DNA adducts and are reflected in higher mutagenicities observed in *Salmonella typhimuium* strain YG1021.

This investigation suggests that there is a relationship between nitroarene mutagenicity and relative rate of reductive metabolism. The initial rates that were observed ranged from 450 pmol/hr/mL (2-NFA) to 3600 pmol/hr/mL for 3-NBA. It was observed that 8-NFA, the most mutagenic compound assayed in YG1021 in this study, shared the same initial rate as 2-NFA, the least mutagenic of the set. This result is believed to be due to toxicity effects, and if a lower dose were used for these experiments, it is expected that this nitroarene would have the most rapid rate of reductive metabolism.

2.3. Nitroarene Structure-Activity Relationships

Since it is difficult to extrapolate high level exposure data to the relatively low human exposures in the environment **[27]**, structure-activity relationship (SAR) approaches to the study of nitroarene mutagenicity have been used in an attempt to better understand this process and predict the mutagenicities observed. Previous studies of nitroarene SARs postulate that the physicochemical properties of nitroarenes directly impact the mutagenic potencies observed **[28, 29, 30]** (Table 10). One of the goals of this research was to examine the possible relationships between the biological activities and physicochemical properties derived from HF/3-21G calculations for 11 nitroarenes whose range of mutagenic potencies are on the same order of larger SAR studies **[34, 37, 117]**.

Compound Class	Physical and Calculated Parameters Investigated	Reference
Nitroarenes	Physical Dimension of Aromatic Ring NO_2 Group Position on Aromatic Ring Relative Conformation of NO_2 Group to Aromatic Plane	Vance and Levin [37] Fu *et al* [38]
Nitroarenes	LUMO Energy (MNDO and STO-3G Determined)	Maynard *et al* [39]
Nitroarenes and Derivatives	LUMO Energy (MNDO Determined) Hydrophobicity Hammett Constants (σ, σ+)	Lopez de Compadre *et al* [34]
Nitroarenes and Derivatives	First Half-Wave Reduction Potential of NO_2 Relative Conformation of NO_2 Group to Aromatic Plane	Klopman *et al* [41] Jung *et al* [44]
Nitrofluoranthenes	First Half-Wave Reduction Potential of NO_2	Shane *et al* [124]
Arylamines	Nitrenium Ion Energies	Ford and Herman [125]
Nitroarenes and Nitrated Heterocyclics	LUMO Energy (PM3 and MNDO Determined) Hydrophobicity	Debnath *et al* [117]

Table 10. Structure-activity relationship investigations of the mutagenicities and carcinogenicities of nitroarenes and aromatic amines.

2.3.1. Mutagenicity vs. Calculated and Experimental Physical Parameters

To assess structure-activity relationships, the experimental parameter believed to be a good index of the ease of nitroreduction, namely the half-wave reduction potential ($E_{½}$) **[25, 41]**, was first investigated. Jung *et al* found that first $E_{½}$ values displayed a fair relationship with mutagenic potency only when the compounds were structurally similar; overall, they observed no correlation existed between nitroarene mutagenic potency and $E_{½}$ **[44]**. The plot of ε_{LUMO} versus $E_{½}$ displayed no correlation for the nitrofluoranthenes, although Shane *et al* stipulate that the same numerical data demonstrate a moderate relationship **[124]**; in this work, the linear regression analysis of the five points yielded an r^2 value of 0.05 and zero slope (-1.12 $\pm$ 2.92).

Half-wave reduction potentials were plotted against the logTA98 and logYG1021 values, and again no correlation was observed between the nitrofluoranthene $E_{½}$ values and mutagenic potency. Electrostatic potentials on the nitrogen of the nitroarene and the *ortho* carbon were plotted versus observed mutagenic potencies and showed no correlation, with r^2 values of 0.09 and 0.11 at a 95% confidence interval, respectively.

Log YG1021 values showed a modest relationship with *ab initio* ε_{LUMO} values (r^2=0.48) and $\Delta\varepsilon$ values (r^2=0.32) (see Figure 21). Favourable or lower values of the ε_{LUMO} may indicate higher mutagenic potencies, however the errors associated with this relationship, particularly the

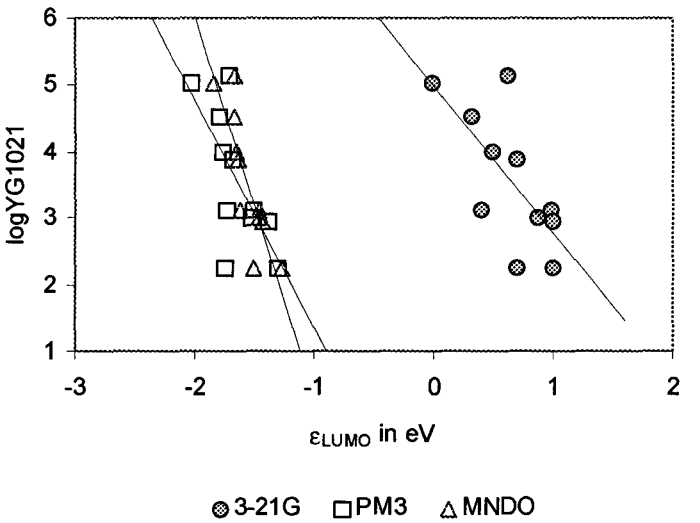

Theory	Slope	r^2 (95%)
HF/3-21G	-2.20 ± 0.77	0.48
PM3	-3.41 ± 1.17	0.49
MNDO	-5.64 ± 1.19	0.71

Figure 21. YG1021 mutagenicities versus ε_{LUMO} values obtained from semi-empirical and *ab initio* calculations.

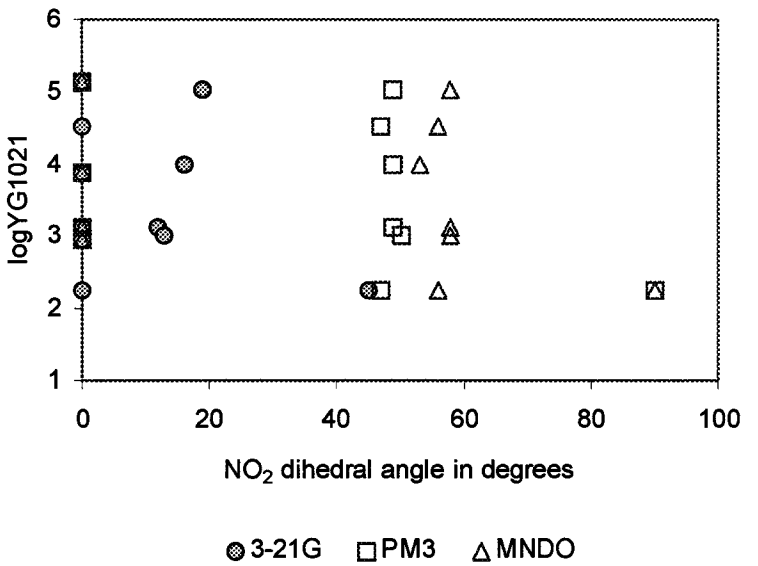

Figure 22. YG1021 mutagenicities versus NO_2 dihedral angles relative to plane of aromatic ring obtained from semi-empirical and *ab initio* calculations.

large changes in predicted mutagenicity for small changes in ε_{LUMO} values, make this parameter's use as a quantitative determinant of mutagenic potency suspect. Lopez de Compadre *et al* comment that the current predictions of nitroarene mutagenicity by SARs should be used with caution since 3-fold differences in activity fall within their standard deviations [**34**]. It was observed that the modest correlation did not improve with the linear regression analysis of the log TA98 versus ε_{LUMO} values for the 66 compounds used in the SAR investigation of Lopez de Compadre *et al* [**34**].

It has been suggested that the dihedral angle of the NO_2 group relative to the aromatic ring plane is an indication of mutagenic potency [**37, 38, 115**], however dipole moments and NO_2 dihedral angles showed little relationship to the mutagenicities observed (Figure 22).

The importance of the hydrophobic effect in biochemical processes has been addressed little in the study of the mutagenicity and carcinogenicity of organic compounds, and this omission has been suggested to be the cause of the mediocre predictive abilities of current SAR investigations [34, 35]. The hydrophobicity of nitroarenes in aqueous media is a measure of loss of entropy rather than gain in enthalpy for the system [30], and is the only entropic factor considered in the assessment of possible indices of mutagenic potency. This parameter has showed correlations with the carcinogenicity of PAH [30], however in this study, the log P values for the nitroarenes showed no correlation with the observed mutagenic potency in YG1021. Specifically, the nitrofluoranthenes and nitropyrenes had equal log P values (see Table 6), even though their mutagenicities ranged over three orders of magnitude.

2.3.2. Relative Rates of Metabolism and Structure-Activity Relationships

Relative rates of metabolism were calculated assuming a first order reaction. By neglecting the 8-nitrofluoranthene point that was considered to be questionable, a good correlation with mutagenic potency was shown in Figure 24 (r^2=0.98, slope=2.72 $\pm$ 0.43, 95% confidence). A fair correlation was found between ε_{LUMO} and relative rate of metabolism with r^2=0.78 and a reasonable error in slope (-1.15 $\pm$ 0.28, 95% confidence) (Figure 25). This suggests that the ε_{LUMO} values of the nitroarenes are not independent of the rates of metabolism observed; these values may have a minor influence on the mutagenic potencies observed in *Salmonella typhimurium* because of this direct relationship to rates of nitroarene metabolism. As shown in Figure 23, larger relative rates of reductive metabolism for the 247 Da molecular weight nitroarene isomers tend to correspond to higher mutagenic potencies in YG1021.

One of the deficiencies of this investigation was that the relative rates of metabolism

over the full range of nitroarene mutagenicities were not determined. Relative rates of metabolism were determined for the 6 nitroarenes possessing higher mutagenic potencies, and the mutagenicity of the most mutagenic compound (8-NFA) had a potency 20 times higher than that of the least mutagenic (1-NP). However, the work completed for this limited set of compounds suggests that there is a good relationship between nitroarene mutagenicity and relative reductive rate of metabolism, and that this correlation is better than any other physicochemical parameter investigated to date as a possible index of mutagenic potency. The compounds 3-nitrofluoranthene and 3-nitrobenzathrone both appear to be more rapidly metabolized than the nitroarenes of lower mutagenicity, 2-nitropyrene, 1-nitropyrene and 2-nitrofluoranthene. These results support the hypothesis that events that occur after nitroarene loss by metabolism, namely the properties of nitroarene metabolites and the interaction of these intermediates with the DNA targets within *Salmonella typhimurium,* may be the primary determinants of mutagenic potency.

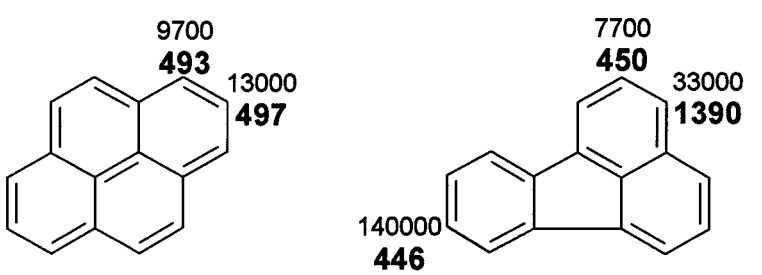

Figure 23. Comparative YG1021 mutagenicites and relative rates of metabolism of nitropyrenes and nitrofluoranthenes.

Top numbers represent the mutagenic potencies of nitroarene isomers in units of revertants per nanomole. Numbers in bold represent the rates of metabolism of nitroarene isomers at 25^{o}C in units of picomoles per hour per mL YG1021 culture.

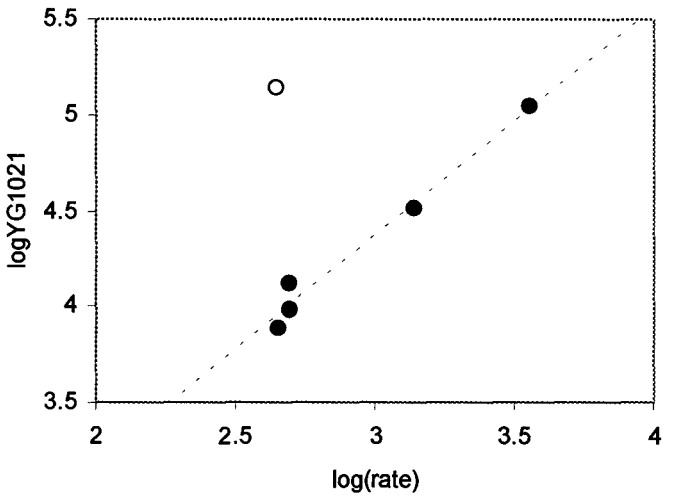

Figure 24. Relative rates of metabolism versus YG1021 mutagenicities.

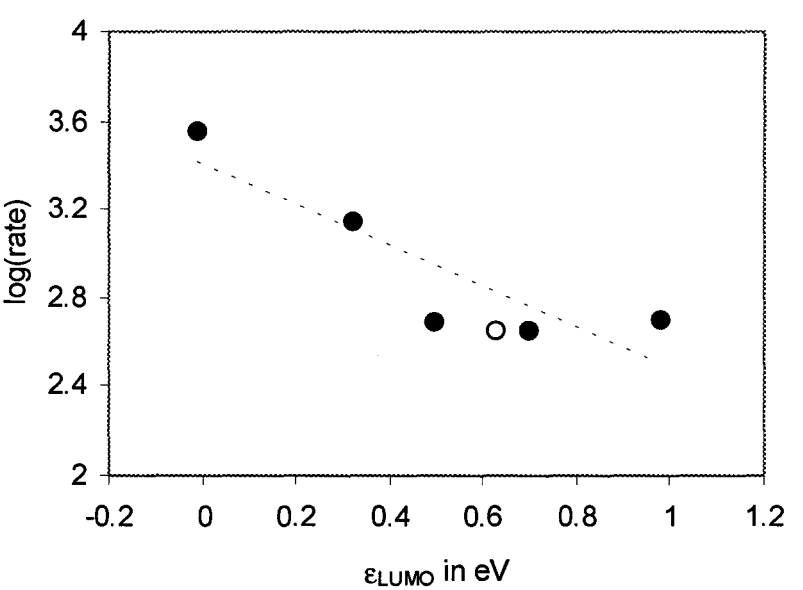

Figure 25. Relative rates of metabolism versus ε_{LUMO} (HF/3-21G).

3. EXPERIMENTAL

3.1. Apparatus and Materials

3.1.1. Gases, Solvents and Chemicals

High purity helium was purchased from Praxair Products Inc. (Mississauga, ON). HPLC grade hexane and nitrobenzene were obtained from BDH Inc. (Toronto, ON). Anhydrous diethyl ether was obtained from Fisher Scientific (Fairlawn, NJ, USA). Distilled in glass grades of acetonitrile, dichloromethane (DCM), methanol, toluene and acetone were obtained from Caledon Laboratories Inc. (Georgetown, ON). PCA grade toluene was purchased from Aldrich Chemicals (St. Louis, MO, USA). Distilled water was purified further for use in HPLC analysis by a Milli-Q Water Purification System (Waters Associates, Milford, MA, USA).

$NaHCO_3$, $Na_2S{\cdot}9H_2O$, concentrated H_2SO_4 and $NaNO_2$ were obtained from BDH Inc. (Toronto, ON). Fuming HNO_3, glacial acetic acid (AcOH), and NaN_3 were purchased from Fisher Scientific (Fairlawn, NJ, USA). KBr and technical grade benzanthrone were obtained from Aldrich Chemicals (St. Louis, MO, USA). $MgSO_4$ and sodium acetate were obtained from Caledon Laboratories, Inc. (Georgetown, ON).

Chrysene and perylene were obtained from Aldrich Chemicals (St. Louis, MO, USA). The compounds 2-nitropyrene, 2-nitrofluoranthene and 3-nitrofluoranthene were obtained from ChemSyn Laboratories (Harrisonville, MO, USA). The compounds 1-nitropyrene, 2-nitrofluorene (Aldrich Chemicals, St. Louis, MO, USA) and 9-nitroanthracene (ICN Pharmaceuticals Inc., Aurora, OH, USA) were recrystallized prior to use. All other nitroarenes were a kind gift from Dr.

M.L. Lee (Brigham-Young University, Provo, UT, USA) and used as received. All PAH and nitroarene standards were shown to be >99% pure by gas chromatographic-mass spectrometric analyses.

3.1.2. General Methods

Melting points were obtained using a Thomas Hoover Uni-Melt capillary melting point apparatus (Arthur H. Thomas Company, Philadelphia, PA, USA) and are uncorrected. Infrared (IR) spectra were recorded on a Bio-Rad FTS-40 FT-IR spectrophotometer and processed using WinIR v. 4.14 software (Bio-Rad Laboratories, Inc., Cambridge, MA, USA). All compounds were prepared for IR analysis as KBr pellets, and all absorption peaks are reported as wavenumbers (cm^{-1}). Ultraviolet (UV) spectra were recorded on a model 8451Hewlett-Packard Diode Array UV spectrophotometer (Hewlett-Packard Co., Mississauga, ON).

3.1.3. Mass Spectrometry and Nuclear Magnetic Resonance

Samples submitted for electron impact (EI) and chemical ionization (CI) mass spectral analyses were analyzed using a Finnigan 4500 mass spectrometer. Details of the experimental conditions are listed in Table 11.

All ^{1}H nuclear magnetic resonance (NMR) spectra were acquired on the Brüker AC-300 spectrometer at 300MHz using a 5mm multiple frequency ^{1}H-^{13}C probe (Brüker Instruments, Milton, ON) at 25°C. Samples were prepared by dissolving each compound in $CDCl_3$ (Cambridge Isotope Labs, Burlington, ON) and followed by filtering through glass wool. Free induction decays (FIDs) were obtained in 64 scans in 16K data points over a 3600Hz spectral width, and were

zero-filled to 32K prior to Fourier transformation. Spectra were processed using exponential multiplication (LB = 0.2 or 0.3 Hz) and in some cases Gaussian multiplication (GB = 0.2 or 0.3 Hz). The chemical shifts (δ) are reported in parts per million (ppm) using the deuterated solvent signal at δ 7.25 (singlet) as a reference. Proton assignments were deduced from chemical shifts and coupling constants derived from ^{1}H-NMR spectra.

Operating Parameter	Setting
Electron Energy	70eV
Emission	100μA
Source Temperature	200°C
Probe Temperature Programming	initial: 30°C rate: 4°C/s final: 300°C
Acceleration Voltage	6 kV
Source Pressure	10^{-6} torr
Resolution (10% valley definition)	1000

Table 11. Experimental conditions used for desorption electron impact mass spectrometry.

3.1.4. Chromatographic Analysis

Silica gel (Baker-Flex, 1B2-F) and neutral alumina (F254-60, Type E) thin layer chromatography sheets were obtained from J.T. Baker Chemicals (Phillipsburg, NJ, USA). Neutral adsorption alumina (grade A540, 80-200 mesh; Fisher Scientific, Fairlawn, NJ, USA) and silica gel (100-200 mesh; Anachemia Science, Montréal, PQ) were used for flash column chromatography.

A Hewlett-Packard Model 1090 Liquid Chromatograph equipped with a diode array detector was used for reversed-phase high-pressure liquid chromatography (HPLC) and analyses were processed using the ChemStation software package (Hewlett-Packard Co., Mississauga, ON). Solvents were degassed using helium gas. Separations were accomplished using a 5μm Vydac 201TP54 reversed phase analytical column (25 cm x 4.6 mm i.d.; Separations Group, Hesperia, CA, USA) and a C_{18} pre-column (1.5cm x 3.2mm i.d.; Chromatographic Specialties, Burlington, ON) with a 20μL injection loop. Column temperature was maintained at 40°C and a mobile phase flow rate of 1.0mL/min was used with the following gradient (elapsed time, mobile phase composition): initial, 60% acetonitrile, 40% water; 10 min., 80% acetonitrile, 20% water; 12 min., 100% acetonitrile; 15 min., 100% acetonitrile; 17 min., 60% acetonitrile, 40% water; 22 min., 60% acetonitrile, 40% water.

GC-MS experiments were performed on a Hewlett-Packard Model 5890 Series II gas chromatograph with electronic pressure control and interfaced to a Hewlett-Packard Model 5971A mass selective detector (Hewlett Packard Co., Mississauga, ON). Analyses were processed using the MS ChemStation v.C.02.00 software package (Hewlett-Packard Co., Mississauga, ON). Splitless on-column sample injections were made using a Hewlett-Packard Model 7673A Automatic Injector onto a DB-17ht column (30m x 0.25mm i.d., 0.15μm film thickness; J & W

Scientific, Folson, CA, USA) that was coupled to a retention gap (fused silica tubing, 0.53mm i.d.; J & W Scientific, Folson, CA, USA).

3.2. Syntheses of Benzanthrone Derivatives

Benzanthrone derivatives were handled under yellow light conditions and were characterized by melting point, nuclear magnetic resonance, low resolution mass spectrometry, HPLC and GC-MS (see Figure 26). NMR multiplicities are reported as follows: s=singlet, d=doublet, dd=doublet of doublets, dt=doublet of triplets, br=broad peak. Benzanthrone was purified by gravity filtration of a DCM mixture of technical grade benzanthrone followed by elution of the filtrate through a silica gel column. Recrystallization from glacial acetic acid yielded pure benzanthrone (mp = 171-172^{o}C) that was shown to be >99% pure by GC-MS analysis.

3.2.1. 3-Nitrobenzanthrone

Benzanthrone was nitrated according to the procedure of Shioda and Kato **[126]**. Benzanthrone (8.01g, 34.8mmol) was placed in a 250mL round bottom flask in a 50^{o}C water bath, and a total of 80mL nitrobenzene was added with stirring until the crystals dissolved. To this yellow solution, fuming HNO_3 (16.05g, 12.1mL) was added dropwise producing a red-coloured solution and a red-brown gas (NO_2). After 90 minutes, a yellow solid began to separate from solution. After 3 hours, the reaction mixture was allowed to cool and the product was collected by vacuum filtration on a medium-fritted glass filter funnel. The filter cake was rinsed three times with 5% $NaHCO_3$ solution followed by two rinses with cold diethyl ether. Drying under vacuum afforded 8.31g of a crude yellow product. Recrystallization from methanol gave 3-nitrobenzanthrone as a fluffy yellow solid (8.22g, 29.9mmol, 86% yield; 60% lit yield **[126]**).

The product 3-nitrobenzanthrone showed:

mp = 248.5-249°C (lit. mp = 252°C [**126**]).

R_f (60% DCM/hexane, silica) = 0.26 (R_f benzanthrone = 0.59).

t_R (HPLC) = 6.65min.

^{1}H NMR (300MHz, $CDCl_3$, δ): 7.667 (H9, dt), 7.819 (H10, dt), 7.994 (H5, dd), 8.363 (H11, d), 8.398 (H1, d), 8.505 (H2, d), 8.513 (H8, dd), 8.845 (H4, dd), 8.945 (H6, dd).

MS [EI] (RI%) found: 275 [M] (100%), 245 [M-NO] (43%), 229 [M-NO_2] (15%), 217 [M-CNO_2] (51%).

IR (υ, KBr, cm^{-1}): 1666, 1516, 1334.

UV (λ_{max}, DCM, nm): 390, 410.

3.2.2. 3-Aminobenzanthrone

The reduction of 3-nitrobenzanthrone was adapted from the method Shioda and Kato [**126**]. A sample of 3-nitrobenzanthrone (7.77g, 28.3mmol) was added to a 250mL round bottom flask containing 13%w/w Na_2S aqueous solution (97.54g) under N_2 atmosphere. After 2 minutes, the mixture turned blue-black in colour. After stirring at room temperature for 30 minutes, the reaction mixture was slowly heated and allowed to reflux for 1 hour. The deep red-coloured mixture was vacuum filtered hot through a fine-fritted glass filter funnel and the product was rinsed three times with hot water and left to air-dry overnight. The filtrate product was recrystallized from toluene to afford 3-aminobenzanthrone as a maroon-coloured powder (5.40g, 22.0mmol, 78% yield; 86% lit. yield [**126**]).

The product 3-aminobenzanthrone showed:

mp = 243-244°C (lit. mp = 246°C [**126**]).

R_f (60% DCM/hexane, alumina) = 0.14 (R_f 3-nitrobenzanthrone = 0.65).

t_R (HPLC) = 4.17min.

^{1}H NMR (300MHz, $CDCl_3$, δ): 4.626 (amine H, br), 6.912 (H2, d), 7.435 (H10, dt), 7.681 (H9, dt), 7.750 (H5, dd), 8.213 (H11, dd), 8.237 (H4, dd), 8.283 (H1, d), 8.471 (H6, dd), 8.830 (H8, dd),

MS [EI] (RI%) found: 245 [M] (100%), 217 [M-CO] (13%), 189 [M-CO-C_2H_2] (18%).

IR (υ, KBr, cm^{-1}): 3454, 3318, 3229, 1637, 1572, 1465, 1314.

UV (λ_{max}, DCM, nm): 505.

3.2.3. 3-Azidobenzanthrone

The diazotization of 3-aminobenzanthrone was adapted from the method Shioda and Kato [**126**]. A sample of 3-aminobenzanthrone (1.96g, 8.01mmol) was added to a 50mL round bottom flask containing concentrated H_2SO_4 (19.6g, 10.7mL). $NaNO_2$ (613mg, 8.79mmol) was added with stirring to the dark red reaction mixture. After 2 minutes, the reaction mixture was poured into a 250mL round bottom flask containing ice (80g) in water (80mL) to yield a light brown frothy mixture. TLC plates showed that the starting material was consumed after 36 minutes. After 55 minutes, sodium acetate (4.02g, 49.0mmol) was added in order to facilitate separation of the diazonium salt from solution. After stirring for 5 minutes, the product was vacuum filtered on a medium-fritted glass filter funnel. The diazonium salt product was then added to NaN_3 solution (80mL, 8.46mM) in a 250mL round bottom flask under N_2 atmosphere to produce a blue-black mixture. After stirring in an ice bath for two hours, the reaction mixture was vacuum filtered on a medium fritted glass filter funnel and rinsed three times with a total of 20mL chilled 3:1 diethyl ether/methanol to yield a yellow-brown crude product. The crude product was chromatographed on alumina (4cm i.d. x 5cm) with initial column washes of 10% and 20% DCM/hexane. Fractions eluted with 50% DCM/hexane and 100% DCM were dried under vacuum

to afford the novel compound 3-azidobenzanthrone as a bright yellow solid (448 mg, 1.65 mmol, 21% yield).

The product 3-azidobenzanthrone showed:

R_f (60% DCM/hexane, alumina) = 0.60 (R_f 3-aminobenzanthrone = 0.11).

^{1}H NMR (300MHz, $CDCl_3$, δ): 7.414 (H11, d), 7.534 (H9, s), 7.735 (H10, dt), 7.793 (H5, dd), 8.267 (H1, d), 8.411 (H2, d), 8.484 (H8, dd), 8.510 (H4, dd), 8.798 (H6, dd).

MS [EI] (RI%) found: 271 [M] (12%), 243 [M-N_2] (100%), 215 [M-N_2-CO] (32%), 214 [M-N_2-HCO] (73%)

HRMS (EI) found exact mass = 271.0757 g/mol (Resolution (10% valley definition) = 40 000)

calculated mass ($C_{17}H_9N_3$) = 271.0746 g/mol (-0.0011 g/mol)

UV (λ_{max}, DCM, nm): 390, 410.

The product 3-azidobenzanthrone was submitted to the W. Leigh group for preliminary laser flash photolysis experiments. The long-lived carbonyl triplet that obscured the nitrene signal was found to be quenched by hexatriene in acetonitrile solution to afford observation of the nitrene species.

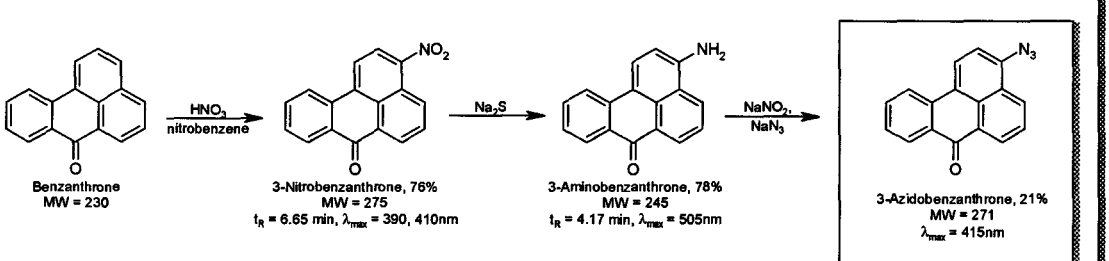

Figure 26. Synthesized derivatives of benzanthrone.

3.3. Molecular Modelling

3.3.1. Semi-Empirical Calculations

MNDO and PM3 calculations were performed using version 5.01 of HyperChem for Windows 95 and NT program (Hypercube, Inc., Gainesville, FL, USA) on a 133 MHz personal computer equipped with 16 Mb RAM. Molecular dynamics calculations using MM+ and a 0.1 RMS level of iterative convergence were used to pre-minimize the geometric structures of the nitroarenes. Nitroarene structures were then optimized with both MNDO and PM3 at 0.001 RMS levels of iterative convergence. All nitroarenes generated energy-minimized structures with the ring plane coplanar with the nitro groups. In the cases of compounds with *peri*-hydrogens, another calculation was performed where one of the NO bond dihedral angles was set to 48° and 90° (in the case of 9-NA only). The molecular indices examined in this study included ε_{LUMO}, ε_{HOMO}, and $\Delta\varepsilon$ (ε_{LUMO}-ε_{HOMO}), which were expressed in electron volts (eV), C-N torsion angles, N-C-C and O-N-O bond angles, which were expressed in degrees, C-N bond lengths, which were expressed in angstroms (Å), and atomic charge on the nitrogen and *ortho*-carbon. Vibrational frequencies were determined in order to ascertain whether the geometry-optimized structures were minima or transition states. Molecular orbital energy values were compared to those reported by Lopez de Compadre *et al* [**34**].

3.3.2. *Ab Initio* Calculations

Ab initio calculations using the HF/3-21G basis set was performed using version 5.0 of the Spartan program for UNIX (Wavefunction, Inc., Irvine, CA, USA) on a 250 MHz Octane workstation equipped with 2 Gb Synchronous DRAM (Silicon Graphics, Inc., Mountain View, CA,

USA). The semi-empirical method PM3 was used for geometry optimization prior to single point energy calculations using the 3-21G basis set. Geometry optimizations of the nitroarenes were then completed at the HF/3-21G level with no restrictions placed on nitro group dihedral angles. The molecular indices examined in this study included ε_{LUMO}, ε_{HOMO}, and $\Delta\varepsilon$ (ε_{LUMO}-ε_{HOMO}), which were expressed in atomic units (au), C-N torsion angles, N-C-C and O-N-O bond angles, which were expressed in degrees, C-N bond lengths, which were expressed in angstroms (Å), electrostatic potentials and hydrophobicity (log P). Vibrational frequencies were calculated to determine whether minimized structures were minima or transition states. Single point calculations at the HF/3-21G level on 3-21G geometry-optimized nitroarene structures were completed to determine electrostatic potential surfaces.

3.4. Ames Reversion Assay

3.4.1. Solutions and Media

The procedures are the methods reported by Maron and Ames [23]. All solutions were made using water purified by a Milli-Q Water Purification System (Waters Associates, Milford, MA, USA), and were reduced in total volume. All solutions and media, with the exception of the antibiotic solutions, were sterilized using an Amsco 2021 Gravity Sterilizer (Eagle Series, Canadian Sterilizer Corp., London, ON) for 30 minutes at 121°C after preparation. Empty glass bottles and flasks, lids and pipet tips were sterilized for 30 minutes at 121°C, followed by 20 minutes drying time.

Oxoid Nutrient Broth #2 (Oxoid Ltd., Basingstoke, UK) was prepared according to stock bottle directions. Top agar was made using granulated agar and NaCl (Caledon Laboratories Ltd., Georgetown, ON). Minimal glucose agar plates were made using granulated agar (Becton

Dickinson and Company, Cockeysville, MD, USA), 40% aqueous glucose (assurance grade, BDH Inc., Toronto, ON) solution, and Vogel-Bonner medium E (50X) – an aqueous solution containing $MgSO_4 \cdot 7H_2O$, anhydrous K_2HPO_4, sodium ammonium phosphate (Sigma Chemical Co., St. Louis, MO, USA) and citric acid monohydrate (BDH Inc., Toronto, ON).

An aqueous solution of tetracycline (Sigma Chemical Co., St. Louis, MO, USA) was prepared by dissolving 48.25 mg of the solid in 51mL H_2O. The aqueous mixture was then filter sterilized using an Acrodisc (0.22μm; Pall Gelman Sciences, Mississauga, ON) into a foil-covered, autoclaved Gibco bottle. Solutions of ampicillin (BDH Inc., Toronto, ON) and L-histidine (HCl-monohydrate; BDH Inc., Toronto, ON)/D-biotin (Sigma Chemical Co., St. Louis, MO) were prepared according to recipe **[23]**; 10.50mg of the L-histidine HCl monohydrate was used to created a 100mL aqueous solution containing the correct amount of L-histidine. Tetracycline and ampicillin solutions were stored at $4^{\circ}C$ until used.

Eppendorf varipette tips, pipetors and the combitip used for DMSO autopipetting (Brinkman Instruments, Inc., Westburg, NY, USA) and syringes (Hamilton Co., Reno, NV, USA) were used for the delivery of sub-millilitre volumes. Liquid volumes in excess of 1mL were delivered by disposable serological pipets (borosilicate glass, Corning Glass Works, Corning, NY, USA) using a vacuum pump (Hartz Mountain Pet Supplies Inc., London, ON).

All reversion assays were completed under aseptic conditions in a Biological Hood Class II (Certified by manufacturer, Canadian Cabinets Co. Ltd., Ottawa, ON). The top agar plated in the reversion assay was mixed using a Vortex-Genie (Scientific Industries, Inc., Bohemia, NY, USA) and the plates were developed in a Dry Type Bacteriological Incubator (gravity convection, GS Blue Electric, Blue Island, IL, USA). After 72 hours of incubation, revertants were hand-

counted. Dose-response plots and linear regression analyses were performed using the Microsoft Excel 97 spreadsheet program (Microsoft Corporation, Redmond, WA, USA).

3.4.2. Reversion Assay Methodology

The 1,8-DNP standard and nitroarene sample solutions were prepared by dissolving solid samples in DMSO, and made up to final concentrations ranging from 0.011 to 17μM by serial dilution. These final concentrations were based on previously reported YG1021 mutagenicities **[17, 18]** and were selected to ensure that the top dose would not give a revertant count larger than 3000, which would exceed the linear response range of the Ames reversion assay method.

On the day prior to the reversion assay, the minimal glucose agar plates were labelled and placed agar-surface down in a dry-type incubator to allow the plates and the incubator to equilibrate at 37°C. Culture medium used to grow the YG1021 culture was prepared by placing aliquots of ampicillin (75μL, 50mg/mL) and tetracycline (100μL, 6.25μg/mL) solutions into a 100mL aluminum foil-wrapped Gibco bottle with an Eppendorf pipet. Oxoid nutrient broth #2 (15mL) was then placed into the bottle. *S. typhimurium* YG1021 stock, previously prepared by J. Villella according to the reported procedure **[23]** and stored at –70°C, was used to innoculate the nutrient broth. The capped and foil-wrapped bottle was placed into a 37°C water bath for a 10-hour growth period with agitation.

The final dilutions of the DMSO solutions of the positive standard 1,8-DNP and the nitroarene samples were aliquoted in duplicate into test tubes at the time of the reversion assay. The volumes of 10, 20, 30, 40 and 50μL of these solutions were placed in each test tube, with

additional aliquots of DMSO added to give a total constant volume of 50μL in each test tube. Two aliquots of 50μL DMSO were placed into separate test tubes to serve as negative controls. The reversion assay of these latter two test tubes indicated the number of spontaneous reversions occurring during the reversion assay.

To each test tube containing a 50μL sample aliquot, 2mL of melted top agar at 45°C was added by glass pipet using a vacuum pump. The tubes were placed into a 45°C water bath to maintain the agar's liquid state prior to the addition of bacterial culture and plating. A 100μL aliquot of fresh YG1021 culture medium was added sequentially to each test tube by Eppendorf pipet. Each test tube was then mixed for 2 seconds with a vortex mixer and the solution was poured onto the surface of the labelled minimal glucose agar plate and evenly distributed. The agar plates were placed into the dry-type incubator, agar surface-up, in stacks of 3 to 5, until set. After about 3 hours, the plates were flipped agar surface-down to prevent condensation from dripping onto the agar surface, and then the bacteria were incubated for a total of 72 hours at 37°C. At the end of this incubation period, the plates were removed sequentially according to the order of plating and the revertant colonies were hand counted (see Figure 27).

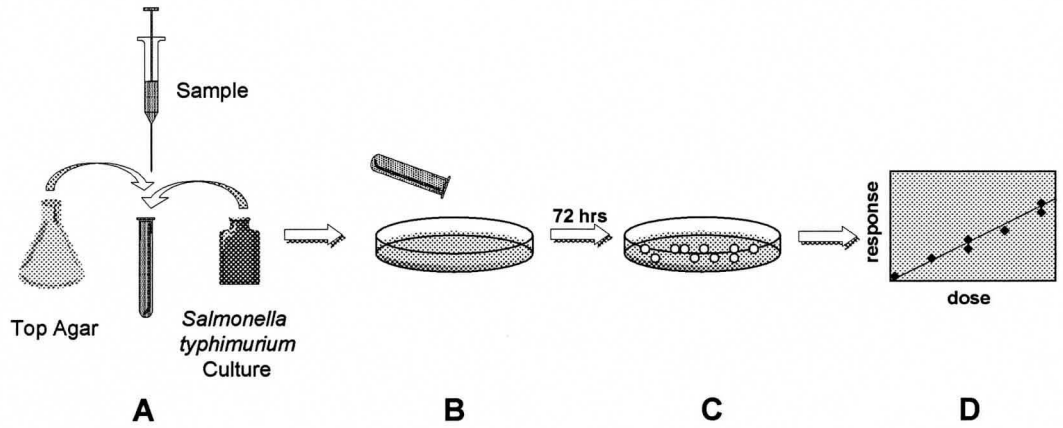

Figure 27. Ames reversion assay methodology. Modified from [23].
A: Sample dose contained in 50μL DMSO is mixed with 2mL melted top agar and 100μL YG1021 bacterial culture. *B:* Mixture distributed onto minimal glucose agar and incubated at 37°C for 72 hours. *C*: Revertant colonies are counted. *D*: Sample mutagenicity is determined from linear dose response.

3.5. Relative Rates of Nitroarene Metabolism

3.5.1. Nitroarene Metabolism in *Salmonella typhimurium* YG1021

The nitroarene sample solutions were prepared by dissolving solid samples into toluene, and made to a final concentration of 45μM by serial dilution. This final concentration was selected based on the mutagenicities determined in this study, to ensure that the *Salmonella* were provided with a nitroarene dose lower than that which would induce toxicity effects in the Ames reversion assay.

Overnight cultures of *Salmonella typhimurium* strain YG1021 (1 to 2 x 10^9 organisms/mL, 2 mL) in Oxoid no. 2 broth (25g/L, Oxoid Inc., Bassingstoke, UK) were incubated with 45μL of unlabelled nitroarene in DMSO solution in a test tube at 25°C. Separate reactions

were stopped at various times by the addition of 3 mL of 2:1 ethyl acetate/acetone and extracted with a further 2 x 2mL of the same solvent. The organic phases were evaporated to dryness under N_2 stream.

3.5.2. Sample Preparation and Analysis

Dried extracts were re-suspended in DCM (200μL) to which hexane (5mL) was added to yield a sample with an organic solvent strength of approximately 4% DCM/hexane. The mixture was run through a neutral alumina SepPak Lite SPE cartridge (Waters Associates, Burlington, ON) that had first been washed with DCM and conditioned in 100% hexane. The SPE cartridge was washed with hexane (3mL) and the collected solvent was discarded. The cartridge was then eluted with DCM (5mL). The eluent was taken to near dryness by N_2 stream then transferred to GC analysis tube insert. After the sample was taken to dryness by N_2 stream, an internal standard containing chrysene and perylene in toluene (10μL, 20mM) was added to the sample and the residue was allowed to dissolve. The GC tube was then capped for GC-MS analysis via injection by the automatic injector.

Nitropyrene and nitrofluoranthene incubation extracts were analyzed using GC-MS method A, and 3-nitrobenzanthrone incubation extracts were analyzed using GC-MS method B (see Tables 12 and 13). Extraction recoveries were determined by the abundance of 1-nitropyrene-d_9 contained in the sample. The peak areas of the 1-nitropyrene-d_9, PAH and nitroarenes in periodically chromatographed standards were used to determine response factors for the GC-MS analyses. These response factors were used in the quantitation of extracted nitroarenes using chrysene and perylene.

	Method A	Method B
Flow velocity	36 cm/s	36 cm/s
Solvent Delay	5.0 min	5.0 min
Injection Volume	1 μL	2 μL
Oven Temperature Program	initial temp. 80°C 80-220°C at 20°C/min 220-300°C at 5°C/min	initial temp. 80°C 80-220°C at 25°C/min 220-300°C at 5°C/min
Total Run Time	23.0 min	21.6 min

Table 12. Protocols for GC-MS analysis methods A and B.

SIM Ion Group (Method A)	Time (min)	Ions Monitored (m/z)	Ion Dwell Time (ms)
1	5.0 - 23.0	189, 198, 200, 201, 208, 210, 217, 226, 228, 247, 250, 252, 256, 259	21

SIM Ion Group (Method B)	Time (min)	Ions Monitored (m/z)	Ion Dwell Time (ms)
1	5.0 - 15.5	198, 208, 210, 226, 228, 256	67
2	15.5 - 21.6	189, 200, 201, 217, 229, 245, 250, 252, 275, 287	35

Table 13. Ion groupings used in selected ion monitoring program for methods A and B.

4. CONCLUSIONS AND FUTURE WORK

The results of this work cast serious doubts on the reported correlations between nitroarene structural and calculated parameters, and the mutagenic potencies of those nitroarenes in the Ames reversion assay. The factors previously claimed to be major determinants of nitroarene mutagenicity, specifically log P **[34, 117]**, ε_{LUMO} **[34, 40, 117]** and $E_{½}$ **[44, 125]**, have shown very poor correlations with Ames mutagenicities in this study; the use of these parameters as predictors of the mutagenic potency of nitroarenes is questionable.

HF/3-21G *ab initio* geometry and energy optimizations were performed for 13 nitroarenes, and this study is the first to report the use of this level of calculations to investigate this class of compounds. These *ab initio* calculations gave higher quality calculation results than the semi-empirical methods (PM3 and MNDO) reported previously **[34, 40, 117]**. These *ab initio* calculations also showed similar trends in molecular orbital energies compared to semi-empirical calculations. The lack of correlation between the physicochemical quantities calculated in this study, and the nitroarene mutagenicities observed, challenges the broadly accepted hypotheses that ε_{LUMO} values and NO_2 group dihedral angles are useful predictors of mutagenic potencies.

The results of these *ab initio* calculations were shown to have some application to nitroarene metabolism by nitroreductase. Electrostatic potential surface maps of thirteen nitroarenes were prepared and examined for any correlation to enzymatic rate or mutagenic potency. It is suggested that the binding pocket or cleft in the enzyme must possess two electropositive regions in order to accommodate the electronegative surfaces of many of the

nitroarene substrates. The electronegative surfaces were associated with the nitro group itself and with a portion of the π system of the aromatic framework.

The relative rates of reductive metabolism were determined for 6 nitroarenes and showed a good correlation with nitroarene mutagenicities. This relationship should be further investigated with a larger set of compounds. In addition, these rates of metabolism showed a fair relationship with ε_{LUMO} values of the nitroarenes, suggesting that this physicochemical parameter is indirectly related to nitroarene mutagenicity.

The results of this work raise serious questions about the indices used in previous structure activity investigations of nitroarene mutagenicity. It is probably more relevant to consider the physical and calculated characteristics of key metabolites and reactive intermediates, such as the *N*-hydroxylarylamines and arylnitrenium ions, which are more proximate chemically to the genotoxic event than are nitroarenes (see Figure 28). Although nitrenium ion energies have been investigated at the AM1 semi-empirical level [**125**], the results of this work indicate that a relatively high level of calculation needs to be performed before drawing important conclusions. *Ab initio* calculations could be used to investigate nitrenium ion and *N*-hydroxylarylamines heats of formation and other physicochemical properties. The experimental determination of nitrene lifetimes by laser flash photolysis [**111, 112**] would also contribute to these investigations.

The GC-MS method was developed and was used to determine the amount of nitroarenes in metabolism experiments using *Salmonella typhimurium* strain YG1021. The method showed good extraction recoveries. Further method development, specifically the use of PAH as recovery standards, needs to be investigated. The sensitivity and chromatographic power of the method would facilitate the monitoring of the formation of arylamine and *N*-

acetylarylamines in the incubations, and this method has the potential to be used in rate determinations at low doses and in a myriad of systems, such as *E. coli* and yeast. Furthermore, the determination of relative rates of oxidative metabolism of nitroarenes and PAH may be more relevant to mammalian systems, and may be related to the bioactivation of these and other compounds in humans.

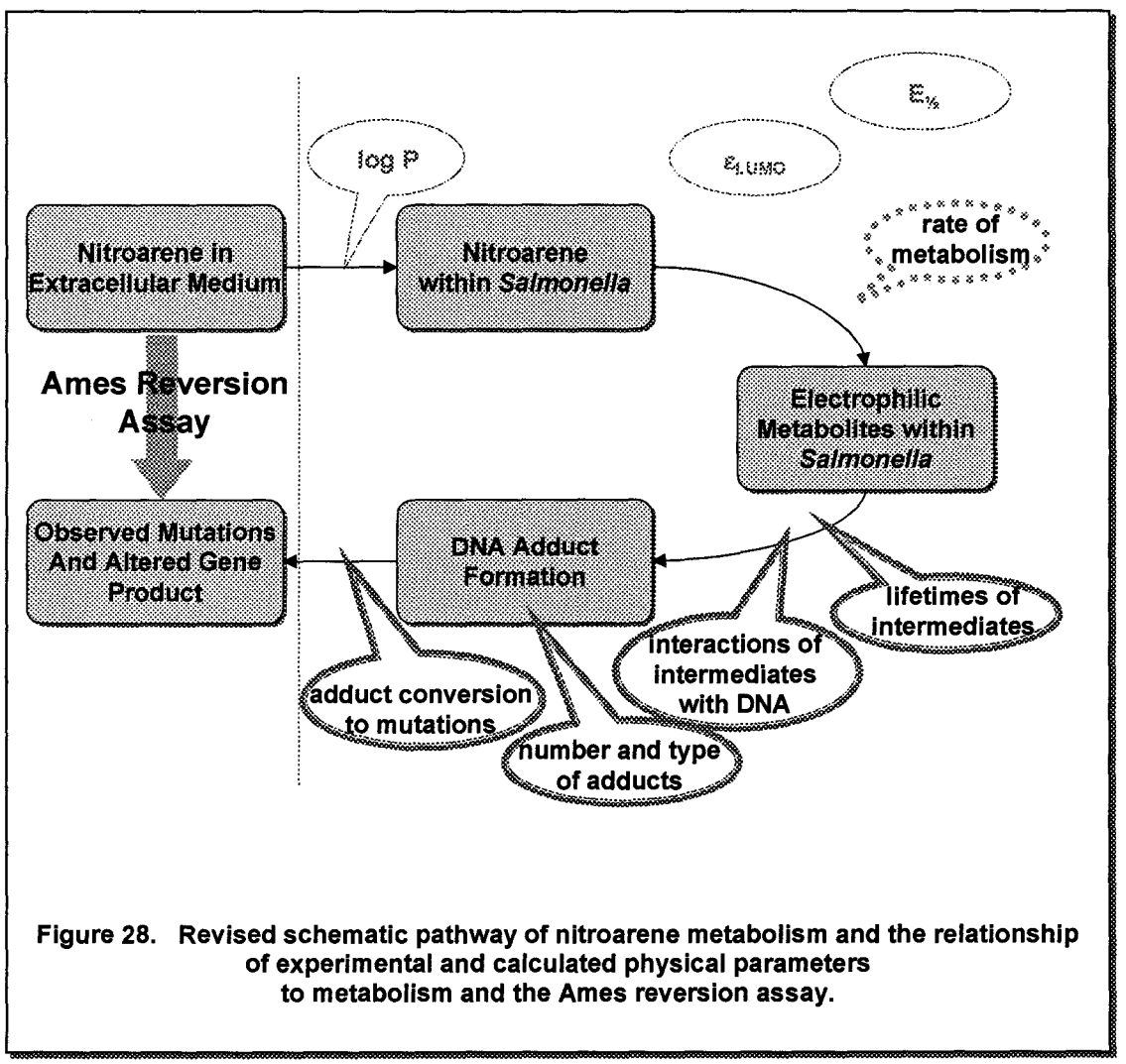

Figure 28. Revised schematic pathway of nitroarene metabolism and the relationship of experimental and calculated physical parameters to metabolism and the Ames reversion assay.

5. REFERENCES

1. Research Triangle Institute, *Toxicological Profile for Polycyclic Aromatic Hydrocarbons*, United States Department of Health and Human Services, Atlanta, 1995.
2. R.G. Harvey, *Polycyclic Aromatic Hydrocarbons: Chemistry and Carcinogenicity*, Cambridge University Press, New York, 1991.
3. K. Naes, J. Knutzen, L. Berglind, Occurance of PAH in marine organisms and sediments from smelter discharge in Norway, *Sci. Tot. Environ.* **163** (1995) 93-106.
4. J. Arey, R. Atkinson, Atmospheric chemistry of gas-phase polycyclic aromatic hydrocarbons: formation of atmospheric mutagens, *Environ. Health Perspect.* **102 (suppl. 4)** (1994) 117-126.
5. S.A. Wise, L.C. Sander, W.E. May, Determination of polycyclic aromatic hydrocarbons by liquid chromatography, *J. Chromatogr.* **642** (1993) 329-349.
6. A.E. Legzdins, B.E. McCarry, D.W. Bryant, Polycyclic Aromatic Compounds in Hamilton Air: Their Mutagenicity, Ambient Concentrations and Relationships with Atmospheric Pollutants, *Polycycl. Aromat. Comp.* **5** (1994) 157-165.
7. C.H. Marvin, L. Allan, B.E. McCarry, D.W. Bryant, Chemico/Biological Investigation of Contaminated Sediment From the Hamilton Harbour Area of Western Lake Ontario, *Environ. Mol. Mutagen.* **22** (1993) 61-70.
8. H.S. Rosenkranz, P.C. Howard, Structural basis of the activity of nitrated polycyclic aromatic hydrocarbons, in: N. Ishinishi, A. Koizumi, R.O. McClellan, W. Stöber (Eds.), *Carcinogenic and Mutagenic Effects of Diesel Engine Exhaust – Proceedings of the International Symposium on Toxicological Effects of Emissions from Diesel Engines Held in Tsukub Science City, Japan, July 26-28*, Elsevier Science Publishers, New York, 1986, pp. 141-169.

9. M.D. Waters, F.B. Daniel, J. Lewtas, M.M. Moure, S. Nesnow (Eds.), *Genetic Toxicology of Complex Mixtures*, Plenum Press, New York, 1990.

10. A. Albagli, H. Oja, L. Dubois, Size-distribution of polycyclic aromatic hydrocarbons in airborne particles, *Environ. Lett.* **6** (1974) 241-251.

11. J. Cvacka, J. Barek, A.G. Fogg, J.C. Moreira, J. Zima, High-performance liquid chromatography of nitrated polycyclic aromatic hydrocarbons, *Analyst* **123** (1998) 9R-18R.

12. K.M. Nauss, The HEI Diesel Working Group, Critical Issues in Assessing the Carcinogenicity of Diesel Exhaust: A Synthesis of Current Knowledge, in: *Diesel Exhaust: A Critical Analysis of Emissions, Exposure, and Health Effects*, Health Effects Institute, Cambridge, 1986, pp. 11-61.

13. R. Mermelstein, E.C. McCoy, H.S. Rosenkranz, The Mutagenic Properties of Nitroarenes: Structure Activity Relationships, in: P.C. Howard, S.S. Hecht, F.A. Beland (Eds.), *Nitroarenes: Occurance, Metabolism and Biological Impact*, Plenum Press, New York, 1990, pp. 205-230.

14. D. Schuetzle, T. Jensen, Analysis of Nitrated Polycyclic Aromatic Hydrocarbons (NitroPAH) by Mass Spectrometry, in: C.M. White (Ed.), *Nitrated Polycyclic Aromatic Hydrocarbons – Chromatographic Methods*, Dr. Alfred Hüthig Verlag, Heidelberg, 1985, pp. 121-168.

15. C.M. White, Analysis of Nitrated Polycyclic Aromatic Hydrocarbons by Gas Chromatography, in: C.M. White (Ed.), *Nitrated Polycyclic Aromatic Hydrocarbons – Chromatographic Methods*, Dr. Alfred Hüthig Verlag, Heidelberg, 1985, pp. 1-86.

16. H.S. Rosenkranz, Mutagenic and carcinogenic nitroarenes in diesel emissions: risk identification, *Mutat. Res.* **140** (1984) 1-6.

17. A.E. Legzdins, *Chemical and Biological Characterizations of Southern Ontario Urban Air Particulate*, Ph.D. Dissertation, McMaster University, Hamilton, 1996.

18. T. Enya, H. Suzuki, T. Watanabe, T. Hirayama, Y. Hisamatsu, 3-Nitrobenzanthrone, a Powerful Bacterial Mutagen and Suspected Human Carcinogen Found in Diesel Exhaust and Airborne Particulates, *Environ. Sci. Technol.* **31** (1997) 2772-2776.

19. W.F. Busby Jr., H. Smith, C.L. Crespi, B.W. Penman, S.L. Lafleur, Mutagenicity of the atmospheric transformation products 2-nitrofluoranthene and 2-nitrodibenzopyranone in Salmonella and human cell forward mutation assays, *Mutat. Res.* **389** (1997) 261-270.

20. L.M. Ball, L.M. Stocking, M.J. Kohan, S.H. Warren, J. Lewtas, Metabolic activation of the genotoxic environmental contaminants 2- and 3-nitrofluoranthene in variants of *Salmonella typhimurium* TA98, *Mutagenesis* **10** (1995) 497-504.

21. E.C. Miller, J.A. Miller, Mechanisms of chemical carcinogenesis, *Cancer* **47** (1981) 1055-1064.

22. J.T. Isaacs, Determination of the number of events required for mammary carcinogenesis in the Sprague-Dawley female rats, *Cancer Res.* **45** (1985) 4827-4832.

23. D.M. Maron, B.N. Ames, Revised methods for the *Salmonella* mutagenicity test, *Mutat. Res.* **113** (1983) 173-215.

24. P.D. Josephy, P. Gruz, T. Nohmi, Recent advances in the construction of bacterial genotoxicity assays, *Mutat. Res.* **386** (1997) 1-23.

25. P.P. Fu, Metabolism of Nitro-Polycyclic Aromatic Hydrocarbons, *Drug Metab. Rev.* **22** (1990) 209-268.

26. H. Tokiwa, Y. Ohnishi, Mutagenicity and carcinogenicity of nitroarenes and their sources in the environment, *Crit. Rev. Toxicol.* **17** (1986) 23-60.

27. D. Schuetzle, J.A. Frazier, Factors influencing the emission of vapor and particulate phase components from diesel engines, in: N. Ishinishi, A. Koizumi, R.O. McClellan, W. Stöber (Eds.), *Carcinogenic and Mutagenic Effects of Diesel Engine Exhaust – Proceedings of the International Symposium on Toxicological Effects of Emissions from Diesel Engines Held in Tsukub Science City, Japan, July 26-28, 1986*, Elsevier Science Publishers, New York, 1986, pp. 41-64.

28. M.R. Frierson, G. Klopman, H.S. Rosenkranz, Structure-Activity Relationships (SARs) Among Mutagens and Carcinogens: A Review, *Environ. Mutagen.* **8** (1986) 283-327.

29. R. Benigni, C. Andreoli, A. Giuliani, Quantitative structure-activity relationships: principles and applications to mutagenicity and carcinogenicity, *Mutat. Res.* **221** (1989) 197-216.

30. C. Hansch, Structure-activity relationships of chemical mutagens and carcinogens, *Sci. Tot. Environ.* **109/110** (1991) 17-29.

31. W.A. Vance, Y.Y. Wang, H.S. Okamoto, Disubstituted amino-, nitroso-, and nitrofluorenes: A physicochemical basis for structure-activity relationship in *Salmonella typhimurium*, *Environ. Mutagen.* **9** (1987) 123-141.

32. M. Watanabe, M. Ishidate Jr., T. Nohmi, A sensitive method for the detection of mutagenic nitroarenes: construction of nitroreductase-overproducing derivatives of *Salmonella typhimurium* strains TA98 and TA100, *Mutat. Res.* **216** (1989) 211-220.

33. R. Benigni, A. Giuliani, Quantitative structure-activity relationship (QSAR) studies in genetic toxicology: mathematical models and the "biological activity" term of the relationship, *Mutat. Res.* **306** (1994) 181-186.

34. R.L. Lopez de Compadre, A.K. Debnath, A.J. Shusterman, C.Hansch, LUMO energies and hydrophobicity as determinants of mutagenicity by nitroaromatic compounds in *Salmonella typhimurium*, *Environ. Mol. Mutagen.* **15** (1990) 44-55.

35. A.S. Debnath, R.L. Lopez de Compadre, A.J. Shusterman, C. Hansch, Quantitative Structure-Activity Relationship Investigation of the Role of Hydrophobicity in Regulating Mutagenicity in the Ames Test: 2. Mutagenicity of Aromatic and Heteroaromatic Nitro Compounds in *Salmonella typhimurium* TA100, *Environ. Mol. Mutagen.* **19** (1992) 53-70.

36. R. Collander, The permeability of nitella cells to nonelectrolytes, *Physiol. Plantarum* **7** (1914) 420-445.

37. W.A. Vance, D.E. Levin, Structural Features of Nitroaromatics That Determine Mutagenic Activity in *Salmonella typhimurium*, *Environ. Mutagen.* **6** (1984) 797-811.

38. P.P. Fu, M.W. Chou, D.W. Miller, G.L. White, R.H. Heflich, F.A. Beland, The orientation of the nitro-substituent predicts the direct-acting bacterial mutagenicity of nitrated polycyclic aromatic hydrocarbons, *Mutat. Res.* **143** (1985) 173-181.

39. A.T. Maynard, L.G. Pederon, H.S. Posner, J.D. McKinney, An *ab initio* study of the relationship between nitroarene mutagenicity and electron affinity, *Mol. Pharmacol.* **29** (1986) 629-636.

40. P.P. Fu, R.H. Heflich, L.S. Von Tunglin, H.Z. Miranda, F.E. Evans, Mirosomal metabolism of 1-nitrobenzo[e]pyrene to a highly mutagenic K-region dihydrodiol, *Carcinogenesis* **9** (1988) 951-958.

41. G. Klopman, D.A. Tonucci, M. Holloway, H.S. Rosenkranz, Relationship between polarographic reduction potential and mutagenicity of nitroarenes, *Mutat. Res.* **126** (1984) 139-144.

42. G.H. Loew, D. Spangler, R.J. Spanggord, Computer-Assisted Risk Assessment: Mechanistic Structure Activity Studies of Mutagenic Nitroaromatic Compounds, in: M. Tichý (Ed.), *QSAR in Toxicology and Xenobiochemistry*, Elsevier Science Publishers, New York, 1985, pp. 111-126.

43. E.P. Eddy, E.C. McCoy, H.S. Rosenkranz, R. Mermelstein, Dichotomy in the mutagenicity and genotoxicity of nitropyrenes: Apparent effect of the number of electrons involved in nitroreduction, *Mutat. Res.* **161** (1986) 109-111.

44. H. Jung, A.U. Shaikh, R.H. Heflich, P.P. Fu, Nitro Group Orientation, Reduction Potential, and Direct-Acting Mutagenicity of Nitro-Polycyclic Aromatic Hydrocarbons, *Environ. Mol. Mutagen.* **17** (1991) 169-180.

45. A. Pross, *Theoretical and Physical Principles of Organic Reactivity*, John Wiley and Sons, Inc., Toronto, 1995.

46. A. Hinchliffe, *Modeling Molecular Structures*, John Wiley & Sons, Inc., Toronto, 1996.

47. I.N. Levine, *Physical Chemistry*, McGraw-Hill, Inc., Toronto, 1995.

48. M.J.S. Dewar, W. Thiel, Ground States of Molecules. 38. The MNDO Method. Approximations and Parameters, *J. Am. Chem. Soc.* **99** (1977) 4899-4907.

49. J.A. Pople, D.P. Santry, G.A. Segal, Self-Consistent Molecular-Orbital Theory. V. Intermediate Neglect of Differential Overlap, *J. Chem. Phys.* **47** (1967) 2026-2033.

50. J.J.P. Stewart, Optimization of Parameters for Semiempirical Methods I. Method. *J. Comput. Chem.* **10** (1989) 209-220.

51. J.J.P. Stewart, Mopac: a semiempirical molecular orbital program, *J. Comput. Aided Mol. Design* **4** (1990) 1-105.

52. J.J.P. Stewart, Optimization of Parameters for Semiempirical Methods II. Applications, *J. Comput. Chem.* **10** (1989) 221-264.

53. G.H. Peslherbe, W.L. Hase, Semiempirical MNDO, AM1, and PM3 direct dynamics trajectory studies of formaldehyde unimolecular dissociation, *J. Chem. Phys.* **104** (1996) 7882-7894.

54. K. Yamagiwa, K. Ichikawa, Experimental study of the pathogenesis of carcinoma, *J. Cancer Res.* **3** (1918) 1-29.

55. B. Singer, D. Grunberger, *Molecular Biology of Mutagens and Carcinogens*, Plenum Press, New York, 1983.

56. R. Dabestani, R.H. Sik, A.G. Motten, C.F. Chignell, Spectroscopic Studies of Cutaneous Photosensitizing Agents. XVII. Benzanthrone, *Photochem. Photobiol.* **55** (1992) 533-539.

57. S.E. Manahan, *Toxicologcial Chemistry*, 2nd ed, Lewis Publishers, Inc., Boca Raton, 1992.

58. F.A. Beland, D.T. Beranek, K.L. Dooley, R.H. Heflich, E. Kadlubar, Arylamine-DNA adducts in vitro and in vivo: their role in bacterial mutagenesis and urinary carcinogenesis, *Environ. Health Perspect.* **49** (1983) 125-134.

59. P.C. Howard, R.H. Heflich, F.E. Evans, F.A. Beland, Formation of DNA adducts *in vitro* and in *Salmonella typhimurium* upon metabolic reduction of the environmental mutagen 1-nitropyrene, *Cancer Res.* **43** (1983) 2052-2058.

60. R.H. Heflich, E.K. Fifer, Z. Djurić, F.A. Beland, DNA Adduct Formation and Mutation Induction by Nitropyrenes in Salmonella and Chinese Hamster Ovary Cells: Relationships with Nitroreduction and Acetylation, *Environ. Health Perspect.* **62** (1985) 135-143.

61. M.V. Reddy, K. Randerath, Nuclease P1-mediated enhancement of sensitivity of ^{32}P-postlabelling test for structurally diverse DNA adducts, *Carcinogenesis* **5** (1986) 231-243.

62. C. Gupta, ^{32}P-Postlabelling analysis of bulky aromatic adducts, in: D.H. Phillips, M. Castegnaro, H. Bartsch (Eds.), *Postlabelling Methods for Detection of DNA Adducts*, Oxford University Press, New York, 1993, pp. 11-23.

63. L.M. Prescott, J.P. Harley, D.A. Klein, *Microbiology*, William C. Brown Publishers, Dubuqué, 1996.

64. M.E. Winkler, Biosynthesis of Histidine, in: F.C. Neidhart (Ed.), Escherchia coli *and* Salmonella – *Cellular and Molecular Biology*, 2nd ed., ASM Press, Washington, 1996, pp. 485-505.

65. P. Andrews, *The Fate of Dinitropyrenes in* Salmonella typhimurium*: Metabolism and DNA Adduct Formation*, Ph.D. Dissertation, McMaster University, Hamilton.

66. F. Hutchinson, Mutagenesis, in: F.C. Neidhart (Ed.), Escherchia coli *and* Salmonella – *Cellular and Molecular Biology*, 2nd ed., ASM Press, Washington, 1996, pp. 2218-2235.

67. M. Watanabe, T. Nishino, K. Takio, T. Sofuni, T. Nohmi, Purification and Characterization of Wild-type and Mutant "Classical" Nitroreductases of *Salmonella typhimurium*, *J. Biol. Chem.* **273** (1998) 23922-23928.

68. C. Lu, D.R. McCalla, B.E. McCarry, The 1-nitropyrene reductase of *Salmonella typhimurium*, *Chem.-Biol. Interact.* **43** (1983) 67-71.

69. P.C. Howard, F.A. Beland, F.E. Evans, R.H. Heflich, G.E. Milo, F.F. Kadlubar, 1-Nitropyrene: *In Vitro* Metabolism and DNA Adduct Formation, in: P.C. Howard, S.S. Hecht, F.A. Beland (Eds.), *Nitroarenes: Occurance, Metabolism and Biological Impact*, Plenum Press, new York, 1990, pp. 103-120.

70. R.P. Mason, J.L. Holtzman, The Mechanism of Microsomal and Mitochondrial Nitroreductase. Electron Spin Resonance Evidence for Nitroaromatic Free Radical Intermediates, *Biochemistry* **14** (1975) 1626-1632.

71. C. Elkhouri, *The Synthesis and Mutagenicity of 1-Nitrosopyrene and 1-Nitroso-8-Nitropyrene*, M.Sc. Dissertation, McMaster University, Hamilton, 1985.

72. F.A. Beland, F.F. Kadlubar, Metabolic activation and DNA adducts of aromatic amines and nitroaromatic hydrocarbons, in: C.S. Cooper, P.L. Grover (Eds.), *Handbook of Experimental Pharmacology*, Springer-Verlag, Berlin, 1990, pp. 267-325.

73. F.F. Kadlubar, J.A. Miller, E.C. Miller, Hepatic microsomal *N*-glucuronidation and binding of *N*-hydroxyarylamines in relation to urinary bladder carcinogenesis, *Cancer Res.* **37** (1977) 805-814.

74. S. Yu, R.H. Heflich, L.S. Von Tungeln, K. El-Bayoumy, F.F. Kadlubar, P.P. Fu, Comparitive direct-acting mutagenicity of 1- and 2-nitropyrene: Evidence for 2-nitropyrene mutagenesis by both guanine and adenine adducts, *Mutat. Res.* **250** (1991) 145-152.

75. W.W. Weber, I.B. Glowinski, Acetylation, in: W.B. Jakoby (Ed.), *Enzymatic Basis of Detoxication, vol. II*, Academic Press, Toronto, 1980, pp. 169-186.

76. N. Sera, K. Fukuhara, N. Miyata, H. Tokiwa, Mutagenicity of nitrophenanthrene derivatives for *Salmonella typhimurium*: effects of nitroreductase and acetyltransferase, *Mutat. Res.* **349** (1996) 137-144.

77. R.P.P. Fuchs, N. Schwartz, M.P. Duane, Hot spots of frameshift mutations induced by the ultimate carcinogen *N*-acetoxy-*N*-2-acetylaminofluorene, *Nature* **294** (1981) 657-659.

78. R. Dulbecco (Ed.), *Encyclopedia of Human Biology*, Academic Press, Toronto, 1991.

79. E.R. Nestmann, A Mutagen is a Mutagen, Not Necessarily a Carcinogen, in: D.M. Shankel, P.E. Hartman, T. Kada, A. Hollaender (Eds.), *Antimutagenesis and Anticarcinogenesis Mechanisms*, Plenum Press, New York, 1986, pp. 423-424.

80. P.F. Rosser, P. Ramchandran, R. Sangaiah, R.N. Austin, A. Gold, L.M. Ball, Role of O-acetyltransferase in activation of oxidised metabolites of the genotoxic environmental pollutant 1-nitropyrene, *Mutat. Res.* **369** (1986) 209-220.

81. P.P. Fu, D.H. Herreno-Saenz, L.S. Von Tungeln, J.O. Lay, Y.-S. Wu, J.-S. Lai, F.E. Evans, DNA Adducts and Carcinogenicity of Nitro-polycyclic Aromatic Hydrocarbons, *Environ. Health Perspect.* **102(suppl. 6)** (1994) 177-183.

82. J.R. Thorton-Manning, W.L. Campbell, B.S. Hass, J.J. Chen, P.P. Fu, C.E. Cerniglia, R.H. Heflich, Role of nitroreductase in the synergistic mutational response induced by mixtures of 1- and 3-nitrobenzo[*a*]pyrene in *Salmonella typhimurium*, *Environ. Mol. Mutagen.* **13** (1989) 203-210.

83. H. Lee, S.H. Cherng,. T.-Y. Liu, Bacterial Mutagenicity, Metabolism, and DNA Adduct Formation by Binary Mixtures of Benzo[a]pyrene and 1-Nitropyrene, *Environ. Mol. Mutagen.* **24** (1994) 229-234.

84. Y.-H. Chae, T. Thomas, F.P. Guengerich, P.P. Fu, K. El-Bayoumy, Comparative Metabolism of 1-, 2-, and 4-Nitropyrnee by Human Hepatic and Pulmonary Microsomes, *Cancer Res.* **59** (1999) 1473-1480.

85. J. Ding, P. Vouros, CEC-MS for the separation and identification of isomeric PAH-DNA adducts derived from in vitro reactions, *Am. Lab.* (1998) 15-29.

86. D.A. Skoog, D.M. West, F.J. Holler, *Analytical Chemisty – An Introduction*, Saunders College Publishing, Toronto, 1994.

87. J. Wellemans, R.L. Cerny, M.L. Gross, Tandem Mass Spectrometry for the Determination of Deoxyribonucleic Acid Damage by Polycyclic Aromatic Hydrocarbons, *Analyst* **119** (1994) 497-503.

88. M.L. Lee, M. Novotny, K.D. Bartle, Gas Chromatography/Mass Spectrometric and Nuclear Magnetic Resonance Spectrometric Studies of Carcinogenic Polynuclear Aromatic Hydrocarbons in Tobacco and Marijuana Smoke Condensates, *Anal. Chem.* **48** (1976) 405-416.

89. R.W. Giese, P. Vouros, Analysis of NO_2-PAH adducts by mass spectrometry, in: P.C. Howard, S.S. Hecht, F.A. Beland (Eds.), *Nitroarenes: Occurance, Metabolism and Biological Impact*, Plenum Press, New York, 1990, pp. 211-217.

90. J.A. Sweetman, F.W. Karasek, D. Schuetzle, Decomposition of nitropyrene during gas chromatographic-mass spectrometric analysis of air particulate and fly-ash samples, *J. Chromatogr.* **247** (1982) 245-254.

91. F.W. McLafferty, F. Tureček, *Interpretation of Mass Spectra, 4th ed.*, University Science Books, Sausalito, 1993.

92. F. Radner, Nitration of Polycyclic Aromatic Hydrocarbons with Dinitrogen Tetroxide. A Simple and Selective Synthesis of Mononitro Derivatives, *Acta Chem. Scand., Sect. B* **37** (1983) 65-67.

93. W.J. Mills, *The Synthesis and Characterization of Some N-hydroxyaminopyrenes*, M.Sc. Dissertation, McMaster University, Hamilton, 1990.

94. K. Lauer, K.-I. Atarashi, Die Nitrierung des 1,9-Benzanthrons mittels Stickstoffdioxyds und die Formulierung des 1,9-Benzanthrons, *Chem. Ber.* **65** (1935) 1373-1376.

95. G.L. Squadrito, F.R. Fronczek, D.F. Church, W.A. Pryor, Anomalous nitration of fluoranthene with nitrogen dioxide in carbon tetrachloride, *J. Am. Chem. Soc.* **109** (1987) 6535-6537.

96. B. Zielinska, J. Arey, R. Atkinson, T. Ramdahl, A.M. Winer, J.N. Pitts Jr., Reaction of Dinitrogen Pentoxide with Fluoranthene, *J. Am. Chem. Soc.* **108** (1986) 4126-4132.

97. E. Bamberger, R. Seligman, Oxydation aliphatischer Casen vom Typus, *Chem. Ber.* **36** (1903) 685-700.

98. K. El-Bayoumy, S.S. Hecht, Identification and mutagenicity of metabolites of 1-nitropyrene formed by rat liver, *Cancer Res.* **48** (1988) 4526-4560.

99. Y. Yost. H.R. Gutmann, Hindered *N*-Arylhydroxamic Acids from Arylamines *via* Nitroso-compounds, *J. Chem. Soc., Sect. C* (1970) 2497-2499.

100. R.P. Mason, P.D. Josephy, Free Radical Mechanism of Nitroreductase, in: D.E. Rickert (Ed.), *Toxicity of Nitroaromatic Compounds*, Plenum Press, New York, 1985, pp. 121-140.

101. I.D. Entwistle, T. Gilkerson, R.A.W. Johnstone, R.P. Telford, Rapid Catalytic Transfer Reduction of Aromatic Nitro Compounds to Hydroxylamines, *Tetrahedron* **34** (1978) 213-215.

102. W.B. Melchior Jr., M.M. Marques, F.A. Beland, Mutations induced by aromatic amine DNA adducts in pBR322, *Carcinogenesis* **15** (1994) 889-899.

103. D.T. Beranek, G.L. White, R.H. Heflich, F.A. Beland, Aminofluorene-DNA adduct formation in *Salmonella typhimurium* exposed to the carcinogen N-hydroxy-2-acetylaminofluorene, *Proc. Nat. Acad. Sci. U.S.A.* **79** (1982) 5175-5178.

104. P.C. Howard, E.C. McCoy, H.S. Rosenkranz, Sequential and differing nitroreductive pathways for mutagenic nitropyrenes in *Salmonella typhimurium*, *Mutagenesis* **2** (1987) 431-432.

105. W.G. Humphreys, F.F. Kadlubar, F.P. Guengerich, Mechanism of C^8 alkylation of guanine residues by activated arylamines: Evidence for initial adduct formation at the N^7 position, *Proc. Nat. Acad. Sci. U.S.A.* **89** (1992) 8278-8282.

106. M.C. Kloetzel, W. King, J.H. Menkes, Fluoranthene Derivatives. III. 2-Nitrofluoranthene and 2-Aminofluoranthene, *J. Am. Chem. Soc.* **78** (1956) 1165-1168.

107. H.K. Porter, The Zinin Reduction of Nitroarenes, in J.E. Baldwin, R. Bittman, W.G. Dauben, J. Fried, R.F. Heck, A.S. Kende, W. Leimgruber, J.A. Marshall, B.C. McKusick, J. Meinwald, B.M. Trost, B. Weinstein (Eds.), *Organic Reactions, vol. 20*, John Wiley & Sons, Inc., New York, 1973, pp. 455-481.

108. H. Zollinger, *Diazo Chemistry I – Aromatic and Heteroaromatic Compounds*, VCH, Inc., New York, 1994.

109. A. Marcinek, E. Leyva, D. Whitt, M.S. Platz, Evidence for Stepwise Nitrogen Extrusion and Ring Expansion upon Photolysis of Phenyl Azide, *J. Am. Chem. Soc.* **115** (1993) 8609-8612.

110. E. Leyva, R. Sagredo, Photochemistry of Fluorophenyl Azides in Diethylamine. Nitrene Reaction Versus Ring Expansion, *Tetrahedron* **54** (1998) 7367-7374.

111. R.A. McClelland, P.A. Davidse, G. Hadzialic, Electron-Deficient Strong Bases. Generation of the 4-Biphenylyl- and 2-Fluorenylnitrenium Ions by Nitrene Protonation in Water, *J. Am. Chem. Soc.* **117** (1995) 4173-4174.

112. D. Wild, A. Dirr, I. Fasshauer, D. Henschler, Photolysis of arylazides and generation of highly electrophilic DNA-binding and mutagenic intermediates, *Carcinogenesis* **10** (1989) 335-341.

113. J. Trotter, The Crystal Structures of Some Anthracene Derivatives. IV. 9,10-Dinitroanthracene, *Acta Crystallogr., Sect. B* **12** (1959) 232-236.

114. J. Trotter, The Crystal Structures of Some Anthracene Derivatives. V. 9-Nitroanthracene, *Acta Crystallogr., Sect. B* **12** (1959) 237-242.

115. H. Jung, A.U. Shaikh, R.H. Heflich, P.P. Fu, Nitrogroup orientation, reduction potential, and direct-acting mutagenicity of nitro-polycyclic aromatic hydrocarbons, *Environ. Mol. Mutagen.* **17** (1991) 169-180.

116. D.E. Koshland Jr., The Key-Lock Theory and the Induced Fit Theory, *Angew. Chem. Intl. Ed. Engl.* **33** (1994) 2375-2378.

117. A.K. Debnath, R.L. Lopez de Compadre, G. Debnath, A.J. Shusterman, C. Hansch, Structure-activity relationship of mutagenic aromatic and heteroaromatic nitro compounds. Correlation with molecular orbital enegies and hydrophobicity, *J. Med. Chem.* **34** (1991), 786-797.

118. A.K. Ghose, A. Pritchett, G.M. Crippen, Atomic physicochemical parameters for three dimensional structure directed quantitative structure-activity relationships. III. Modeling hydrophobic interactions, *J. Comput. Chem.* **9** (1988) 80-90.

119. J. Tomasi, Use of the Electrostatic Potential as a Guide to Understanding Molecular Properties, in: P. Politzer, D.G. Trublar (Eds.), *Chemical Applications of Atomic and Molecular Electrostatic Potentials: Reactivity, Structure, Scattering, and Energetics of Organic, Inorganic, and Biological Systems*, Plenum Press, New York, 1981, pp. 257-294.

120. J.V. Pothuluri, D.R. Doerge, M.I. Churchwell, P.P. Fu, C.E. Cerniglia, Fungal Metabolism of Nitrofluoranthenes, *J. Toxicol. Environ. Health, Pt. A* **53** (1998) 153-174.

121. R. Modica, M. Fiume, I. Bartosek, Gas-liquid chromatographic assay of polycyclic aromatic hydrocarbon mixtures: specifically modified method for rat tissues, *J. Chromatogr.* **247** (1982) 352-355.

122. C.-L. Li, *Separation and characterization of thia-arenes and high mass polycyclic aromatic hydrocarbons in coal tar*, M.Sc. Dissertation, McMaster University, Hamilton, 1997.

123. M. Kranendonk, J.N. Commandeur, A. Laires, J. Rueff, N.P. Vermeulen, Characterization of enzyme activity and cofactors involved in bioactivation and bioinactivation of chemical carcinogens in the tester strains *Escherchia coli* K12 MX100 and *Salmonella typhimurium* LT2 TA100, *Mutagenesis* **12** (1997) 245-254.

124. B.S. Shane, G.L. Squadrito, D.F. Church, W.A. Pryor, Comparative mutagenicity of nitrofluoranthenes in *Salmonella typhimurium* TA98, TA98NR, and TA98/1,8-DNP6, *Environ. Mol. Mutagen.* **17** (1991) 130-138.

125. G.P. Ford, P.S. Herman, Relative Stabilities of Nitrenium Ions Derived from Polycyclic Aromatic Amines. Relationship to Mutagenicity, *Chem.-Biol. Interact.* **65** (1992) 1-18.

126. H. Shioda, S. Kato, Mononitration of benzanthrone, *Chem. Abs.* (1957) 16393; [*Yuki Gosei Kagaku Kyokaishi* **15** (1957) 361-364].

6. Appendices

Appendix 1. Electronic Surface Maps derived from *Ab Initio* Calculations

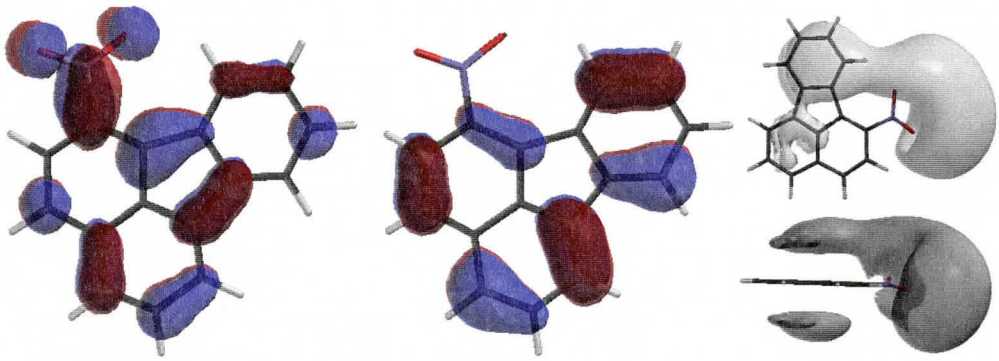

LUMO HOMO Electrostatic Potential

1-Nitrofluoranthene.

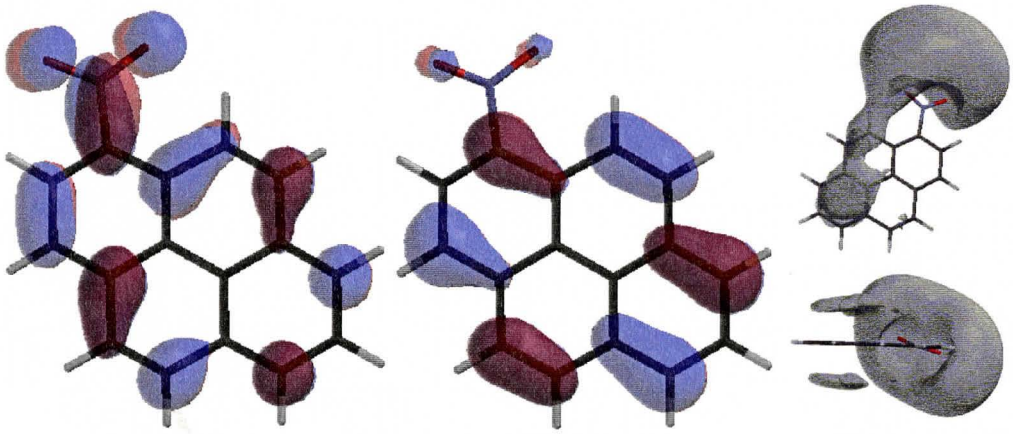

LUMO HOMO Electrostatic Potential

1-Nitropyrene.

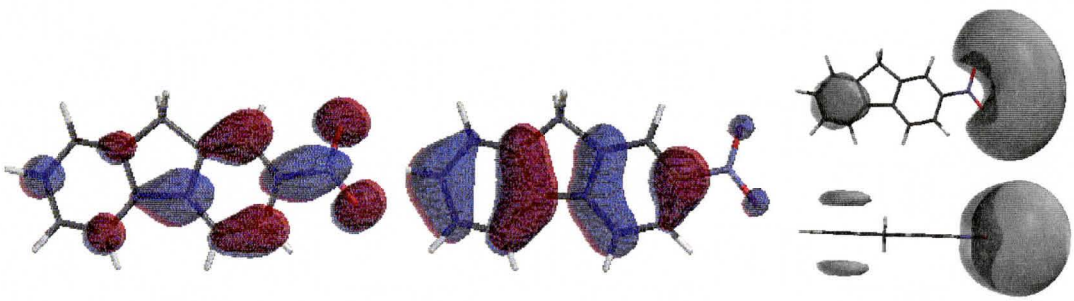

LUMO HOMO Electrostatic Potential

2-Nitrofluorene.

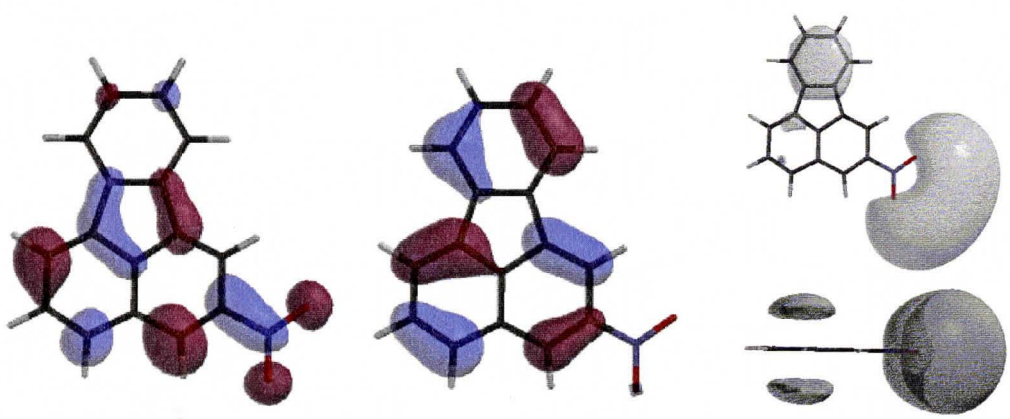

LUMO HOMO Electrostatic Potential

2-Nitrofluoranthene.

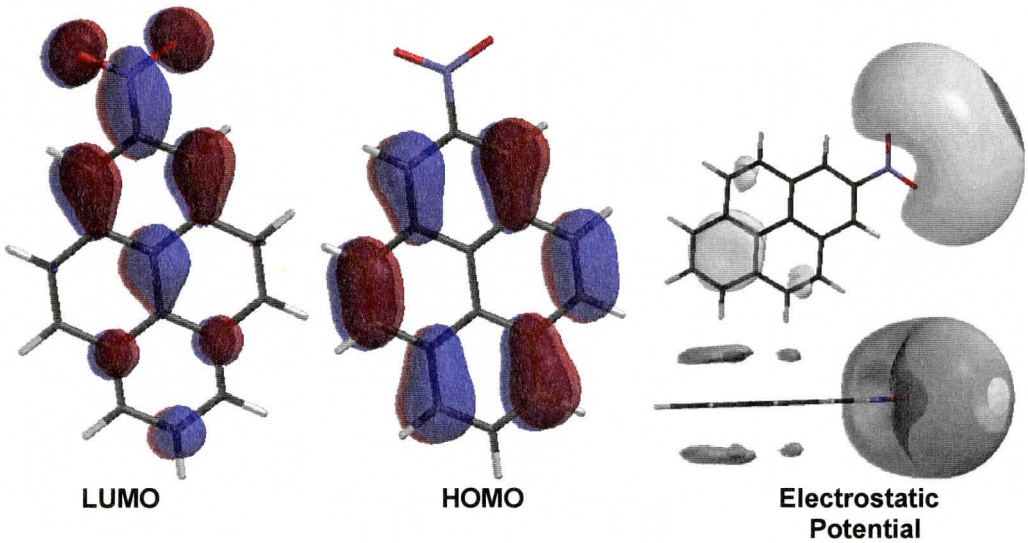

2-Nitropyrene.

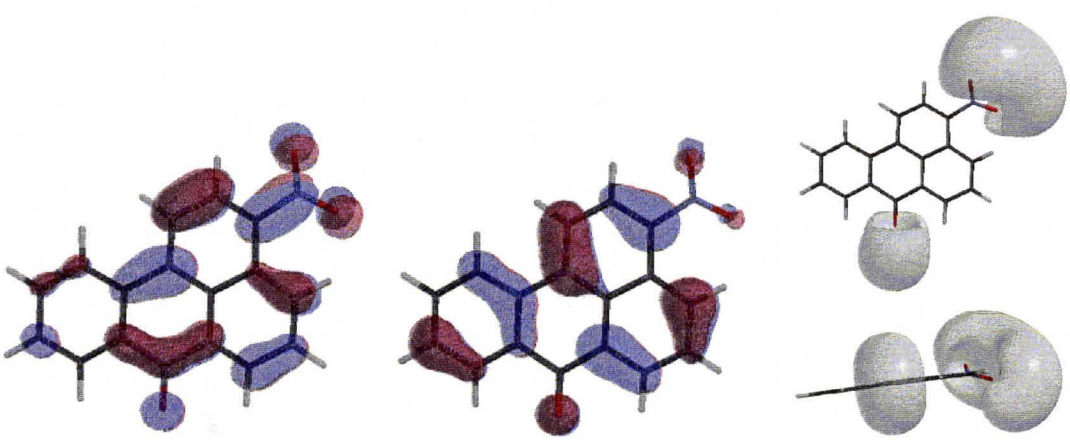

3-Nitrobenzanthrone.

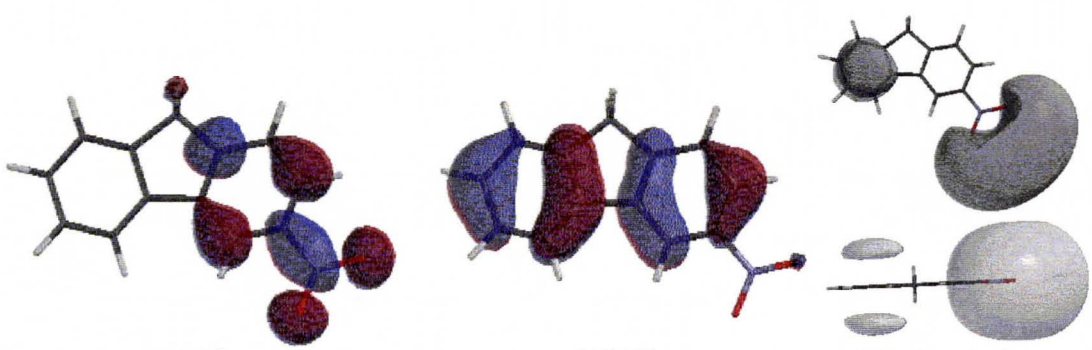

LUMO HOMO Electrostatic Potential

3-Nitrofluorene.

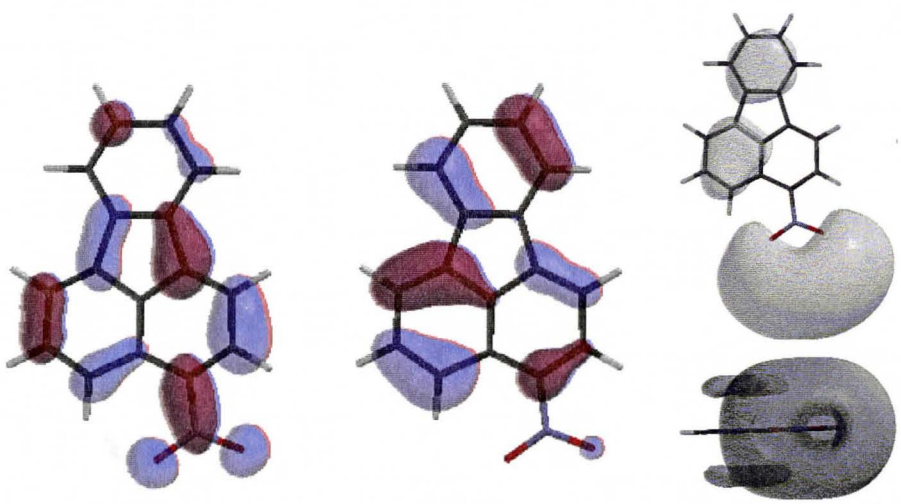

LUMO HOMO Electrostatic Potential

3-Nitrofluoranthene.

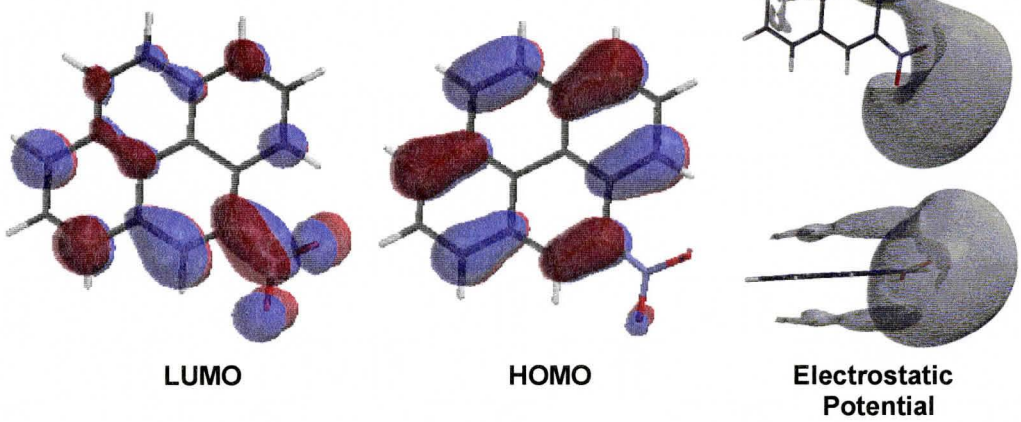

LUMO HOMO Electrostatic Potential

4-Nitropyrene.

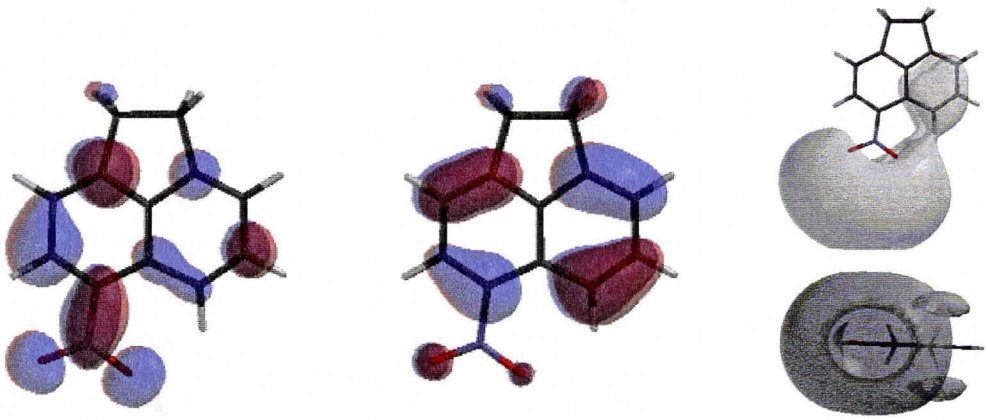

LUMO HOMO Electrostatic Potential

5-Nitroacenaphthene.

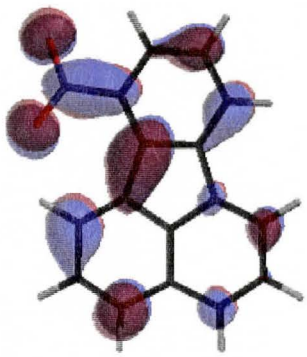

LUMO

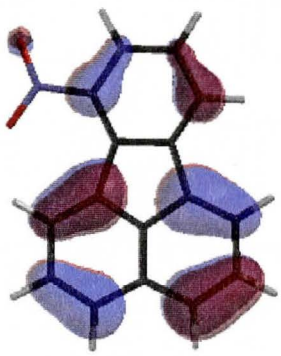

HOMO

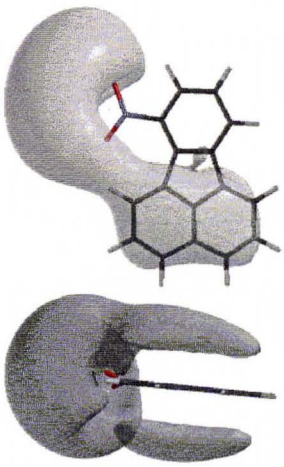

Electrostatic Potential

7-Nitrofluoranthene.

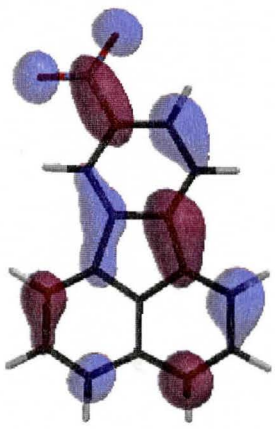

LUMO

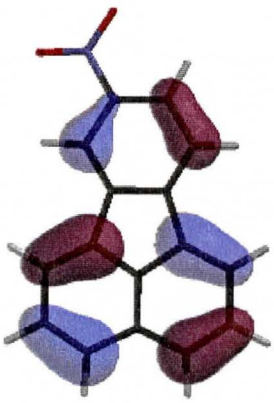

HOMO

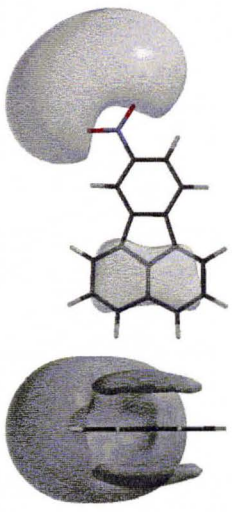

Electrostatic Potential

8-Nitrofluoranthene.

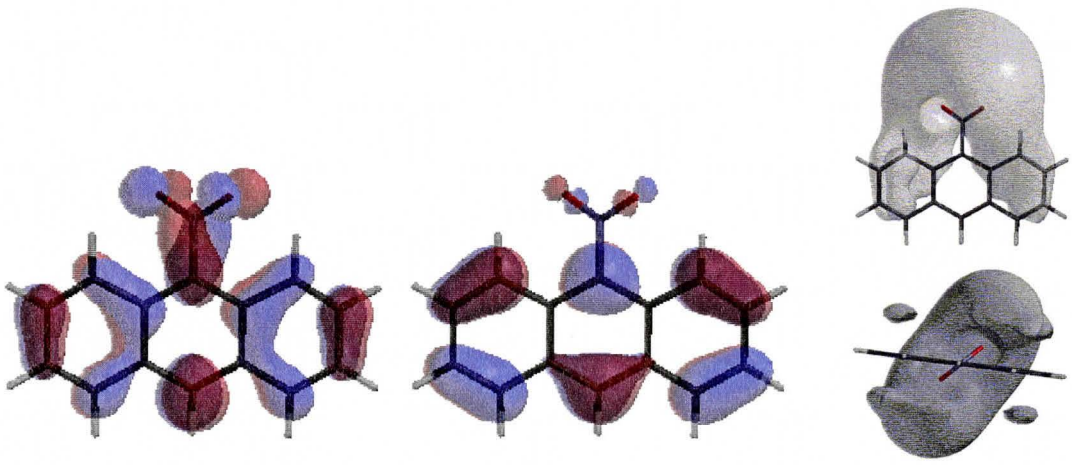

9-Nitroanthracene.

Appendix 2. Selected Output from *Ab Initio* Calculations using HF/3-21G Basis Set

Appendix 2 Contents

1-Nitrofluoranthene. Geometry Optimization.

```
Run type: Geometry optimization
          Numerical Frequency
Model: RHF/3-21G(*)
Number of shells:  75
  37 S shells
  38 SP shells
Number of basis functions: 189
Number of electrons: 128
Use of molecular symmetry disabled
Molecular charge:   0
Spin multiplicity:  1

Point Group = C1  Order =  1 Nsymop =  1
This system has  78 degrees of freedom
```

Atom	Label	Cartesian Coordinates (Angstroms) X	Y	Z
H	H1	1.1817987	-3.3739856	0.0243869
C	C1	0.4942542	-2.6760158	0.4581139
C	C11	1.1573532	-0.5855563	-0.9580573
C	C2	0.4312195	-1.3843824	0.0493675
C	C3	-1.2708224	-2.2597636	2.0841300
C	C4	-0.4939782	-0.5102715	0.6558432
C	C5	-0.3806664	-3.1051462	1.4940271
C	C6	-1.3474285	-0.9031776	1.6665765
C	C7	-0.4255045	0.8004306	0.0999979
H	H3	-0.3295362	-4.1263180	1.8156575
H	H4	-2.8969249	-0.1514917	2.9810998
H	H5	-1.9167842	-2.6082450	2.8655079
C	C8	-1.2804067	1.7173191	0.6438020
H	H11	0.8244580	2.6696652	-1.8141092
N	N1	-1.3699066	3.0937241	0.2166815
C	C9	-2.1641566	1.3485902	1.6943868
H	H2	-2.7976157	2.1141939	2.0801393
C	C10	-2.2126210	0.0911325	2.1932772
C	C12	2.2236335	1.2932209	-2.6558991
C	C13	0.6525551	0.7365045	-0.9445982
C	C14	2.1700470	-0.9539032	-1.8076281
C	C15	2.7064444	0.0013882	-2.6648235
C	C16	1.1925141	1.6728544	-1.8007748
H	H12	2.6428028	2.0228301	-3.3194364
H	H9	2.5449640	-1.9580524	-1.8109848
H	H10	3.4984286	-0.2700375	-3.3339904
O	O1	-0.8155382	3.4268764	-0.8455842
O	O2	-2.0185824	3.8776166	0.9328910

```
E(HF)  =     -810.6108233 a.u.

Dipole moment:  X =   1.103224  Y =  -5.270350  Z =   0.963351
Total Dipole:   5.470076 Debye

Frequencies and reduced mass in atomic units are:
```

mode	(cm-1)	AU	mass
1	-0.2129E-04	-0.1715E-16	-0.2174E+16
2	-0.1043E-04	-0.4120E-17	-0.3658E+16
3	0.6756E-05	0.1727E-17	0.1335E+17
4	0.8746E-05	0.2894E-17	0.7652E+16
5	0.1365E-04	0.7047E-17	0.3991E+16
6	0.1701E-04	0.1095E-16	0.3598E+16
7	30.54	0.3530E-04	45.00
8	76.47	0.2213E-03	75.27
9	127.4	0.6138E-03	37.49

10	133.8	0.6771E-03	50.91
11	214.1	0.1735E-02	19.78
12	235.1	0.2092E-02	22.44
13	254.1	0.2444E-02	25.84
14	327.0	0.4047E-02	16.16
15	336.6	0.4288E-02	11.39
16	343.6	0.4467E-02	11.22
17	414.8	0.6513E-02	10.70
18	482.2	0.8799E-02	13.22
19	494.7	0.9263E-02	10.79
20	507.6	0.9750E-02	9.178
21	532.7	0.1074E-01	13.58
22	556.2	0.1171E-01	9.086
23	596.2	0.1345E-01	10.43
24	631.9	0.1511E-01	12.19
25	646.1	0.1580E-01	8.538
26	700.4	0.1857E-01	9.165
27	707.2	0.1893E-01	9.694
28	718.8	0.1955E-01	7.254
29	739.1	0.2067E-01	7.031
30	753.5	0.2148E-01	11.47
31	823.9	0.2569E-01	6.623
32	836.4	0.2648E-01	8.330
33	847.3	0.2717E-01	9.955
34	875.4	0.2900E-01	4.475
35	890.4	0.3000E-01	3.285
36	922.2	0.3219E-01	5.211
37	964.5	0.3521E-01	8.318
38	988.1	0.3695E-01	7.883
39	1007.	0.3840E-01	4.691
40	1008.	0.3842E-01	5.627
41	1055.	0.4211E-01	3.310
42	1086.	0.4460E-01	3.722
43	1087.	0.4473E-01	7.736
44	1104.	0.4613E-01	7.989
45	1121.	0.4759E-01	8.987
46	1152.	0.5021E-01	2.857
47	1174.	0.5220E-01	3.256
48	1181.	0.5278E-01	6.657
49	1193.	0.5390E-01	7.560
50	1200.	0.5450E-01	3.381
51	1215.	0.5587E-01	6.370
52	1219.	0.5620E-01	5.266
53	1264.	0.6044E-01	6.872
54	1278.	0.6180E-01	6.552
55	1285.	0.6248E-01	6.696
56	1324.	0.6639E-01	6.015
57	1335.	0.6747E-01	7.192
58	1342.	0.6815E-01	6.213
59	1374.	0.7146E-01	5.881
60	1395.	0.7363E-01	6.077
61	1414.	0.7570E-01	6.602
62	1456.	0.8027E-01	6.379
63	1460.	0.8067E-01	5.383
64	1505.	0.8574E-01	5.778
65	1533.	0.8888E-01	5.988
66	1585.	0.9511E-01	5.518
67	1593.	0.9606E-01	4.265
68	1616.	0.9881E-01	4.951
69	1633.	0.1009	4.922
70	1645.	0.1024	5.221
71	1745.	0.1153	5.861
72	1763.	0.1176	5.915
73	1782.	0.1202	5.861
74	1785.	0.1206	5.915
75	1801.	0.1227	5.907
76	3357.	0.4264	1.187

```
  77     3358.       0.4267       1.176
  78     3369.       0.4295       1.176
  79     3372.       0.4302       1.189
  80     3377.       0.4316       1.193
  81     3384.       0.4334       1.217
  82     3386.       0.4337       1.218
  83     3447.       0.4496       1.188
  84     3493.       0.4616       1.180

Zero-point vibrational energy is   141.480 kcal/mol

Standard Thermodynamic quantities at   298.15 K  and     1.00 atm

Translational Enthalpy:          0.889 kcal/mol
Rotational Enthalpy:             0.889 kcal/mol
Vibrational Enthalpy:          147.069 kcal/mol
Translational Entropy:          42.414  cal/mol.K
Rotational Entropy:             33.101  cal/mol.K
Vibrational Entropy:            33.869  cal/mol.K
```

1-Nitrofluoranthene. Single Point Calculation of Electrostatic Potentials using Optimized Geometry.

```
Run type: Single point energy
Model: RHF/3-21G(*)
Number of shells:  75
  37 S shells
  38 SP shells
Number of basis functions: 189
Number of electrons: 128
Use of molecular symmetry disabled
Molecular charge:   0
Spin multiplicity:  1

Atomic Charges from Electrostatic Potential

Resolution:   1  points per atomic unit
8478 of  27753 gridpoints used in calculation

   Atom     Charge
   ----   -----------
   H  1     0.185350
   C  2    -0.200471
   C  3     0.115320
   C  4    -0.018244
   C  5    -0.300740
   C  6    -0.010135
   C  7    -0.119178
   C  8     0.223004
   C  9     0.040285
   H 10     0.167613
   H 11     0.196484
   H 12     0.194152
   C 13    -0.137255
   H 14     0.234152
   N 15     0.941864
   C 16    -0.182335
   H 17     0.210120
   C 18    -0.274596
   C 19    -0.182659
   C 20    -0.005655
   C 21    -0.265943
   C 22    -0.109108
```

```
   C 23     -0.187229
   H 24      0.160070
   H 25      0.187822
   H 26      0.157422
   O 27     -0.518116
   O 28     -0.501992

Total Charge =  0.000000

RMS fit:     1.145666
RRMS fit:    0.135945

Dipole moment from formal charges:
x =    1.1472, y =  -5.3081, z =    0.9667  =    5.5160 debye
```

1-Nitropyrene. Geometry Optimization.

```
Run type: Geometry optimization
          Numerical Frequency
Model: RHF/3-21G(*)
Number of shells:  75
  37 S shells
  38 SP shells
Number of basis functions: 189
Number of electrons: 128
Use of molecular symmetry disabled
Molecular charge:   0
Spin multiplicity:  1

Point Group = C1  Order =  1 Nsymop =  1
This system has  78 degrees of freedom
```

Atom	Label	Cartesian Coordinates (Angstroms) X	Y	Z
H	H1	-0.4259771	2.7390418	-3.2436524
C	C1	-0.2596783	2.0883908	-2.4157315
H	H2	1.6938743	2.8006959	-2.0130860
C	C2	0.9233801	2.1136437	-1.7275527
C	C3	-1.1246415	0.3221398	-0.9931596
C	C4	1.1294530	1.2487849	-0.6586959
C	C5	-1.2748391	1.2188943	-2.0561717
C	C6	0.1103573	0.3449418	-0.2922295
C	C7	2.3676345	1.2558241	0.0789663
N	N1	-2.4772471	1.3112808	-2.8605801
C	C16	-1.8914304	-1.4804514	0.4393583
C	C15	-2.1216294	-0.6396412	-0.5755276
C	C8	2.5698906	0.4174917	1.1008019
H	H6	3.1241250	1.9549199	-0.2176980
H	H7	3.4947748	0.4298802	1.6436151
C	C9	1.5587588	-0.5269107	1.5025061
C	C10	1.7581119	-1.4072679	2.5585968
C	C11	0.3363356	-0.5542729	0.7994368
C	C12	0.7738841	-2.3063768	2.9225347
H	H8	2.6880411	-1.3839971	3.0924316
H	H9	0.9420869	-2.9795570	3.7389371
C	C13	-0.4248849	-2.3408037	2.2378576
H	H10	-1.1870279	-3.0399348	2.5214689
C	C14	-0.6586023	-1.4737129	1.1771698
H	H4	-2.6462113	-2.1872181	0.7245584
H	H11	-3.0481618	-0.6608842	-1.0943128
O	O1	-2.3863018	1.9134674	-3.9495167
O	O2	-3.5440755	0.8216316	-2.4403252

```
E(HF)  =     -810.6339666 a.u.

Dipole moment:  X =   4.678431  Y =  -1.299858  Z =   4.070485
Total Dipole:   6.336102 Debye

Frequencies and reduced mass in atomic units are:
```

mode	(cm-1)	AU	mass
1	-0.2557E-04	-0.2475E-16	-0.1315E+16
2	-0.9459E-05	-0.3386E-17	-0.6807E+16
3	0.1427E-04	0.7702E-17	0.1687E+16
4	0.1584E-04	0.9494E-17	0.3025E+16
5	0.1907E-04	0.1376E-16	0.2604E+16
6	0.6659E-04	0.1678E-15	0.1327E+15
7	43.27	0.7086E-04	24.21
8	73.37	0.2037E-03	61.73
9	120.2	0.5469E-03	46.71

10	204.3	0.1580E-02	23.62
11	228.7	0.1979E-02	18.71
12	246.2	0.2294E-02	18.02
13	297.5	0.3349E-02	14.64
14	325.9	0.4019E-02	12.29
15	346.5	0.4545E-02	12.56
16	385.1	0.5612E-02	11.42
17	461.5	0.8059E-02	11.37
18	467.7	0.8277E-02	13.73
19	498.7	0.9413E-02	12.55
20	535.2	0.1084E-01	13.33
21	567.0	0.1217E-01	9.075
22	571.6	0.1236E-01	12.06
23	583.4	0.1288E-01	8.617
24	614.9	0.1431E-01	10.31
25	621.0	0.1459E-01	11.21
26	635.4	0.1528E-01	10.22
27	672.5	0.1711E-01	8.212
28	687.9	0.1791E-01	9.832
29	774.8	0.2272E-01	9.889
30	775.9	0.2279E-01	7.814
31	803.7	0.2445E-01	6.630
32	814.9	0.2513E-01	8.800
33	853.6	0.2757E-01	5.879
34	863.6	0.2823E-01	9.647
35	888.3	0.2986E-01	3.251
36	909.9	0.3133E-01	10.05
37	938.9	0.3336E-01	3.066
38	943.0	0.3365E-01	8.308
39	999.2	0.3778E-01	4.621
40	1018.	0.3926E-01	5.740
41	1024.	0.3966E-01	4.087
42	1038.	0.4076E-01	7.806
43	1087.	0.4474E-01	2.865
44	1138.	0.4901E-01	7.735
45	1165.	0.5140E-01	3.018
46	1178.	0.5250E-01	3.246
47	1195.	0.5405E-01	7.430
48	1198.	0.5429E-01	3.597
49	1203.	0.5477E-01	6.728
50	1211.	0.5546E-01	6.995
51	1214.	0.5573E-01	4.185
52	1270.	0.6101E-01	7.197
53	1291.	0.6305E-01	7.060
54	1307.	0.6462E-01	7.049
55	1316.	0.6551E-01	6.570
56	1323.	0.6625E-01	6.220
57	1346.	0.6858E-01	6.320
58	1368.	0.7083E-01	6.034
59	1385.	0.7260E-01	6.590
60	1392.	0.7331E-01	6.513
61	1405.	0.7475E-01	5.330
62	1434.	0.7777E-01	5.921
63	1455.	0.8008E-01	5.938
64	1507.	0.8589E-01	6.140
65	1561.	0.9216E-01	5.722
66	1583.	0.9485E-01	5.026
67	1590.	0.9561E-01	4.856
68	1612.	0.9835E-01	4.316
69	1656.	0.1038	5.498
70	1661.	0.1044	5.448
71	1724.	0.1125	5.833
72	1753.	0.1162	5.896
73	1758.	0.1169	5.752
74	1795.	0.1220	5.956
75	1817.	0.1249	5.929
76	3352.	0.4253	1.154

```
  77     3355.        0.4260        1.173
  78     3359.        0.4269        1.181
  79     3363.        0.4280        1.185
  80     3375.        0.4310        1.241
  81     3380.        0.4325        1.208
  82     3385.        0.4336        1.220
  83     3448.        0.4499        1.189
  84     3492.        0.4614        1.184

Zero-point vibrational energy is   141.869 kcal/mol

Standard Thermodynamic quantities at   298.15 K  and     1.00 atm

Translational Enthalpy:          0.889 kcal/mol
Rotational Enthalpy:             0.889 kcal/mol
Vibrational Enthalpy:          147.283 kcal/mol
Translational Entropy:          42.414  cal/mol.K
Rotational Entropy:             33.026  cal/mol.K
Vibrational Entropy:            31.845  cal/mol.K
```

1-Nitropyrene. Single Point Calculation of Electrostatic Potentials using Optimized Geometry.

```
Run type: Single point energy
Model: RHF/3-21G(*)
Number of shells:  75
  37 S shells
  38 SP shells
Number of basis functions: 189
Number of electrons: 128
Use of molecular symmetry disabled
Molecular charge:   0
Spin multiplicity:  1

Atomic Charges from Electrostatic Potential

Resolution:   1  points per atomic unit
8858 of  29667 gridpoints used in calculation

   Atom     Charge
   ----   -----------
   H  1     0.200374
   C  2    -0.071057
   H  3     0.205810
   C  4    -0.357221
   C  5     0.238823
   C  6     0.255298
   C  7    -0.268938
   C  8    -0.073067
   C  9    -0.282252
   N 10     0.938968
   C 11    -0.197591
   C 12    -0.341890
   C 13    -0.222413
   H 14     0.192384
   H 15     0.190101
   C 16     0.146568
   C 17    -0.270701
   C 18    -0.012187
   C 19    -0.126308
   H 20     0.189479
   H 21     0.169597
   C 22    -0.271937
```

```
   H 23      0.188989
   C 24      0.164547
   H 25      0.179493
   H 26      0.253608
   O 27     -0.507891
   O 28     -0.510588

Total Charge =  0.000000

RMS fit:    1.091503
RRMS fit:   0.121642

Dipole moment from formal charges:
x =    4.7119, y =  -1.3460, z =    4.1100  =    6.3958 debye
```

2-Nitrofluorene. Geometry Optimization.

```
Run type: Geometry optimization
          Numerical Frequency
Model: RHF/3-21G(*)
Number of shells:  66
  34 S shells
  32 SP shells
Number of basis functions: 162
Number of electrons: 110
Use of molecular symmetry enabled
Molecular charge:   0
Spin multiplicity:  1

Point Group = CS  Order =  1 Nsymop =  2
This system has  46 degrees of freedom
```

Atom	Label	Cartesian Coordinates (Angstroms) X	Y	Z
H	H9	-2.2613739	0.0000000	3.2221486
H	H10	-0.4777503	0.0000000	4.9148474
C	C11	-0.8867882	0.0000000	1.5871045
H	H12	1.8758658	0.0000000	4.2443846
C	C16	1.4607274	0.0000000	2.1541892
C	C14	-1.2323249	0.0000000	2.9205173
C	C15	-0.2234713	0.0000000	3.8736129
C	C13	0.4552314	0.0000000	1.2061390
C	C1	0.5277657	0.0000000	-0.2646733
C	C7	-1.7883152	0.0000000	0.3597483
C	C12	1.1106190	0.0000000	3.4942571
H	H11	2.4927755	0.0000000	1.8641092
C	C2	0.1132378	0.0000000	-2.9628991
C	C3	1.6204376	0.0000000	-1.1123373
C	C4	-0.7745087	0.0000000	-0.7752750
C	C5	-0.9919840	0.0000000	-2.1286702
C	C6	1.4045319	0.0000000	-2.4772157
H	H1	2.6199184	0.0000000	-0.7282290
H	H8	-2.4169493	0.8835130	0.3289318
H	H4	-1.9703810	0.0000000	-2.5567516
H	H5	2.2150951	0.0000000	-3.1714413
N	N1	-0.0951012	0.0000000	-4.3929172
H	H3	-2.4169493	-0.8835130	0.3289318
O	O1	-1.2718533	0.0000000	-4.8028284
O	O2	0.9115452	0.0000000	-5.1256836

```
E(HF)  =    -697.6464167 a.u.

Dipole moment:  X =   0.208849  Y =   0.000000  Z =   6.200368
Total Dipole:   6.203884 Debye

Frequencies and reduced mass in atomic units are:
```

mode	(cm-1)	AU	mass
1	-0.1864E-04	-0.1314E-16	-0.2637E+16
2	-0.1635E-04	-0.1012E-16	-0.7630E+16
3	-0.5763E-05	-0.1257E-17	-0.1471E+17
4	0.1597E-04	0.9657E-17	0.3400E+16
5	0.2014E-04	0.1535E-16	0.1020E+16
6	0.2530E-04	0.2423E-16	0.1288E+16
7	65.24	0.1611E-03	161.6
8	67.44	0.1721E-03	42.28
9	149.7	0.8485E-03	50.75
10	159.7	0.9646E-03	53.16
11	200.9	0.1527E-02	21.80
12	272.7	0.2814E-02	46.85

13	275.6	0.2874E-02	19.11
14	348.7	0.4601E-02	13.23
15	364.7	0.5034E-02	10.49
16	485.4	0.8915E-02	11.81
17	502.4	0.9553E-02	11.81
18	506.4	0.9704E-02	10.81
19	546.1	0.1128E-01	11.41
20	554.2	0.1162E-01	8.542
21	594.0	0.1335E-01	11.11
22	615.0	0.1431E-01	11.43
23	645.2	0.1576E-01	8.106
24	723.7	0.1982E-01	10.97
25	738.8	0.2066E-01	9.827
26	763.2	0.2204E-01	7.114
27	809.9	0.2482E-01	9.871
28	821.9	0.2556E-01	7.084
29	839.2	0.2665E-01	9.384
30	861.6	0.2810E-01	4.843
31	901.0	0.3072E-01	9.263
32	909.6	0.3131E-01	5.838
33	965.7	0.3530E-01	8.185
34	1006.	0.3831E-01	3.250
35	1018.	0.3925E-01	4.566
36	1056.	0.4217E-01	4.912
37	1110.	0.4665E-01	9.170
38	1129.	0.4825E-01	2.839
39	1140.	0.4918E-01	8.228
40	1157.	0.5065E-01	3.796
41	1181.	0.5279E-01	7.577
42	1184.	0.5301E-01	3.408
43	1202.	0.5470E-01	3.422
44	1217.	0.5603E-01	7.712
45	1226.	0.5687E-01	6.802
46	1261.	0.6015E-01	6.646
47	1289.	0.6286E-01	6.389
48	1294.	0.6341E-01	6.585
49	1304.	0.6430E-01	6.176
50	1328.	0.6678E-01	6.856
51	1335.	0.6743E-01	2.181
52	1349.	0.6890E-01	6.559
53	1379.	0.7194E-01	6.138
54	1402.	0.7439E-01	6.227
55	1428.	0.7716E-01	6.182
56	1442.	0.7867E-01	5.596
57	1469.	0.8163E-01	4.142
58	1575.	0.9391E-01	5.778
59	1604.	0.9732E-01	3.724
60	1624.	0.9976E-01	4.811
61	1639.	0.1016	5.042
62	1644.	0.1023	5.008
63	1747.	0.1155	5.906
64	1754.	0.1164	5.980
65	1778.	0.1196	5.786
66	1779.	0.1198	5.846
67	3217.	0.3916	0.9496
68	3257.	0.4014	1.127
69	3354.	0.4256	1.194
70	3360.	0.4273	1.173
71	3372.	0.4302	1.186
72	3381.	0.4326	1.194
73	3386.	0.4340	1.227
74	3425.	0.4438	1.198
75	3436.	0.4468	1.194

Zero-point vibrational energy is 128.553 kcal/mol

Standard Thermodynamic quantities at 298.15 K and 1.00 atm

```
Translational Enthalpy:        0.889 kcal/mol
Rotational Enthalpy:           0.889 kcal/mol
Vibrational Enthalpy:        133.369 kcal/mol
Translational Entropy:        41.944  cal/mol.K
Rotational Entropy:           32.226  cal/mol.K
Vibrational Entropy:          28.516  cal/mol.K
```

2-Nitrofluorene. Single Point Calculation of Electrostatic Potentials using Optimized Geometry.

```
Run type: Single point energy
Model: RHF/3-21G(*)
Number of shells:  66
  34 S shells
  32 SP shells
Number of basis functions: 162
Number of electrons: 110
Use of molecular symmetry enabled
Molecular charge:   0
Spin multiplicity:  1

Atomic Charges from Electrostatic Potential

Resolution:   1  points per atomic unit
8019 of  18981 gridpoints used in calculation

   Atom     Charge
   ----   -----------
   H  1     0.161167
   H  2     0.153258
   C  3    -0.064568
   H  4     0.173641
   C  5    -0.193810
   C  6    -0.187029
   C  7    -0.115805
   C  8     0.073367
   C  9     0.050888
   C 10     0.043656
   C 11    -0.204144
   H 12     0.172296
   C 13    -0.076833
   C 14    -0.189035
   C 15    -0.036884
   C 16    -0.183742
   C 17    -0.177986
   H 18     0.176934
   H 19     0.066637
   H 20     0.198113
   H 21     0.203375
   N 22     0.885572
   H 23     0.066637
   O 24    -0.498932
   O 25    -0.496773

Total Charge =  0.000000

RMS fit:    1.098784
RRMS fit:   0.123389

Dipole moment from formal charges:
x =   0.2326, y =   0.0000, z =   6.2801  =   6.2844 debye
```

2-Nitrofluoranthene. Geometry Optimization.

```
Run type: Geometry optimization
          Numerical Frequency
Model: RHF/3-21G(*)
Number of shells:  75
  37 S shells
  38 SP shells
Number of basis functions: 189
Number of electrons: 128
Use of molecular symmetry disabled
Molecular charge:   0
Spin multiplicity:  1

Point Group = C1  Order =  1 Nsymop =  1
This system has  78 degrees of freedom
```

Atom	Label	Cartesian Coordinates (Angstroms) X	Y	Z
H	H1	0.6726691	-0.0547210	3.5437162
C	C1	-0.0323612	-0.0410278	2.7365633
C	C11	1.6666747	-0.0145251	0.7252738
C	C2	0.3633471	-0.0223831	1.4376014
C	C3	-2.3772566	-0.0255831	2.0534084
C	C4	-0.6274001	-0.0051226	0.4326308
C	C5	-1.4270141	-0.0423586	3.0302567
C	C6	-1.9834431	-0.0059539	0.6863291
C	C7	-0.0600626	0.0130889	-0.8620284
H	H3	-1.7292650	-0.0571277	4.0582762
H	H4	-3.8977789	0.0136813	-0.3493386
H	H5	-3.4187793	-0.0270737	2.3076745
C	C8	-0.8833997	0.0310863	-1.9374216
H	H11	2.2618091	0.0344345	-2.6209711
H	H7	-0.5438370	0.0456778	-2.9487802
C	C9	-2.2783470	0.0302992	-1.6874264
N	N1	-3.1666672	0.0493470	-2.8338847
C	C10	-2.8338595	0.0128487	-0.4448612
C	C12	3.7534837	0.0080928	-1.0838098
C	C13	1.4103828	0.0069012	-0.6637107
C	C14	2.9598037	-0.0243928	1.1939103
C	C15	4.0051606	-0.0128886	0.2762196
C	C16	2.4485603	0.0181764	-1.5654799
H	H12	4.5722473	0.0166887	-1.7751104
H	H9	3.1648712	-0.0406582	2.2460083
H	H10	5.0174393	-0.0203904	0.6280396
O	O1	-4.3937659	0.0486629	-2.6204095
O	O2	-2.6432123	0.0652205	-3.9626754

```
E(HF)  =    -810.6144138 a.u.

Dipole moment:  X =   3.465612  Y =  -0.080226  Z =   4.861496
Total Dipole:   5.970850 Debye

Frequencies and reduced mass in atomic units are:
```

mode	(cm-1)	AU	mass
1	-0.1643E-04	-0.1022E-16	-0.1929E+16
2	-0.4548E-05	-0.7827E-18	-0.3103E+17
3	0.9495E-05	0.3412E-17	0.4210E+16
4	0.1249E-04	0.5902E-17	0.5377E+16
5	0.1389E-04	0.7298E-17	0.2316E+16
6	0.6222E-04	0.1465E-15	0.3443E+15
7	62.39	0.1473E-03	14.74
8	84.87	0.2726E-03	54.33
9	121.5	0.5586E-03	49.88

10	153.7	0.8935E-03	38.68
11	154.2	0.8996E-03	47.53
12	249.2	0.2350E-02	16.39
13	258.7	0.2532E-02	25.67
14	307.3	0.3575E-02	15.57
15	348.4	0.4593E-02	11.11
16	349.8	0.4632E-02	12.10
17	373.9	0.5290E-02	16.20
18	490.2	0.9092E-02	10.80
19	497.3	0.9358E-02	12.06
20	502.9	0.9572E-02	8.817
21	552.3	0.1155E-01	8.515
22	559.0	0.1183E-01	12.83
23	591.1	0.1322E-01	11.70
24	650.2	0.1600E-01	7.966
25	663.7	0.1667E-01	9.918
26	687.3	0.1788E-01	10.33
27	706.3	0.1888E-01	8.916
28	706.5	0.1889E-01	7.392
29	726.2	0.1996E-01	7.272
30	761.8	0.2196E-01	10.54
31	788.3	0.2351E-01	7.091
32	820.1	0.2545E-01	8.678
33	874.6	0.2895E-01	4.092
34	878.3	0.2919E-01	9.383
35	879.7	0.2929E-01	5.400
36	910.9	0.3140E-01	4.624
37	933.3	0.3296E-01	8.487
38	971.5	0.3571E-01	5.744
39	995.7	0.3752E-01	7.898
40	1036.	0.4066E-01	3.085
41	1080.	0.4412E-01	8.491
42	1088.	0.4480E-01	2.901
43	1106.	0.4629E-01	8.039
44	1115.	0.4706E-01	9.227
45	1119.	0.4740E-01	2.869
46	1127.	0.4808E-01	2.973
47	1152.	0.5019E-01	3.720
48	1162.	0.5107E-01	7.581
49	1177.	0.5245E-01	3.453
50	1180.	0.5271E-01	3.355
51	1195.	0.5406E-01	6.662
52	1199.	0.5437E-01	7.664
53	1243.	0.5843E-01	6.575
54	1276.	0.6158E-01	6.442
55	1282.	0.6221E-01	6.719
56	1323.	0.6622E-01	6.930
57	1336.	0.6757E-01	6.956
58	1349.	0.6889E-01	5.804
59	1371.	0.7114E-01	5.933
60	1399.	0.7405E-01	7.031
61	1410.	0.7521E-01	5.797
62	1453.	0.7994E-01	4.918
63	1487.	0.8366E-01	5.717
64	1502.	0.8543E-01	5.755
65	1539.	0.8961E-01	5.984
66	1562.	0.9230E-01	5.431
67	1597.	0.9652E-01	5.154
68	1616.	0.9882E-01	5.081
69	1625.	0.9989E-01	5.097
70	1643.	0.1022	5.273
71	1746.	0.1154	5.877
72	1780.	0.1199	5.799
73	1781.	0.1200	5.942
74	1793.	0.1216	5.903
75	1801.	0.1227	5.916
76	3354.	0.4258	1.195

77	3358.	0.4267	1.185
78	3361.	0.4275	1.177
79	3369.	0.4294	1.184
80	3372.	0.4303	1.183
81	3384.	0.4334	1.213
82	3387.	0.4340	1.226
83	3426.	0.4442	1.184
84	3437.	0.4471	1.198

Zero-point vibrational energy is 141.111 kcal/mol

Standard Thermodynamic quantities at 298.15 K and 1.00 atm

Translational Enthalpy:	0.889	kcal/mol
Rotational Enthalpy:	0.889	kcal/mol
Vibrational Enthalpy:	146.705	kcal/mol
Translational Entropy:	42.414	cal/mol.K
Rotational Entropy:	33.362	cal/mol.K
Vibrational Entropy:	32.720	cal/mol.K

2-Nitrofluoranthene. Single Point Calculation of Electrostatic Potential using Optimized Geometry.

Run type: Single point energy
Model: RHF/3-21G(*)
Number of shells: 75
37 S shells
38 SP shells
Number of basis functions: 189
Number of electrons: 128
Use of molecular symmetry disabled
Molecular charge: 0
Spin multiplicity: 1

Atomic Charges from Electrostatic Potential

Resolution: 1 points per atomic unit
8873 of 21945 gridpoints used in calculation

Atom	Charge
H 1	0.177933
C 2	-0.165209
C 3	0.017276
C 4	0.047706
C 5	-0.307326
C 6	-0.110142
C 7	-0.162604
C 8	0.306858
C 9	0.028692
H 10	0.174693
H 11	0.232674
H 12	0.202590
C 13	-0.225461
H 14	0.191477
H 15	0.216725
C 16	-0.049862
N 17	0.902664
C 18	-0.313438
C 19	-0.150350
C 20	0.076632
C 21	-0.203690
C 22	-0.146642

```
  C 23     -0.231472
  H 24      0.159273
  H 25      0.175669
  H 26      0.156029
  O 27     -0.501220
  O 28     -0.499472

Total Charge =  0.000000

RMS fit:     1.217774
RRMS fit:    0.141495

Dipole moment from formal charges:
x =    3.4819, y =  -0.0811, z =    4.9167  =    6.0253 debye
```

2-Nitropyrene. Geometry Optimization.

```
Run type: Geometry optimization
          Numerical Frequency
Model: RHF/3-21G(*)
Number of shells:  75
  37 S shells
  38 SP shells
Number of basis functions: 189
Number of electrons: 128
Use of molecular symmetry enabled
Molecular charge:   0
Spin multiplicity:  1
```

		Cartesian Coordinates (Angstroms)		
Atom	Label	X	Y	Z
N	N1	0.0000000	0.0000000	-4.5078570
C	C1	0.0000000	0.0000000	-3.0595601
H	H2	-2.1116695	0.0000000	-2.9640205
C	C2	-1.2065775	0.0000000	-2.3975347
C	C3	1.2230265	0.0000000	-1.0128223
C	C4	-1.2230265	0.0000000	-1.0128223
C	C5	1.2065775	0.0000000	-2.3975347
C	C6	0.0000000	0.0000000	-0.3084463
C	C7	-2.4581487	0.0000000	-0.2644706
H	H5	2.1116695	0.0000000	-2.9640205
C	C16	2.4562079	0.0000000	1.0725859
C	C15	2.4581487	0.0000000	-0.2644706
C	C8	-2.4562079	0.0000000	1.0725859
H	H6	-3.3793188	0.0000000	-0.8130950
H	H7	-3.3783302	0.0000000	1.6199351
C	C9	-1.2216902	0.0000000	1.8235595
C	C10	-1.2011958	0.0000000	3.2124703
C	C11	0.0000000	0.0000000	1.1196548
C	C12	0.0000000	0.0000000	3.8962804
H	H8	-2.1273374	0.0000000	3.7530007
H	H9	0.0000000	0.0000000	4.9680170
C	C13	1.2011958	0.0000000	3.2124703
H	H10	2.1273374	0.0000000	3.7530007
C	C14	1.2216902	0.0000000	1.8235595
H	H4	3.3783302	0.0000000	1.6199351
H	H11	3.3793188	0.0000000	-0.8130950
O	O1	-1.1032742	0.0000000	-5.0836528
O	O2	1.1032742	0.0000000	-5.0836528

```
E(HF)  =    -810.6387966 a.u.

Dipole moment:  X =   0.000000  Y =   0.000000  Z =   6.323348
Total Dipole:   6.323348 Debye

Frequencies and reduced mass in atomic units are:
```

mode	(cm-1)	AU	mass
1	-0.2916E-04	-0.3218E-16	-0.1125E+16
2	-0.1922E-04	-0.1398E-16	-0.6280E+15
3	0.4249E-05	0.6833E-18	0.4992E+17
4	0.5741E-05	0.1247E-17	0.1296E+17
5	0.3617E-04	0.4950E-16	0.7102E+15
6	0.4573E-04	0.7914E-16	0.2885E+15
7	62.46	0.1477E-03	71.44
8	64.55	0.1577E-03	15.44
9	176.0	0.1172E-02	34.26
10	177.1	0.1187E-02	19.04
11	182.6	0.1262E-02	29.06
12	246.1	0.2291E-02	16.86

13	287.7	0.3132E-02	18.37
14	321.3	0.3908E-02	12.27
15	352.4	0.4700E-02	10.07
16	388.8	0.5720E-02	13.02
17	454.7	0.7824E-02	11.62
18	502.3	0.9547E-02	12.21
19	524.8	0.1042E-01	13.64
20	538.6	0.1098E-01	11.88
21	558.5	0.1181E-01	11.78
22	573.0	0.1243E-01	8.726
23	591.3	0.1323E-01	7.911
24	604.3	0.1382E-01	12.77
25	606.0	0.1390E-01	7.868
26	632.4	0.1513E-01	11.08
27	641.9	0.1559E-01	12.62
28	662.5	0.1661E-01	7.936
29	786.7	0.2342E-01	8.244
30	787.3	0.2346E-01	6.668
31	790.5	0.2365E-01	6.922
32	829.1	0.2602E-01	6.343
33	849.9	0.2733E-01	9.608
34	850.4	0.2736E-01	9.781
35	886.4	0.2974E-01	2.320
36	908.7	0.3125E-01	10.04
37	931.9	0.3287E-01	2.895
38	969.4	0.3556E-01	4.859
39	980.8	0.3640E-01	7.684
40	995.9	0.3753E-01	5.611
41	1043.	0.4120E-01	7.717
42	1079.	0.4407E-01	2.818
43	1111.	0.4670E-01	8.226
44	1127.	0.4805E-01	2.711
45	1147.	0.4980E-01	3.431
46	1168.	0.5161E-01	3.647
47	1172.	0.5196E-01	3.086
48	1186.	0.5322E-01	8.561
49	1187.	0.5332E-01	3.420
50	1195.	0.5400E-01	6.444
51	1208.	0.5520E-01	7.114
52	1220.	0.5631E-01	7.672
53	1290.	0.6299E-01	7.005
54	1317.	0.6564E-01	6.432
55	1332.	0.6710E-01	7.201
56	1334.	0.6733E-01	5.948
57	1361.	0.7007E-01	6.261
58	1377.	0.7180E-01	5.989
59	1398.	0.7393E-01	6.489
60	1400.	0.7422E-01	5.974
61	1407.	0.7488E-01	6.612
62	1437.	0.7816E-01	5.793
63	1454.	0.8003E-01	5.911
64	1535.	0.8919E-01	5.868
65	1553.	0.9127E-01	5.211
66	1575.	0.9384E-01	5.927
67	1590.	0.9570E-01	4.268
68	1613.	0.9848E-01	4.274
69	1644.	0.1023	6.020
70	1661.	0.1044	5.448
71	1738.	0.1143	5.628
72	1759.	0.1170	5.950
73	1767.	0.1182	5.705
74	1797.	0.1221	5.999
75	1821.	0.1255	5.930
76	3351.	0.4250	1.154
77	3352.	0.4252	1.138
78	3354.	0.4256	1.172
79	3362.	0.4276	1.175

```
  80      3374.        0.4307        1.260
  81      3374.        0.4309        1.259
  82      3382.        0.4327        1.222
  83      3427.        0.4445        1.170
  84      3428.        0.4446        1.200

Zero-point vibrational energy is   141.700 kcal/mol

Standard Thermodynamic quantities at   298.15 K  and     1.00 atm

Translational Enthalpy:          0.889 kcal/mol
Rotational Enthalpy:             0.889 kcal/mol
Vibrational Enthalpy:          147.114 kcal/mol
Translational Entropy:          42.414  cal/mol.K
Rotational Entropy:             31.746  cal/mol.K
Vibrational Entropy:            31.336  cal/mol.K
```

2-Nitropyrene. Single Point Calculation of Electrostatic Potentials using Optimized Geometry.

```
Run type: Single point energy
Model: RHF/3-21G(*)
Number of shells:  75
  37 S shells
  38 SP shells
Number of basis functions: 189
Number of electrons: 128
Use of molecular symmetry enabled
Molecular charge:   0
Spin multiplicity:  1

Atomic Charges from Electrostatic Potential

Resolution:   1  points per atomic unit
8664 of  20387 gridpoints used in calculation

  Atom     Charge
  ----   -----------
  N  1     0.909815
  C  2    -0.045226
  H  3     0.224384
  C  4    -0.287353
  C  5     0.162158
  C  6     0.162158
  C  7    -0.287353
  C  8    -0.003910
  C  9    -0.255913
  H 10     0.224384
  C 11    -0.265745
  C 12    -0.255913
  C 13    -0.265745
  H 14     0.197266
  H 15     0.190678
  C 16     0.239888
  C 17    -0.364930
  C 18    -0.061800
  C 19    -0.050562
  H 20     0.205573
  H 21     0.161948
  C 22    -0.364930
  H 23     0.205573
  C 24     0.239888
  H 25     0.190678
```

```
  H 26      0.197266
  O 27     -0.501138
  O 28     -0.501138

Total Charge =  0.000000

RMS fit:     1.075295
RRMS fit:    0.123781

Dipole moment from formal charges:
x =    0.0000, y =    0.0000, z =    6.3711   =    6.3711 debye
```

3-Nitrobenzanthrone. Geometry Optimization.

```
Run type: Geometry optimization
          Numerical Frequency
Model: RHF/3-21G(*)
Number of shells:  81
  39 S shells
  42 SP shells
Number of basis functions: 207
Number of electrons: 142
Use of molecular symmetry disabled
Molecular charge:   0
Spin multiplicity:  1

Point Group = C1  Order =  1 Nsymop =  1
This system has  84 degrees of freedom
```

Atom	Label	Cartesian Coordinates (Angstroms) X	Y	Z
H	H1	2.0210973	0.3283494	2.0793524
C	C1	1.3664868	0.7686765	1.3606937
C	C11	0.5209577	-1.4806903	0.6986238
C	C2	0.5486150	0.0002782	0.5828173
C	C3	0.5656658	2.7944639	0.3645187
C	C4	-0.2956883	0.6484898	-0.3712244
C	C5	1.3779263	2.1596960	1.2447246
C	C6	-0.3037711	2.0606391	-0.4893818
C	C7	-1.1348349	-0.1137512	-1.2228425
H	H3	2.0302322	2.7431624	1.8541847
H	H4	-1.1622124	3.7133753	-1.5512254
N	N1	0.6568381	4.2438487	0.3599803
C	C8	-1.9296874	0.4945579	-2.1452836
C	C17	-1.1736017	-1.5889955	-1.1461904
H	H7	-2.5466833	-0.1149943	-2.7723463
C	C9	-1.9322520	1.8899203	-2.2677288
H	H8	-2.5587615	2.3574472	-2.9997222
C	C10	-1.1492748	2.6540516	-1.4638113
C	C12	0.4375777	-4.2729513	0.8760140
C	C13	-0.3051870	-2.2282568	-0.1363219
C	C14	1.3036294	-2.1640704	1.6291638
C	C15	1.2618890	-3.5393479	1.7153618
C	C16	-0.3418898	-3.6120544	-0.0450939
O	O1	-1.8913498	-2.2475997	-1.8802620
H	H9	1.9487013	-1.6322863	2.2944693
H	H10	1.8731482	-4.0401446	2.4394243
H	H11	-0.9915838	-4.1435265	-0.7087521
H	H12	0.4073944	-5.3413279	0.9450602
O	O2	1.6733279	4.7483310	0.8747773
O	O3	-0.2767091	4.9147097	-0.1189796

```
E(HF)  =    -922.7300161 a.u.

Frequencies and reduced mass in atomic units are:
```

mode	(cm-1)	AU	mass
1	-0.1788E-04	-0.1209E-16	-0.2194E+16
2	-0.1549E-04	-0.9082E-17	-0.2558E+16
3	-0.7928E-05	-0.2378E-17	-0.5221E+16
4	0.1325E-04	0.6643E-17	0.5983E+16
5	0.1854E-04	0.1301E-16	0.1962E+16
6	0.1776E-03	0.1194E-14	0.1584E+14
7	41.78	0.6606E-04	96.49
8	58.45	0.1293E-03	72.61
9	66.69	0.1683E-03	67.08
10	128.5	0.6250E-03	47.86

11	189.2	0.1355E-02	17.54
12	197.7	0.1479E-02	30.05
13	207.8	0.1634E-02	26.58
14	267.8	0.2713E-02	14.69
15	288.4	0.3147E-02	14.22
16	339.1	0.4351E-02	15.06
17	358.2	0.4856E-02	10.91
18	392.8	0.5839E-02	13.97
19	397.2	0.5971E-02	11.89
20	431.0	0.7029E-02	10.99
21	482.2	0.8798E-02	9.350
22	510.2	0.9849E-02	11.93
23	513.6	0.9982E-02	9.508
24	536.7	0.1090E-01	10.47
25	545.6	0.1127E-01	10.22
26	603.7	0.1379E-01	8.772
27	625.8	0.1482E-01	11.21
28	646.6	0.1582E-01	10.88
29	681.8	0.1759E-01	9.756
30	704.4	0.1877E-01	8.019
31	741.1	0.2079E-01	7.379
32	744.0	0.2095E-01	11.48
33	756.4	0.2165E-01	8.008
34	788.5	0.2353E-01	6.774
35	842.0	0.2683E-01	8.356
36	845.2	0.2703E-01	6.673
37	882.7	0.2948E-01	10.35
38	892.8	0.3016E-01	4.350
39	899.8	0.3064E-01	8.200
40	935.0	0.3308E-01	3.586
41	962.7	0.3507E-01	5.713
42	999.7	0.3782E-01	7.625
43	1029.	0.4004E-01	3.143
44	1030.	0.4013E-01	4.728
45	1052.	0.4186E-01	7.798
46	1095.	0.4537E-01	5.314
47	1127.	0.4807E-01	8.302
48	1150.	0.5001E-01	8.142
49	1156.	0.5054E-01	2.850
50	1166.	0.5141E-01	3.486
51	1187.	0.5331E-01	7.265
52	1208.	0.5521E-01	3.593
53	1211.	0.5547E-01	3.659
54	1215.	0.5582E-01	7.449
55	1220.	0.5637E-01	3.949
56	1236.	0.5784E-01	7.456
57	1270.	0.6105E-01	6.326
58	1287.	0.6267E-01	6.715
59	1301.	0.6408E-01	7.015
60	1321.	0.6604E-01	6.694
61	1324.	0.6629E-01	6.911
62	1344.	0.6835E-01	6.053
63	1359.	0.6988E-01	5.412
64	1365.	0.7049E-01	5.995
65	1398.	0.7394E-01	6.629
66	1413.	0.7551E-01	6.261
67	1437.	0.7810E-01	6.264
68	1452.	0.7980E-01	5.935
69	1467.	0.8148E-01	5.879
70	1531.	0.8876E-01	5.452
71	1580.	0.9446E-01	5.406
72	1616.	0.9886E-01	4.913
73	1634.	0.1011	4.861
74	1657.	0.1040	5.140
75	1662.	0.1045	5.390
76	1740.	0.1146	5.891
77	1747.	0.1156	5.866

78	1773.	0.1189	5.781
79	1778.	0.1196	5.840
80	1794.	0.1218	5.923
81	1896.	0.1360	6.620
82	3364.	0.4284	1.189
83	3380.	0.4324	1.197
84	3383.	0.4331	1.182
85	3402.	0.4380	1.191
86	3404.	0.4385	1.190
87	3407.	0.4393	1.214
88	3430.	0.4452	1.175
89	3444.	0.4488	1.183
90	3483.	0.4590	1.183

Zero-point vibrational energy is 149.287 kcal/mol

Standard Thermodynamic quantities at 298.15 K and 1.00 atm

Translational Enthalpy:	0.889	kcal/mol
Rotational Enthalpy:	0.889	kcal/mol
Vibrational Enthalpy:	155.776	kcal/mol
Translational Entropy:	42.734	cal/mol.K
Rotational Entropy:	33.812	cal/mol.K
Vibrational Entropy:	39.732	cal/mol.K

3-Nitrobenzanthrone. Single Point Calculation of Electrostatic Potentials using Optimized Geometry.

Run type: Single point energy
Model: RHF/3-21G(*)
Number of shells: 81
39 S shells
42 SP shells
Number of basis functions: 207
Number of electrons: 142
Use of molecular symmetry disabled
Molecular charge: 0
Spin multiplicity: 1

Atomic Charges from Electrostatic Potential

Resolution: 1 points per atomic unit
9094 of 26973 gridpoints used in calculation

Atom	Charge
H 1	0.176666
C 2	-0.163902
C 3	0.216767
C 4	-0.140648
C 5	-0.230988
C 6	0.187493
C 7	-0.104459
C 8	0.141746
C 9	-0.372738
H 10	0.200437
H 11	0.230138
N 12	0.937871
C 13	0.022704
C 14	0.756635
H 15	0.160267
C 16	-0.198244
H 17	0.173385

```
  C 18    -0.229995
  C 19    -0.185130
  C 20    -0.239995
  C 21    -0.286318
  C 22    -0.073981
  C 23    -0.083237
  O 24    -0.563888
  H 25     0.187429
  H 26     0.152208
  H 27     0.172438
  H 28     0.162212
  O 29    -0.501703
  O 30    -0.503170

Total Charge =  0.000000

RMS fit:    1.109441
RRMS fit:   0.132932

Dipole moment from formal charges:
x =   1.4589, y =  -3.7790, z =   1.7727  =   4.4217 debye
```

3-Nitrofluoranthene. Geometry Optimization.

```
Run type: Geometry optimization
          Numerical Frequency
Model: RHF/3-21G(*)
Number of shells:  75
  37 S shells
  38 SP shells
Number of basis functions: 189
Number of electrons: 128
Use of molecular symmetry disabled
Molecular charge:   0
Spin multiplicity:  1

Point Group = C1  Order =  1 Nsymop =  1
This system has  78 degrees of freedom
```

Atom	Label	Cartesian Coordinates (Angstroms) X	Y	Z
H	H1	3.3271280	-0.0035377	-0.7823854
C	C1	2.5252208	-0.0141724	-0.0717380
C	C11	0.5181973	0.0356749	-1.7574705
C	C2	1.2245607	0.0024078	-0.4510156
C	C3	1.8477757	-0.0618609	2.2789049
C	C4	0.2186094	-0.0132252	0.5424005
C	C5	2.8151654	-0.0467254	1.3187521
C	C6	0.4711162	-0.0449168	1.9035075
C	C7	-1.0710673	0.0077181	-0.0389856
H	H3	3.8424692	-0.0599513	1.6243174
N	N1	-0.6411725	-0.0882454	4.1659994
H	H5	2.1112779	-0.0862568	3.3089227
C	C8	-2.1606347	-0.0033615	0.7718082
H	H11	-2.8268367	0.0698882	-2.3593729
H	H7	-3.1616377	0.0113151	0.3929766
C	C9	-1.9474971	-0.0355665	2.1648722
H	H8	-2.7830522	-0.0450658	2.8282292
C	C10	-0.7004132	-0.0556914	2.7201716
C	C12	-1.2867547	0.0930244	-3.8486852
C	C13	-0.8694369	0.0388454	-1.5067910
C	C14	0.9907845	0.0611397	-3.0478771
C	C15	0.0738881	0.0899345	-4.0952082
C	C16	-1.7708644	0.0673435	-2.5442885
H	H12	-1.9755664	0.1153780	-4.6691314
H	H9	2.0431631	0.0590236	-3.2510138
H	H10	0.4287159	0.1099611	-5.1063119
O	O1	-1.7190278	-0.0958445	4.7938776
O	O2	0.4758891	-0.1072322	4.7155347

```
E(HF)  =     -810.6120438 a.u.

Dipole moment:  X =    0.190688  Y =    0.131462  Z =   -5.975425
Total Dipole:   5.979912 Debye

Frequencies and reduced mass in atomic units are:
```

mode	(cm-1)	AU	mass
1	-0.1318E-04	-0.6579E-17	-0.2640E+16
2	0.6661E-05	0.1679E-17	0.4930E+16
3	0.1465E-04	0.8125E-17	0.4167E+16
4	0.1782E-04	0.1201E-16	0.2509E+16
5	0.1824E-04	0.1259E-16	0.2212E+16
6	0.3811E-04	0.5498E-16	0.8809E+15
7	33.72	0.4304E-04	32.53
8	69.77	0.1842E-03	56.45
9	128.8	0.6277E-03	53.39

10	164.7	0.1027E-02	27.64
11	183.0	0.1268E-02	43.47
12	198.7	0.1493E-02	27.12
13	276.5	0.2894E-02	15.83
14	311.5	0.3672E-02	13.52
15	327.4	0.4056E-02	17.60
16	383.4	0.5563E-02	9.921
17	403.3	0.6154E-02	10.69
18	485.7	0.8926E-02	13.17
19	492.1	0.9165E-02	10.17
20	506.8	0.9722E-02	8.324
21	535.4	0.1085E-01	10.55
22	565.9	0.1212E-01	11.51
23	615.6	0.1434E-01	11.46
24	633.7	0.1520E-01	12.27
25	644.2	0.1570E-01	8.429
26	661.3	0.1655E-01	9.959
27	714.8	0.1933E-01	6.904
28	718.9	0.1956E-01	9.314
29	740.7	0.2076E-01	7.237
30	762.3	0.2199E-01	10.70
31	804.1	0.2447E-01	6.662
32	828.1	0.2595E-01	8.634
33	871.5	0.2874E-01	5.298
34	877.9	0.2917E-01	9.775
35	883.7	0.2955E-01	4.685
36	907.5	0.3116E-01	8.784
37	919.9	0.3202E-01	4.330
38	996.1	0.3755E-01	5.753
39	1006.	0.3828E-01	7.959
40	1025.	0.3979E-01	2.720
41	1046.	0.4140E-01	3.614
42	1095.	0.4538E-01	8.049
43	1098.	0.4566E-01	3.008
44	1110.	0.4666E-01	8.957
45	1126.	0.4796E-01	2.871
46	1127.	0.4803E-01	7.598
47	1169.	0.5176E-01	7.306
48	1181.	0.5277E-01	3.345
49	1193.	0.5386E-01	3.142
50	1198.	0.5429E-01	7.906
51	1211.	0.5551E-01	6.814
52	1215.	0.5583E-01	3.388
53	1268.	0.6088E-01	6.562
54	1277.	0.6171E-01	6.553
55	1282.	0.6216E-01	6.740
56	1313.	0.6524E-01	7.218
57	1331.	0.6706E-01	6.311
58	1339.	0.6788E-01	5.915
59	1364.	0.7045E-01	6.178
60	1401.	0.7425E-01	6.532
61	1416.	0.7588E-01	6.398
62	1451.	0.7968E-01	5.153
63	1478.	0.8264E-01	6.104
64	1494.	0.8444E-01	5.767
65	1540.	0.8970E-01	5.760
66	1566.	0.9280E-01	5.060
67	1592.	0.9591E-01	5.082
68	1617.	0.9893E-01	5.089
69	1628.	0.1002	4.972
70	1641.	0.1019	5.190
71	1749.	0.1157	5.880
72	1766.	0.1180	5.918
73	1778.	0.1196	5.800
74	1792.	0.1215	5.906
75	1799.	0.1225	5.938
76	3355.	0.4260	1.195

```
  77     3362.       0.4277        1.193
  78     3363.       0.4281        1.184
  79     3374.       0.4308        1.183
  80     3380.       0.4322        1.186
  81     3387.       0.4342        1.220
  82     3389.       0.4345        1.212
  83     3438.       0.4473        1.172
  84     3480.       0.4582        1.180

Zero-point vibrational energy is   141.321 kcal/mol

Standard Thermodynamic quantities at   298.15 K  and     1.00 atm

Translational Enthalpy:         0.889 kcal/mol
Rotational Enthalpy:            0.889 kcal/mol
Vibrational Enthalpy:         146.926 kcal/mol
Translational Entropy:         42.414  cal/mol.K
Rotational Entropy:            33.134  cal/mol.K
Vibrational Entropy:           33.884  cal/mol.K
```

3-Nitrofluoranthene. Single Point Calculation of Electrostatic Potentials using Optimized Geometry.

```
Run type: Single point energy
Model: RHF/3-21G(*)
Number of shells:  75
  37 S shells
  38 SP shells
Number of basis functions: 189
Number of electrons: 128
Use of molecular symmetry disabled
Molecular charge:   0
Spin multiplicity:  1

Atomic Charges from Electrostatic Potential

Resolution:   1  points per atomic unit
8538 of  20615 gridpoints used in calculation

  Atom     Charge
  ----   -----------
  H  1     0.173615
  C  2    -0.163656
  C  3     0.038734
  C  4    -0.035235
  C  5    -0.363747
  C  6    -0.017801
  C  7    -0.098962
  C  8     0.272019
  C  9     0.046873
  H 10     0.155062
  N 11     0.984789
  H 12     0.254656
  C 13    -0.243069
  H 14     0.177796
  H 15     0.195355
  C 16    -0.075559
  H 17     0.201522
  C 18    -0.317494
  C 19    -0.178046
  C 20     0.054357
  C 21    -0.188865
  C 22    -0.153255
```

```
  C 23     -0.191253
  H 24      0.168343
  H 25      0.177563
  H 26      0.163427
  O 27     -0.520039
  O 28     -0.517133

Total Charge =  0.000000

RMS fit:     1.151437
RRMS fit:    0.131848

Dipole moment from formal charges:
x =    0.1510, y =  -0.0164, z =  -6.0341  =    6.0360 debye
```

3-Nitrofluorene. Geometry Optimization.

```
Run type: Geometry optimization
          Numerical Frequency
Model: RHF/3-21G(*)
Number of shells:  66
  34 S shells
  32 SP shells
Number of basis functions: 162
Number of electrons: 110
Use of molecular symmetry enabled
Molecular charge:   0
Spin multiplicity:  1

Point Group = CS  Order =  1 Nsymop =  2
This system has  46 degrees of freedom
```

Atom	Label	Cartesian Coordinates (Angstroms) X	Y	Z
H	H9	-1.2515739	0.0000000	3.8115924
H	H10	1.0160754	0.0000000	4.7645432
C	C11	-0.5437596	0.0000000	1.7964759
H	H12	2.9790808	0.0000000	3.3026096
C	C16	1.8505625	0.0000000	1.4947789
C	C14	-0.3956648	0.0000000	3.1653372
C	C15	0.8854299	0.0000000	3.7007263
C	C13	0.5755740	0.0000000	0.9642997
C	C1	0.1185264	0.0000000	-0.4372090
C	C7	-1.8212367	0.0000000	0.9664561
C	C12	1.9972866	0.0000000	2.8730413
H	H11	2.7132180	0.0000000	0.8581827
C	C2	-1.2555768	0.0000000	-2.8351908
C	C3	0.8341103	0.0000000	-1.6124047
C	C4	-1.2795959	0.0000000	-0.4555345
C	C5	-1.9689809	0.0000000	-1.6484598
C	C6	0.1230362	0.0000000	-2.7972486
H	H1	1.9012433	0.0000000	-1.6404467
H	H8	-2.4216909	0.8834694	1.1563555
H	H4	-3.0401334	0.0000000	-1.6683484
N	N1	0.8551040	0.0000000	-4.0465305
H	H6	-1.7455043	0.0000000	-3.7832127
H	H3	-2.4216909	-0.8834694	1.1563555
O	O1	2.0987862	0.0000000	-3.9833439
O	O2	0.1973746	0.0000000	-5.1028246

```
E(HF)  =     -697.6459541 a.u.

Dipole moment:  X =  -2.967381  Y =   0.000000  Z =   5.363829
Total Dipole:   6.129928 Debye

Frequencies and reduced mass in atomic units are:
```

mode	(cm-1)	AU	mass
1	-0.4279E-04	-0.6930E-16	-0.9857E+15
2	0.1328E-04	0.6669E-17	0.3018E+16
3	0.1337E-04	0.6765E-17	0.3477E+16
4	0.1340E-04	0.6799E-17	0.3682E+16
5	0.2177E-04	0.1793E-16	0.2509E+16
6	0.2726E-04	0.2812E-16	0.8319E+15
7	62.13	0.1461E-03	39.73
8	87.19	0.2877E-03	73.82
9	127.0	0.6107E-03	82.95
10	147.5	0.8231E-03	55.60
11	205.9	0.1605E-02	42.18
12	292.7	0.3242E-02	23.84

13	297.3	0.3345E-02	18.80
14	346.9	0.4555E-02	12.75
15	352.3	0.4697E-02	13.16
16	483.9	0.8860E-02	11.95
17	499.2	0.9429E-02	12.97
18	500.6	0.9485E-02	11.65
19	509.3	0.9817E-02	10.95
20	551.3	0.1150E-01	8.676
21	587.9	0.1308E-01	10.96
22	655.1	0.1624E-01	10.44
23	657.2	0.1634E-01	7.680
24	717.3	0.1947E-01	11.38
25	739.8	0.2071E-01	9.664
26	776.3	0.2280E-01	6.986
27	811.8	0.2494E-01	7.366
28	823.8	0.2568E-01	9.330
29	853.6	0.2757E-01	9.434
30	857.0	0.2779E-01	5.438
31	880.1	0.2932E-01	9.205
32	902.2	0.3080E-01	5.643
33	950.9	0.3422E-01	8.697
34	984.0	0.3665E-01	4.100
35	1024.	0.3968E-01	3.178
36	1075.	0.4377E-01	5.211
37	1114.	0.4700E-01	9.414
38	1133.	0.4855E-01	3.316
39	1139.	0.4909E-01	3.438
40	1148.	0.4986E-01	8.239
41	1182.	0.5289E-01	3.367
42	1188.	0.5341E-01	7.363
43	1198.	0.5429E-01	3.430
44	1215.	0.5589E-01	7.645
45	1228.	0.5707E-01	6.698
46	1253.	0.5937E-01	6.545
47	1281.	0.6205E-01	6.384
48	1293.	0.6324E-01	6.554
49	1316.	0.6557E-01	6.111
50	1332.	0.6714E-01	5.696
51	1334.	0.6730E-01	2.177
52	1339.	0.6782E-01	7.192
53	1385.	0.7264E-01	6.212
54	1399.	0.7404E-01	6.171
55	1431.	0.7746E-01	4.943
56	1432.	0.7762E-01	6.404
57	1473.	0.8210E-01	4.310
58	1582.	0.9468E-01	5.856
59	1598.	0.9661E-01	3.903
60	1618.	0.9903E-01	4.600
61	1638.	0.1016	5.028
62	1649.	0.1029	4.969
63	1750.	0.1159	5.893
64	1754.	0.1165	6.020
65	1779.	0.1197	5.827
66	1781.	0.1201	5.796
67	3215.	0.3913	0.9495
68	3256.	0.4013	1.124
69	3352.	0.4253	1.194
70	3359.	0.4271	1.176
71	3371.	0.4300	1.185
72	3374.	0.4308	1.199
73	3386.	0.4339	1.226
74	3431.	0.4456	1.191
75	3436.	0.4468	1.193

Zero-point vibrational energy is 128.521 kcal/mol

Standard Thermodynamic quantities at 298.15 K and 1.00 atm

```
Translational Enthalpy:        0.889 kcal/mol
Rotational Enthalpy:           0.889 kcal/mol
Vibrational Enthalpy:        133.335 kcal/mol
Translational Entropy:        41.944  cal/mol.K
Rotational Entropy:           32.346  cal/mol.K
Vibrational Entropy:          28.397  cal/mol.K
```

3-Nitrofluorene. Single Point Calculation of Electrostatic Potentials using Optimized Geometry.

```
Run type: Single point energy
Model: RHF/3-21G(*)
Number of shells:  66
  34 S shells
  32 SP shells
Number of basis functions: 162
Number of electrons: 110
Use of molecular symmetry enabled
Molecular charge:   0
Spin multiplicity:  1

Atomic Charges from Electrostatic Potential

Resolution:   1  points per atomic unit
8145 of  20387 gridpoints used in calculation

  Atom     Charge
  ----   -----------
  H  1     0.168910
  H  2     0.151915
  C  3     0.089906
  H  4     0.165868
  C  5    -0.111917
  C  6    -0.239291
  C  7    -0.113936
  C  8    -0.120074
  C  9     0.123976
  C 10    -0.105054
  C 11    -0.204653
  H 12     0.159933
  C 13    -0.113792
  C 14    -0.214275
  C 15     0.035140
  C 16    -0.237582
  C 17    -0.101394
  H 18     0.212875
  H 19     0.096786
  H 20     0.183334
  N 21     0.865006
  H 22     0.185744
  H 23     0.096786
  O 24    -0.489214
  O 25    -0.484998

Total Charge =  0.000000

RMS fit:    1.171258
RRMS fit:   0.132867

Dipole moment from formal charges:
x =  -2.9629, y =   0.0000, z =   5.4030  =   6.1620 debye
```

4-Nitropyrene. Geometry Optimization.

```
Run type: Geometry optimization
          Numerical Frequency
Model: RHF/3-21G(*)
Number of shells:  75
  37 S shells
  38 SP shells
Number of basis functions: 189
Number of electrons: 128
Use of molecular symmetry disabled
Molecular charge:   0
Spin multiplicity:  1

Point Group = C1  Order =  1 Nsymop =  1
This system has  78 degrees of freedom
```

Atom	Label	Cartesian Coordinates (Angstroms) X	Y	Z
H	H3	-1.0061997	2.6966218	-3.4246860
C	C1	-0.8379281	2.0217869	-2.6095074
H	H2	1.1006008	2.7876611	-2.2231658
C	C2	0.3663972	2.0761882	-1.9334000
C	C3	-1.6040952	0.2450921	-1.1959906
C	C4	0.6244269	1.2147322	-0.8721907
C	C5	-1.8172796	1.1237600	-2.2491354
C	C6	-0.3770762	0.2790663	-0.4998408
C	C7	1.8635032	1.1746061	-0.1125402
H	H5	-2.7493818	1.0954905	-2.7784050
C	C16	-2.4129530	-1.5604322	0.2111689
C	C15	-2.6135953	-0.7078772	-0.7977977
C	C8	2.0585190	0.2985848	0.8814832
N	N1	2.9770011	2.0731766	-0.3740909
H	H7	2.9948646	0.3060424	1.3941665
C	C9	1.0545433	-0.6386825	1.2735576
C	C10	1.2631841	-1.5334070	2.3168821
C	C11	-0.1656398	-0.6419745	0.5746996
C	C12	0.2743339	-2.4285237	2.6707901
H	H8	2.1976832	-1.5224865	2.8424951
H	H9	0.4391456	-3.1162426	3.4754162
C	C13	-0.9288760	-2.4421402	1.9893179
H	H10	-1.6923152	-3.1417661	2.2685713
C	C14	-1.1694615	-1.5619593	0.9411376
H	H4	-3.1704621	-2.2629806	0.4981052
H	H11	-3.5380125	-0.7103368	-1.3412935
O	O1	4.0835724	1.7755463	0.1222198
O	O2	2.7855008	3.1004537	-1.0479675

```
E(HF)  =     -810.6326745 a.u.

Dipole moment:  X =  -4.255358  Y =  -3.681990  Z =   1.205392
Total Dipole:   5.754832 Debye

Frequencies and reduced mass in atomic units are:
```

mode	(cm-1)	AU	mass
1	-0.4334E-04	-0.7108E-16	-0.4387E+15
2	-0.2509E-04	-0.2382E-16	-0.7611E+15
3	-0.2051E-04	-0.1593E-16	-0.1929E+16
4	0.6641E-05	0.1669E-17	0.6694E+16
5	0.1066E-04	0.4301E-17	0.5698E+16
6	0.2269E-04	0.1948E-16	0.2080E+16
7	39.66	0.5951E-04	24.08
8	76.10	0.2192E-03	72.73
9	127.4	0.6145E-03	35.70

10	178.8	0.1210E-02	32.03
11	235.9	0.2107E-02	18.09
12	261.5	0.2589E-02	18.42
13	295.2	0.3298E-02	15.51
14	333.9	0.4218E-02	11.14
15	334.8	0.4241E-02	12.24
16	397.4	0.5977E-02	14.22
17	429.1	0.6968E-02	12.15
18	466.9	0.8250E-02	12.44
19	475.5	0.8556E-02	11.87
20	528.3	0.1056E-01	13.88
21	560.4	0.1189E-01	12.17
22	563.1	0.1200E-01	9.478
23	586.8	0.1303E-01	8.382
24	614.1	0.1427E-01	13.43
25	632.4	0.1514E-01	7.465
26	663.1	0.1664E-01	8.598
27	689.2	0.1797E-01	9.125
28	705.8	0.1885E-01	10.07
29	762.1	0.2198E-01	7.116
30	780.8	0.2307E-01	9.679
31	809.1	0.2477E-01	6.945
32	811.5	0.2492E-01	9.306
33	856.2	0.2774E-01	5.818
34	865.1	0.2832E-01	9.091
35	898.6	0.3056E-01	4.027
36	909.9	0.3133E-01	9.507
37	914.9	0.3168E-01	3.902
38	973.6	0.3587E-01	8.216
39	982.5	0.3653E-01	4.460
40	1018.	0.3919E-01	5.774
41	1067.	0.4311E-01	7.237
42	1084.	0.4445E-01	2.774
43	1107.	0.4635E-01	2.876
44	1116.	0.4710E-01	8.266
45	1162.	0.5107E-01	3.064
46	1172.	0.5202E-01	3.382
47	1183.	0.5297E-01	8.675
48	1188.	0.5338E-01	5.016
49	1193.	0.5390E-01	5.715
50	1196.	0.5415E-01	3.853
51	1219.	0.5621E-01	7.895
52	1228.	0.5703E-01	7.037
53	1296.	0.6359E-01	7.097
54	1308.	0.6472E-01	6.927
55	1325.	0.6649E-01	6.104
56	1326.	0.6657E-01	6.486
57	1348.	0.6877E-01	6.050
58	1364.	0.7036E-01	5.968
59	1377.	0.7173E-01	6.491
60	1388.	0.7294E-01	6.359
61	1408.	0.7502E-01	6.469
62	1427.	0.7709E-01	5.597
63	1458.	0.8045E-01	6.123
64	1530.	0.8860E-01	5.861
65	1546.	0.9046E-01	5.382
66	1577.	0.9406E-01	5.692
67	1598.	0.9658E-01	4.839
68	1605.	0.9746E-01	4.368
69	1657.	0.1039	5.519
70	1666.	0.1051	5.393
71	1735.	0.1139	5.645
72	1754.	0.1164	5.902
73	1764.	0.1177	5.751
74	1792.	0.1215	5.946
75	1818.	0.1251	5.940
76	3351.	0.4250	1.137

```
  77      3356.        0.4262        1.188
  78      3359.        0.4270        1.180
  79      3363.        0.4279        1.173
  80      3374.        0.4309        1.258
  81      3380.        0.4324        1.213
  82      3385.        0.4337        1.222
  83      3428.        0.4446        1.183
  84      3485.        0.4597        1.175

Zero-point vibrational energy is   141.872 kcal/mol

Standard Thermodynamic quantities at   298.15 K  and     1.00 atm

Translational Enthalpy:          0.889 kcal/mol
Rotational Enthalpy:             0.889 kcal/mol
Vibrational Enthalpy:          147.295 kcal/mol
Translational Entropy:          42.414  cal/mol.K
Rotational Entropy:             33.051  cal/mol.K
Vibrational Entropy:            31.991  cal/mol.K
```

4-Nitropyrene. Single Point Calculation of Electrostatic Potentials using Optimized Geometry.

```
Run type: Single point energy
Model: RHF/3-21G(*)
Number of shells:  75
  37 S shells
  38 SP shells
Number of basis functions: 189
Number of electrons: 128
Use of molecular symmetry disabled
Molecular charge:   0
Spin multiplicity:  1

Atomic Charges from Electrostatic Potential

Resolution:   1  points per atomic unit
8128 of  27753 gridpoints used in calculation

  Atom      Charge
  ----    -----------
  H  1      0.156996
  C  2     -0.078531
  H  3      0.247802
  C  4     -0.336078
  C  5      0.202277
  C  6      0.172244
  C  7     -0.299470
  C  8     -0.042393
  C  9     -0.228941
  H 10      0.190175
  C 11     -0.227437
  C 12     -0.286407
  C 13     -0.168653
  N 14      0.942511
  H 15      0.208287
  C 16      0.165468
  C 17     -0.311481
  C 18     -0.020572
  C 19     -0.083086
  H 20      0.205357
  H 21      0.161185
  C 22     -0.294083
```

```
  H 23      0.197287
  C 24      0.163299
  H 25      0.183740
  H 26      0.194953
  O 27     -0.509594
  O 28     -0.504857

Total Charge =  0.000000

RMS fit:     1.122751
RRMS fit:    0.130041

Dipole moment from formal charges:
x =  -4.3050, y =  -3.7295, z =   1.1910  =   5.8190 debye
```

5-Nitroacenaphthene. Geometry Optimization.

```
Run type: Geometry optimization
          Numerical Frequency
Model: RHF/3-21G(*)
Number of shells:  63
  33 S shells
  30 SP shells
Number of basis functions: 153
Number of electrons: 104
Use of molecular symmetry disabled
Molecular charge:   0
Spin multiplicity:  1

Point Group = C1  Order =  1 Nsymop =  1
This system has  66 degrees of freedom
```

Atom	Label	Cartesian Coordinates (Angstroms) X	Y	Z
H	H1	-3.5158977	-0.0836302	1.4106567
C	C1	-2.5573228	-0.0603634	0.9306364
H	H2	-1.5193506	-0.0462794	2.7705772
C	C2	-1.4376908	-0.0394821	1.7107302
C	C3	-1.2966401	-0.0232360	-1.0859207
C	C4	-0.1533564	-0.0084574	1.1050753
C	C5	-2.5109585	-0.0526968	-0.4845115
C	C6	-0.1344580	-0.0014804	-0.2919036
C	C7	1.1364327	0.0168852	1.7165722
H	H3	-3.4219416	-0.0700315	-1.0489431
C	C11	0.6727110	0.0265705	-2.5417642
C	C12	-0.9007994	-0.0076060	-2.5588605
C	C8	2.2738974	0.0453812	0.9605646
N	N1	1.3201336	0.0139997	3.1493354
H	H7	3.2078670	0.0633707	1.4762557
C	C9	2.2489733	0.0514418	-0.4448209
H	H8	3.1704046	0.0741651	-0.9895788
C	C10	1.0397576	0.0278347	-1.0642793
H	H4	1.0515334	0.9160116	-3.0294865
H	H11	-1.2640317	-0.8921832	-3.0664006
H	H10	1.0897113	-0.8411614	-3.0373911
H	H5	-1.3022397	0.8651793	-3.0579695
O	O1	2.4895215	0.0370444	3.5887376
O	O2	0.3137438	-0.0112762	3.8826892

```
E(HF)  =    -659.9852718 a.u.

Dipole moment:  X =  -1.174141  Y =   0.005408  Z =  -6.516891
Total Dipole:   6.621820 Debye

Frequencies and reduced mass in atomic units are:
```

mode	(cm-1)	AU	mass
1	-0.1197E-03	-0.5419E-15	-0.6410E+14
2	-0.2792E-04	-0.2950E-16	-0.4210E+15
3	-0.1670E-04	-0.1056E-16	-0.3104E+16
4	-0.1664E-04	-0.1048E-16	-0.8242E+16
5	-0.1283E-04	-0.6230E-17	-0.7363E+16
6	0.9809E-05	0.3641E-17	0.9160E+16
7	36.79	0.5121E-04	63.34
8	88.61	0.2971E-03	488.9
9	113.5	0.4876E-03	187.2
10	195.5	0.1447E-02	28.58
11	253.2	0.2427E-02	30.43
12	253.4	0.2431E-02	17.77
13	348.4	0.4594E-02	12.20

14	366.9	0.5093E-02	12.16
15	406.4	0.6249E-02	10.75
16	497.3	0.9360E-02	14.00
17	515.5	0.1006E-01	9.508
18	543.3	0.1117E-01	10.34
19	584.3	0.1292E-01	12.75
20	602.9	0.1376E-01	10.33
21	627.8	0.1492E-01	11.83
22	663.4	0.1665E-01	7.331
23	708.7	0.1901E-01	11.37
24	712.2	0.1920E-01	8.089
25	762.1	0.2198E-01	8.782
26	789.7	0.2360E-01	6.962
27	854.5	0.2763E-01	8.740
28	860.1	0.2799E-01	6.344
29	893.4	0.3021E-01	10.15
30	912.5	0.3151E-01	3.529
31	958.6	0.3478E-01	8.130
32	987.2	0.3688E-01	7.937
33	998.8	0.3775E-01	5.967
34	1008.	0.3848E-01	3.419
35	1079.	0.4403E-01	3.372
36	1080.	0.4415E-01	7.661
37	1123.	0.4773E-01	7.502
38	1148.	0.4985E-01	5.827
39	1195.	0.5402E-01	3.294
40	1195.	0.5403E-01	7.252
41	1218.	0.5616E-01	3.401
42	1222.	0.5648E-01	6.939
43	1277.	0.6169E-01	6.697
44	1303.	0.6420E-01	7.219
45	1331.	0.6704E-01	6.303
46	1338.	0.6778E-01	3.059
47	1343.	0.6829E-01	6.046
48	1367.	0.7072E-01	6.337
49	1383.	0.7234E-01	3.960
50	1392.	0.7334E-01	2.143
51	1411.	0.7533E-01	6.819
52	1423.	0.7664E-01	5.717
53	1464.	0.8110E-01	5.900
54	1487.	0.8373E-01	4.827
55	1558.	0.9183E-01	4.995
56	1574.	0.9372E-01	5.503
57	1611.	0.9821E-01	4.807
58	1627.	0.1002	4.343
59	1645.	0.1024	4.889
60	1647.	0.1027	4.450
61	1755.	0.1165	5.890
62	1776.	0.1193	5.895
63	1793.	0.1216	5.914
64	3227.	0.3942	0.9449
65	3239.	0.3970	0.9413
66	3262.	0.4027	1.202
67	3282.	0.4077	1.088
68	3358.	0.4268	1.199
69	3376.	0.4312	1.189
70	3382.	0.4328	1.206
71	3439.	0.4476	1.172
72	3484.	0.4594	1.178

Zero-point vibrational energy is 124.881 kcal/mol

Standard Thermodynamic quantities at 298.15 K and 1.00 atm

Translational Enthalpy: 0.889 kcal/mol
Rotational Enthalpy: 0.889 kcal/mol
Vibrational Enthalpy: 129.379 kcal/mol

```
Translational Entropy:        41.770  cal/mol.K
Rotational Entropy:           31.651  cal/mol.K
Vibrational Entropy:          27.391  cal/mol.K
```

5-Nitroacenaphthene. Single Point Calculation of Electrostatic Potentials using Optimized Geometry.

```
Run type: Single point energy
Model: RHF/3-21G(*)
Number of shells:  63
  33 S shells
  30 SP shells
Number of basis functions: 153
Number of electrons: 104
Use of molecular symmetry disabled
Molecular charge:   0
Spin multiplicity:  1

Atomic Charges from Electrostatic Potential

Resolution:   1  points per atomic unit
7225 of  18183 gridpoints used in calculation

  Atom     Charge
  ----   -----------
  H  1     0.151362
  C  2    -0.030294
  H  3     0.253006
  C  4    -0.428700
  C  5     0.108759
  C  6     0.371918
  C  7    -0.302029
  C  8    -0.206634
  C  9    -0.365643
  H 10     0.179671
  C 11    -0.091051
  C 12    -0.033670
  C 13     0.013852
  N 14     0.954985
  H 15     0.190309
  C 16    -0.383254
  H 17     0.201345
  C 18     0.201597
  H 19     0.068869
  H 20     0.053984
  H 21     0.066961
  H 22     0.052185
  O 23    -0.519943
  O 24    -0.507584

Total Charge =  0.000000

RMS fit:     0.940457
RRMS fit:    0.099255

Dipole moment from formal charges:
x =  -1.2087, y =   0.0053, z =  -6.5383  =   6.6490 debye
```

7-Nitrofluoranthene. Geometry Optimization.

```
Run type: Geometry optimization
          Numerical Frequency
Model: RHF/3-21G(*)
Number of shells:  75
  37 S shells
  38 SP shells
Number of basis functions: 189
Number of electrons: 128
Use of molecular symmetry disabled
Molecular charge:   0
Spin multiplicity:  1

Point Group = C1  Order =  1 Nsymop =  1
This system has  78 degrees of freedom
```

Atom	Label	Cartesian Coordinates (Angstroms) X	Y	Z
H	H1	2.8644179	1.1645838	0.4426570
C	C1	1.9946332	0.8635086	0.9739055
C	C11	0.4911234	0.0980090	-1.0869839
C	C2	0.9009373	0.3636449	0.3301322
C	C3	0.8990220	0.5954145	3.1408119
C	C4	-0.2082008	-0.0216345	1.1246334
C	C5	1.9706860	0.9747440	2.3908566
C	C6	-0.2548455	0.0695233	2.5026377
C	C7	-1.2739930	-0.5110986	0.3512492
H	H3	2.8406242	1.3711838	2.8753552
H	H4	-1.5353076	-0.3176706	4.1990850
H	H5	0.9204636	0.6910549	4.2089690
C	C8	-2.4130389	-0.9252768	0.9657572
H	H11	-2.5066750	-1.1605568	-2.1335220
H	H7	-3.2505037	-1.3053548	0.4148499
C	C9	-2.4860107	-0.8468107	2.3815392
H	H2	-3.3837402	-1.1737995	2.8670531
C	C10	-1.4508515	-0.3675404	3.1309409
C	C12	-0.9066353	-0.5782488	-3.4299179
C	C13	-0.8313695	-0.4282323	-1.0521096
C	C14	1.0632275	0.2671470	-2.3371970
C	C15	0.3637043	-0.0639046	-3.4930332
C	C16	-1.5131293	-0.7634661	-2.1947483
H	H12	-1.4237635	-0.8321925	-4.3320003
N	N1	2.3982842	0.7808408	-2.5430918
H	H10	0.8465829	0.0948907	-4.4301087
O	O1	3.1630099	0.8579252	-1.5667040
O	O2	2.7213481	1.1033163	-3.7010164

```
E(HF)  =     -810.6109080 a.u.

Dipole moment:  X =  -4.481371  Y =  -1.564878  Z =   1.943049
Total Dipole:   5.129032 Debye

Frequencies and reduced mass in atomic units are:
```

mode	(cm-1)	AU	mass
1	-0.6230E-04	-0.1469E-15	-0.2443E+15
2	-0.1834E-04	-0.1273E-16	-0.1070E+16
3	-0.1166E-04	-0.5144E-17	-0.4192E+16
4	-0.9698E-05	-0.3559E-17	-0.1116E+17
5	-0.7883E-05	-0.2352E-17	-0.1350E+17
6	0.7254E-05	0.1991E-17	0.9358E+16
7	29.19	0.3224E-04	50.44
8	66.19	0.1658E-03	74.98
9	123.5	0.5775E-03	42.29

10	183.7	0.1277E-02	31.55
11	204.0	0.1574E-02	19.30
12	217.6	0.1792E-02	21.42
13	263.5	0.2627E-02	20.89
14	291.9	0.3224E-02	18.86
15	347.9	0.4581E-02	10.97
16	367.0	0.5096E-02	16.92
17	409.5	0.6347E-02	11.17
18	488.2	0.9020E-02	12.09
19	496.2	0.9319E-02	8.835
20	526.0	0.1047E-01	10.47
21	544.2	0.1121E-01	12.69
22	560.9	0.1191E-01	9.541
23	588.7	0.1312E-01	11.05
24	628.4	0.1494E-01	12.55
25	651.1	0.1604E-01	9.230
26	661.2	0.1654E-01	10.64
27	702.8	0.1869E-01	9.456
28	714.0	0.1929E-01	6.939
29	729.8	0.2016E-01	7.557
30	780.5	0.2306E-01	8.179
31	795.0	0.2392E-01	6.823
32	846.1	0.2709E-01	9.960
33	872.4	0.2880E-01	4.106
34	889.2	0.2992E-01	8.191
35	891.9	0.3010E-01	10.09
36	904.4	0.3095E-01	4.095
37	917.3	0.3185E-01	3.895
38	993.1	0.3732E-01	5.329
39	1002.	0.3798E-01	5.674
40	1014.	0.3893E-01	7.806
41	1079.	0.4408E-01	8.374
42	1085.	0.4454E-01	3.140
43	1103.	0.4600E-01	7.726
44	1128.	0.4814E-01	2.930
45	1132.	0.4850E-01	5.057
46	1132.	0.4853E-01	6.992
47	1155.	0.5048E-01	7.994
48	1168.	0.5165E-01	3.298
49	1193.	0.5387E-01	3.340
50	1209.	0.5533E-01	6.935
51	1218.	0.5614E-01	4.483
52	1231.	0.5733E-01	6.775
53	1250.	0.5916E-01	6.967
54	1285.	0.6248E-01	6.726
55	1308.	0.6479E-01	6.577
56	1332.	0.6711E-01	6.254
57	1337.	0.6770E-01	7.082
58	1359.	0.6992E-01	6.199
59	1369.	0.7090E-01	6.029
60	1380.	0.7210E-01	5.808
61	1413.	0.7552E-01	6.443
62	1435.	0.7793E-01	6.659
63	1485.	0.8341E-01	5.889
64	1494.	0.8451E-01	5.795
65	1534.	0.8906E-01	5.753
66	1572.	0.9354E-01	5.348
67	1598.	0.9665E-01	4.787
68	1608.	0.9781E-01	4.865
69	1636.	0.1013	4.909
70	1645.	0.1024	5.222
71	1733.	0.1137	5.925
72	1770.	0.1186	5.877
73	1778.	0.1197	5.910
74	1784.	0.1205	5.843
75	1801.	0.1227	5.901
76	3352.	0.4251	1.173

77	3354.	0.4258	1.173
78	3362.	0.4278	1.190
79	3370.	0.4298	1.190
80	3377.	0.4317	1.216
81	3381.	0.4325	1.211
82	3391.	0.4353	1.203
83	3447.	0.4497	1.188
84	3489.	0.4606	1.182

Zero-point vibrational energy is 141.479 kcal/mol

Standard Thermodynamic quantities at 298.15 K and 1.00 atm

Translational Enthalpy:	0.889	kcal/mol
Rotational Enthalpy:	0.889	kcal/mol
Vibrational Enthalpy:	147.052	kcal/mol
Translational Entropy:	42.414	cal/mol.K
Rotational Entropy:	33.042	cal/mol.K
Vibrational Entropy:	33.884	cal/mol.K

7-Nitrofluoranthene. Single Point Calculation of Electrostatic Potentials using Optimized Geometry.

Run type: Single point energy
Model: RHF/3-21G(*)
Number of shells: 75
37 S shells
38 SP shells
Number of basis functions: 189
Number of electrons: 128
Use of molecular symmetry disabled
Molecular charge: 0
Spin multiplicity: 1

Atomic Charges from Electrostatic Potential
Resolution: 1 points per atomic unit

8683 of 22011 gridpoints used in calculation

Atom	Charge
H 1	0.211183
C 2	-0.110204
C 3	0.031974
C 4	-0.075085
C 5	-0.239852
C 6	0.067994
C 7	-0.189217
C 8	0.177909
C 9	-0.137039
H 10	0.165420
H 11	0.192798
H 12	0.185134
C 13	-0.113716
H 14	0.187076
H 15	0.160770
C 16	-0.163923
H 17	0.163616
C 18	-0.281576
C 19	-0.158191
C 20	0.126074
C 21	-0.098985
C 22	-0.214934

```
  C 23     -0.188015
  H 24      0.173748
  N 25      0.920348
  H 26      0.216318
  O 27     -0.509573
  O 28     -0.500052

Total Charge =  0.000000

RMS fit:     1.164818
RRMS fit:    0.137826

Dipole moment from formal charges:
x =  -4.5171, y =  -1.5545, z =   1.9978  =   5.1780 debye
```

8-Nitrofluoranthene. Geometry Optimization.

```
Run type: Geometry optimization
          Numerical Frequency
Model: RHF/3-21G(*)
Number of shells:  75
  37 S shells
  38 SP shells
Number of basis functions: 189
Number of electrons: 128
Use of molecular symmetry disabled
Molecular charge:   0
Spin multiplicity:  1

Point Group = C1  Order =  1 Nsymop =  1
This system has  78 degrees of freedom
```

Atom	Label	Cartesian Coordinates (Angstroms) X	Y	Z
H	H1	3.2322847	0.0015238	-0.0379016
C	C1	2.4369600	0.0009833	0.6807112
C	C11	0.3979581	0.0003725	-0.9772160
C	C2	1.1304428	0.0004266	0.3114101
C	C3	1.7849527	0.0001926	3.0347458
C	C4	0.1390980	-0.0002541	1.3158746
C	C5	2.7495648	0.0008495	2.0698246
C	C6	0.4105339	-0.0003874	2.6683805
C	C7	-1.1632811	-0.0007407	0.7731274
H	H3	3.7819589	0.0012946	2.3576697
H	H4	-0.5690048	-0.0012284	4.5973203
H	H5	2.0587234	0.0001196	4.0717241
C	C8	-2.2276978	-0.0014105	1.6178952
H	H11	-2.9635337	-0.0010500	-1.5227661
H	H7	-3.2385477	-0.0018027	1.2612847
C	C9	-1.9803552	-0.0015804	3.0183204
H	H2	-2.8206102	-0.0021040	3.6835452
C	C10	-0.7162582	-0.0010884	3.5349023
C	C12	-1.4564297	0.0000231	-3.0319304
C	C13	-0.9909699	-0.0003212	-0.6980775
C	C14	0.8458332	0.0008539	-2.2725970
C	C15	-0.1016707	0.0006619	-3.2839332
C	C16	-1.9116082	-0.0005063	-1.7230920
H	H12	-2.1327656	-0.0000492	-3.8574225
H	H8	1.8828438	0.0013566	-2.5260433
N	N1	0.3518489	0.0011577	-4.6570368
O	O1	1.5818255	0.0014882	-4.8555625
O	O2	-0.5120958	0.0012194	-5.5531572

```
E(HF)  =     -810.6152493 a.u.

Dipole moment:  X =  -1.454638  Y =  -0.001964  Z =   6.356410
Total Dipole:   6.520730 Debye

Frequencies and reduced mass in atomic units are:
```

mode	(cm-1)	AU	mass
1	-0.2565E-04	-0.2489E-16	-0.8246E+15
2	-0.1000E-04	-0.3786E-17	-0.7729E+16
3	-0.9739E-05	-0.3589E-17	-0.3519E+16
4	-0.9157E-05	-0.3173E-17	-0.3854E+16
5	0.1220E-04	0.5636E-17	0.4380E+16
6	0.4706E-04	0.8381E-16	0.6557E+15
7	63.58	0.1530E-03	17.49
8	68.41	0.1771E-03	57.26
9	135.3	0.6928E-03	43.81

10	142.1	0.7645E-03	52.22
11	184.8	0.1292E-02	31.83
12	213.7	0.1728E-02	15.74
13	278.6	0.2937E-02	18.41
14	294.6	0.3284E-02	17.50
15	314.3	0.3739E-02	16.89
16	380.4	0.5477E-02	9.406
17	463.4	0.8126E-02	12.88
18	500.4	0.9476E-02	10.60
19	503.7	0.9600E-02	8.377
20	520.4	0.1025E-01	11.64
21	525.0	0.1043E-01	10.27
22	548.9	0.1140E-01	11.32
23	582.7	0.1285E-01	11.98
24	629.2	0.1498E-01	12.49
25	650.0	0.1599E-01	7.884
26	652.2	0.1610E-01	10.62
27	709.4	0.1904E-01	6.907
28	721.1	0.1968E-01	8.768
29	725.6	0.1992E-01	7.412
30	756.7	0.2167E-01	10.91
31	788.5	0.2353E-01	6.901
32	821.1	0.2552E-01	8.557
33	860.9	0.2805E-01	5.080
34	891.4	0.3007E-01	10.23
35	903.4	0.3088E-01	4.430
36	908.8	0.3126E-01	8.603
37	913.3	0.3157E-01	5.289
38	980.9	0.3641E-01	5.351
39	990.4	0.3712E-01	7.793
40	1015.	0.3901E-01	3.827
41	1067.	0.4309E-01	8.481
42	1084.	0.4445E-01	2.913
43	1092.	0.4516E-01	2.911
44	1100.	0.4579E-01	8.141
45	1125.	0.4793E-01	8.586
46	1138.	0.4897E-01	3.324
47	1165.	0.5137E-01	3.233
48	1172.	0.5199E-01	7.753
49	1176.	0.5231E-01	3.297
50	1197.	0.5425E-01	3.406
51	1204.	0.5482E-01	6.661
52	1215.	0.5582E-01	7.278
53	1241.	0.5824E-01	6.951
54	1279.	0.6193E-01	6.531
55	1313.	0.6520E-01	6.336
56	1328.	0.6674E-01	6.172
57	1334.	0.6737E-01	7.183
58	1366.	0.7057E-01	6.406
59	1369.	0.7092E-01	5.897
60	1399.	0.7402E-01	6.568
61	1420.	0.7635E-01	6.555
62	1432.	0.7760E-01	4.445
63	1488.	0.8385E-01	5.828
64	1495.	0.8456E-01	5.786
65	1538.	0.8954E-01	5.748
66	1568.	0.9304E-01	5.693
67	1592.	0.9597E-01	4.339
68	1612.	0.9838E-01	5.054
69	1627.	0.1002	5.347
70	1639.	0.1016	5.198
71	1748.	0.1157	5.988
72	1778.	0.1197	5.840
73	1780.	0.1200	5.852
74	1790.	0.1213	5.887
75	1801.	0.1227	5.909
76	3354.	0.4256	1.169

77	3355.	0.4260	1.182
78	3366.	0.4288	1.196
79	3367.	0.4291	1.193
80	3381.	0.4325	1.199
81	3382.	0.4328	1.206
82	3383.	0.4331	1.204
83	3431.	0.4455	1.192
84	3437.	0.4469	1.192

Zero-point vibrational energy is 141.194 kcal/mol

Standard Thermodynamic quantities at 298.15 K and 1.00 atm

Translational Enthalpy: 0.889 kcal/mol
Rotational Enthalpy: 0.889 kcal/mol
Vibrational Enthalpy: 146.769 kcal/mol
Translational Entropy: 42.414 cal/mol.K
Rotational Entropy: 33.301 cal/mol.K
Vibrational Entropy: 32.743 cal/mol.K

8-Nitrofluoranthene. Single Point Calculation of Electrostatic Potentials using Optimized Geometry.

Run type: Single point energy
Model: RHF/3-21G(*)
Number of shells: 75
37 S shells
38 SP shells
Number of basis functions: 189
Number of electrons: 128
Use of molecular symmetry disabled
Molecular charge: 0
Spin multiplicity: 1

Atomic Charges from Electrostatic Potential

Resolution: 1 points per atomic unit
9076 of 22971 gridpoints used in calculation

Atom	Charge
H 1	0.188321
C 2	-0.211018
C 3	-0.028773
C 4	0.081516
C 5	-0.350611
C 6	-0.124103
C 7	-0.131220
C 8	0.326449
C 9	0.010499
H 10	0.169009
H 11	0.195720
H 12	0.204510
C 13	-0.180576
H 14	0.185868
H 15	0.181040
C 16	-0.146749
H 17	0.166762
C 18	-0.310719
C 19	-0.127525
C 20	0.107188
C 21	-0.153947
C 22	-0.131213

```
  C 23    -0.226332
  H 24     0.194252
  H 25     0.206245
  N 26     0.911330
  O 27    -0.505521
  O 28    -0.500402

Total Charge =  0.000000

RMS fit:    1.256774
RRMS fit:   0.138827

Dipole moment from formal charges:
x =  -1.4577, y =  -0.0020, z =   6.4433  =   6.6062 debye
```

9-Nitroanthracene. Geometry Optimization.

```
Run type: Geometry optimization
          Numerical Frequency
Model: RHF/3-21G(*)
Number of shells:  69
  35 S shells
  34 SP shells
Number of basis functions: 171
Number of electrons: 116
Use of molecular symmetry disabled
Molecular charge:   0
Spin multiplicity:  1

Point Group = C1  Order =  1 Nsymop =  1
This system has  72 degrees of freedom
```

		Cartesian Coordinates (Angstroms)		
Atom	Label	X	Y	Z
H	H1	0.0106890	-4.5511851	1.5633298
C	C1	0.0175259	-3.6257592	1.0239735
H	H2	-0.0013313	-2.4090299	2.7461507
C	C2	0.0114770	-2.4492948	1.6745953
C	C3	0.0513751	-2.5052729	-1.1198276
C	C4	0.0157628	-1.2103137	0.9552370
C	C5	0.0345653	-3.6446865	-0.4015034
C	C6	0.0360479	-1.2251452	-0.4688673
C	C7	-0.0000246	0.0000042	1.6250253
H	H3	0.0405022	-4.5885520	-0.9088117
N	N1	0.0002247	-0.0000349	-2.5899140
H	H5	0.0908434	-2.5407728	-2.1829375
C	C8	-0.0158310	1.2103302	0.9552597
H	H6	-0.0000216	-0.0000525	2.6981906
C	C9	-0.0115683	2.4493215	1.6746116
C	C10	-0.0360477	1.2251673	-0.4688457
H	H7	-0.0911047	2.5407782	-2.1829393
C	C11	0.0000271	0.0000161	-1.1391504
C	C12	-0.0175722	3.6257853	1.0239814
H	H8	0.0011923	2.4090577	2.7461702
H	H9	-0.0107287	4.5512026	1.5633570
C	C13	-0.0346118	3.6447177	-0.4014998
H	H10	-0.0405388	4.5885820	-0.9088145
C	C14	-0.0514597	2.5052894	-1.1198127
O	O1	-0.7944246	0.7579571	-3.1786189
O	O2	0.7950323	-0.7581101	-3.1783394

```
E(HF)  =    -735.2855280 a.u.

Dipole moment:  X =  -0.000538  Y =  -0.000054  Z =   5.201692
Total Dipole:   5.201692 Debye

Frequencies and reduced mass in atomic units are:
```

mode	(cm-1)	AU	mass
1	-0.1860E-04	-0.1309E-16	-0.9517E+15
2	-0.9308E-05	-0.3279E-17	-0.1670E+17
3	0.5368E-05	0.1091E-17	0.3483E+17
4	0.1492E-04	0.8425E-17	0.2302E+16
5	0.1553E-04	0.9128E-17	0.5831E+16
6	0.6130E-04	0.1422E-15	0.8736E+14
7	88.26	0.2948E-03	84.31
8	96.95	0.3557E-03	29.19
9	131.8	0.6574E-03	32.09
10	142.4	0.7678E-03	43.03
11	247.9	0.2325E-02	15.86

12	258.8	0.2534E-02	20.03
13	272.8	0.2817E-02	22.40
14	309.1	0.3616E-02	12.71
15	397.5	0.5980E-02	13.87
16	401.8	0.6109E-02	10.89
17	442.3	0.7403E-02	16.39
18	454.5	0.7818E-02	13.84
19	485.1	0.8904E-02	11.57
20	550.3	0.1146E-01	9.192
21	571.3	0.1235E-01	9.231
22	591.5	0.1324E-01	8.858
23	641.5	0.1557E-01	9.456
24	669.9	0.1698E-01	10.50
25	710.7	0.1912E-01	10.22
26	719.8	0.1961E-01	11.75
27	729.7	0.2015E-01	10.94
28	798.0	0.2410E-01	7.037
29	805.2	0.2454E-01	8.552
30	866.3	0.2840E-01	3.872
31	882.6	0.2948E-01	6.227
32	887.6	0.2981E-01	3.042
33	895.9	0.3038E-01	8.212
34	940.5	0.3348E-01	8.956
35	963.4	0.3513E-01	4.424
36	1014.	0.3891E-01	3.495
37	1036.	0.4065E-01	7.875
38	1042.	0.4109E-01	5.664
39	1069.	0.4326E-01	8.087
40	1088.	0.4481E-01	9.377
41	1097.	0.4551E-01	8.749
42	1119.	0.4742E-01	4.382
43	1160.	0.5090E-01	2.632
44	1166.	0.5149E-01	3.028
45	1197.	0.5424E-01	6.086
46	1199.	0.5444E-01	3.230
47	1203.	0.5481E-01	5.920
48	1224.	0.5666E-01	7.174
49	1308.	0.6477E-01	7.236
50	1326.	0.6653E-01	6.099
51	1335.	0.6748E-01	7.287
52	1340.	0.6792E-01	5.954
53	1348.	0.6874E-01	6.805
54	1362.	0.7023E-01	6.069
55	1411.	0.7529E-01	6.824
56	1432.	0.7756E-01	5.974
57	1433.	0.7770E-01	5.600
58	1465.	0.8117E-01	6.029
59	1516.	0.8692E-01	5.630
60	1534.	0.8900E-01	6.184
61	1568.	0.9306E-01	3.305
62	1613.	0.9850E-01	4.756
63	1627.	0.1002	4.361
64	1643.	0.1021	4.780
65	1694.	0.1085	6.013
66	1726.	0.1128	5.999
67	1760.	0.1173	5.754
68	1818.	0.1250	5.852
69	1823.	0.1258	5.879
70	3351.	0.4248	1.169
71	3356.	0.4261	1.167
72	3358.	0.4268	1.187
73	3369.	0.4295	1.201
74	3369.	0.4296	1.199
75	3387.	0.4341	1.226
76	3388.	0.4343	1.226
77	3460.	0.4530	1.191
78	3460.	0.4531	1.191

```
Zero-point vibrational energy is   133.160 kcal/mol

Standard Thermodynamic quantities at   298.15 K  and     1.00 atm

Translational Enthalpy:        0.889 kcal/mol
Rotational Enthalpy:           0.889 kcal/mol
Vibrational Enthalpy:        138.208 kcal/mol
Translational Entropy:        42.109  cal/mol.K
Rotational Entropy:           32.441  cal/mol.K
Vibrational Entropy:          28.850  cal/mol.K
```

9-Nitroanthracene. Single Point Calculation of Electrostatic Potentials using Optimized Geometry.

```
Run type: Single point energy
Model: RHF/3-21G(*)
Number of shells:  69
  35 S shells
  34 SP shells
Number of basis functions: 171
Number of electrons: 116
Use of molecular symmetry disabled
Molecular charge:   0
Spin multiplicity:  1

Atomic Charges from Electrostatic Potential

Resolution:   1  points per atomic unit
7793 of  20097 gridpoints used in calculation

  Atom     Charge
  ----   -----------
  H  1     0.156866
  C  2    -0.110921
  H  3     0.181865
  C  4    -0.281981
  C  5    -0.266563
  C  6     0.212034
  C  7    -0.153257
  C  8     0.179977
  C  9    -0.435530
  H 10     0.170489
  N 11     1.018862
  H 12     0.212349
  C 13     0.212022
  H 14     0.245175
  C 15    -0.281973
  C 16     0.180012
  H 17     0.212377
  C 18    -0.393500
  C 19    -0.110935
  H 20     0.181864
  H 21     0.156865
  C 22    -0.153222
  H 23     0.170484
  C 24    -0.266661
  O 25    -0.518360
  O 26    -0.518339

Total Charge =  0.000000

RMS fit:    1.118931
```

```
RRMS fit:   0.125936

Dipole moment from formal charges:
x =  -0.0006, y =  -0.0001, z =   5.2614  =   5.2614 debye
```

Appendix 3. Ames Reversion Assay Dose Response Data

Dose (ng)	Revertants per plate
0	24
0.0335	27
0.0335	48
0.0335	32
0.0335	52
0.0670	37
0.0670	60
0.0670	65
0.0670	71
0.100	70
0.100	56
0.100	72
0.100	81
0.134	102
0.134	116
0.134	110
0.134	97
0.167	161
0.167	159
0.167	151
0.167	141
Revertants/nmol	230000 ± 8.3%
r^2 (95%)	0.88

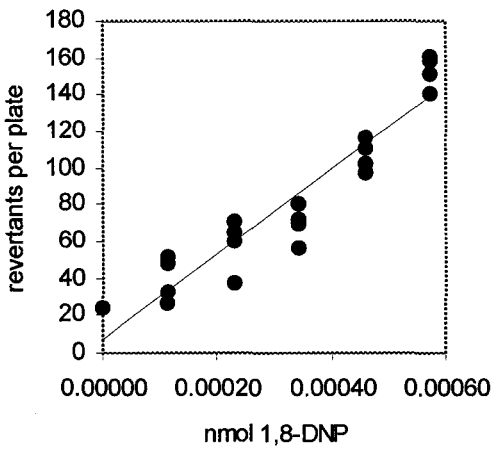

1,8-Dinitropyrene.

Dose (ng)	Revertants per plate
0	24
11.1	86
11.1	49
22.2	157
22.2	186
33.2	165
33.2	218
44.3	221
44.3	245
55.4	331
55.4	332
Revertants/nmol	1300 ± 9.2%
r^2 (95%)	0.93

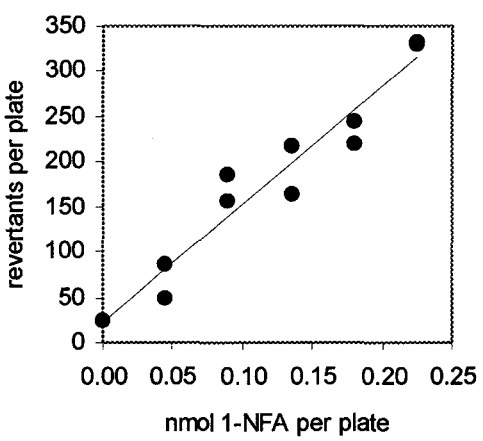

1-Nitrofluoranthene.

Dose (ng)	Revertants per plate
0	25
0	41
2.14	140
2.14	138
4.28	167
4.28	195
6.42	247
6.42	304
8.56	350
8.56	432
10.7	418
10.7	491
Revertants/nmol	9700 ± 6.6%
r^2 (95%)	0.96

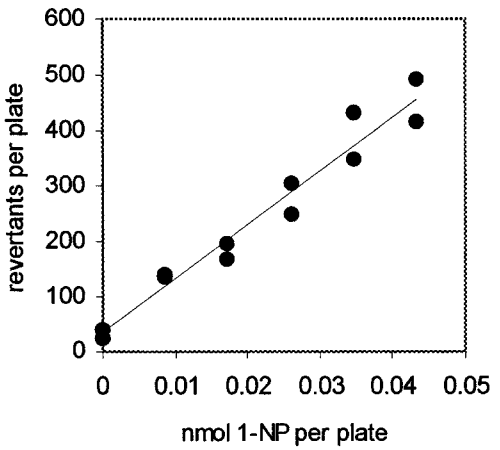

1-Nitropyrene.

Dose (ng)	Revertants per plate
0	24
4.96	293
9.91	382
9.91	532
14.9	636
14.9	702
19.8	690
19.8	220
24.8	811
Revertants/nmol	7700 ± 36%
r^2 (95%)	0.90

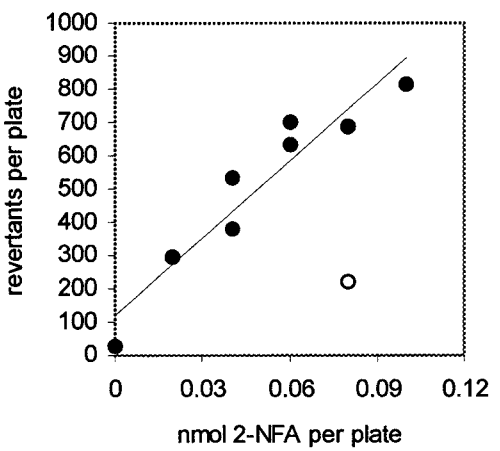

2-Nitrofluoranthene.

O = Point not included in linear regression analysis

Dose (ng)	Revertants per plate
0	25
0	41
36.0	257
36.0	234
72.0	330
72.0	457
108	526
108	520
144	642
144	610
180	842
180	783
Revertants/nmol	870 ± 5.0%
r^2 (95%)	0.97

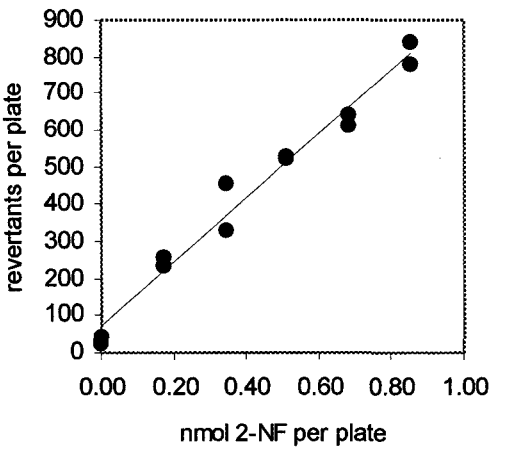

2-Nitrofluorene.

Dose (ng)	Revertants per plate
0	25
0	41
3.96	247
3.96	256
7.93	427
7.93	401
11.9	576
11.9	641
15.9	924
15.9	905
19.8	1033
19.8	1108
Revertants/nmol	13000 ± 3.4%
r^2 (95%)	0.99

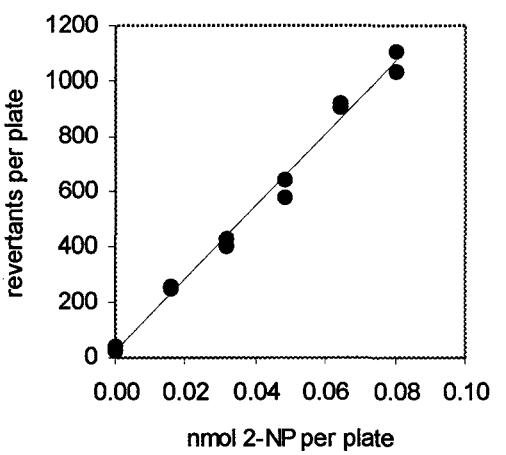

2-Nitropyrene.

Dose (ng)	Revertants per plate
0	24
0.0607	8
0.0607	48
0.121	76
0.121	69
0.182	71
0.182	67
0.243	97
0.243	68
0.303	145
0.303	76
Revertants/nmol	110000 ± 25%
r^2 (95%)	0.83

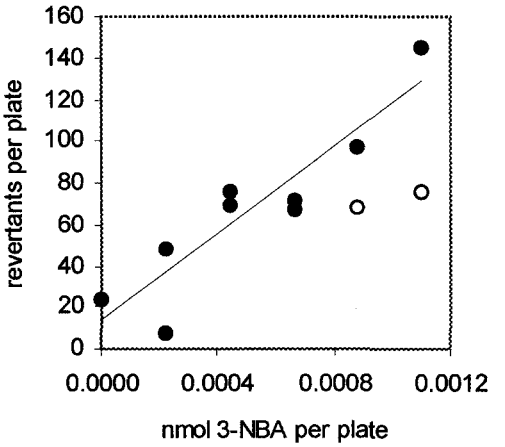

3-Nitrobenzanthrone.
O = Point not included in linear regression analysis

Dose (ng)	Revertants per plate
0	24
0.708	23
0.708	112
1.42	222
1.42	224
2.12	240
2.12	274
2.83	308
2.83	378
3.54	504
3.54	506
Revertants/nmol	33000 ± 8.7%
r^2 (95%)	0.94

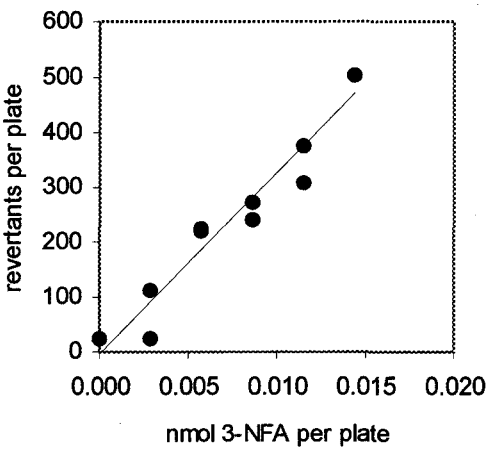

3-Nitrofluoranthene.

Dose (ng)	Revertants per plate
0	25
0	41
33.9	41
33.9	38
67.7	64
67.7	68
102	95
102	114
135	135
135	117
169	131
169	185
Revertants/nmol	170 ± 10%
r^2 (95%)	0.93

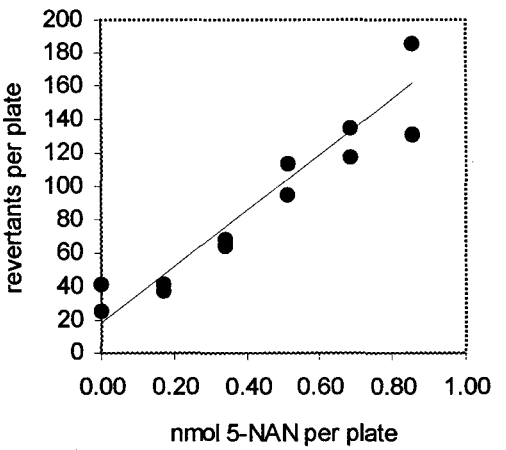

5-Nitroacenaphthene.

Dose (ng)	Revertants per plate
0	24
61.2	142
61.2	459
122	678
122	818
184	902
184	912
245	967
245	921
306	1567
Revertants/nmol	1000 ± 13%
r^2 (95%)	0.88

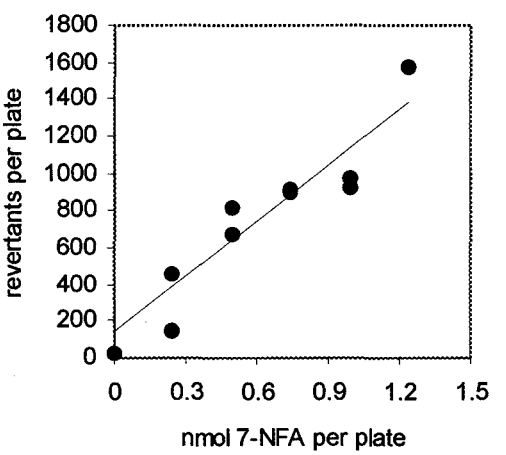

7-Nitrofluoranthene.

Dose (ng)	Revertants per plate
0	24
0.198	83
0.198	183
0.396	294
0.396	278
0.594	301
0.594	390
0.792	513
0.792	460
0.990	23
0.990	440
Revertants/nmol	140000 ± 9.9%
r^2 (95%)	0.94

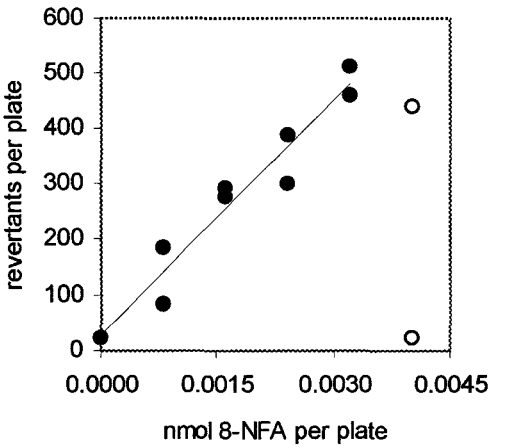

8-Nitrofluoranthene.
O = Point not included in linear regression analysis

Dose (ng)	Revertants per plate
0	25
0	41
37.9	45
37.9	48
75.8	76
75.8	68
114	95
114	89
152	159
152	141
190	154
190	175
Revertants/nmol	170 ± 8.0%
r^2 (95%)	0.94

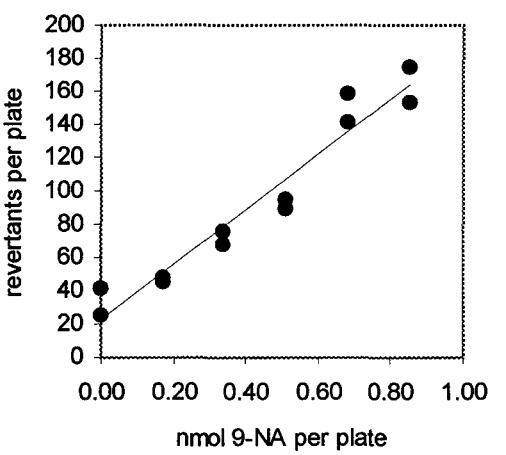

9-Nitroanthracene.

Appendix 4. Relative Rate of Metabolism Data

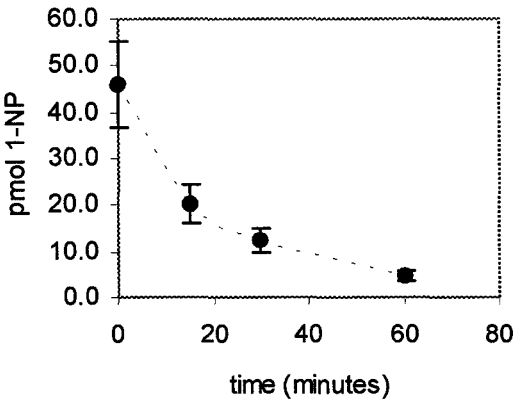

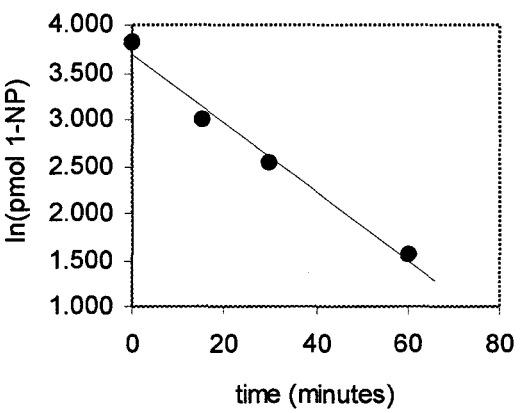

first order rate constant (25°C)	0.0366 min^{-1} (± 6.69%)
first order initial rate (25°C)	493 ± 46 pmol/h/mL culture

1-Nitropyrene.
Error bars represent the estimated error for each data point (20%), where 20% equals the average relative error for 8 sets of duplicate analyses.

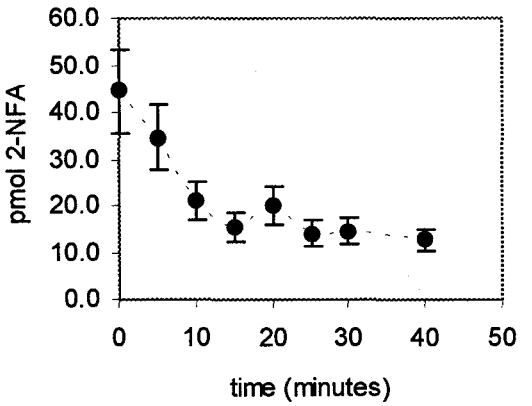

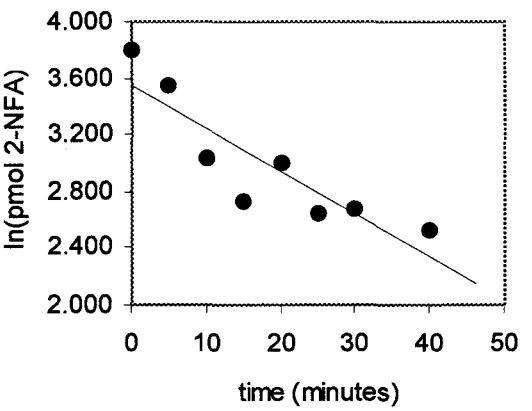

first order rate constant (25°C)	0.0333 min^{-1} (± 13.0%)
first order initial rate (25°C)	450 ± 58 pmol/h/mL culture

2-Nitrofluoranthene.

Error bars represent the estimated error for each data point (20%), where 20% equals the average relative error for 8 sets of duplicate analyses

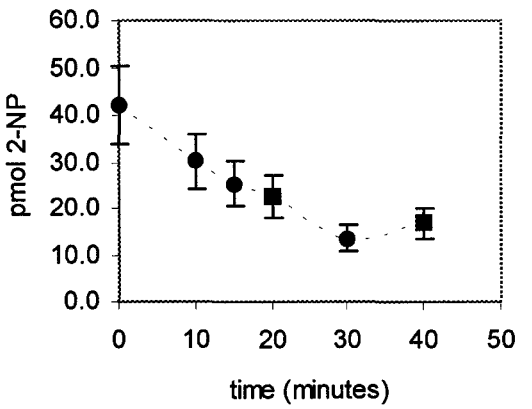

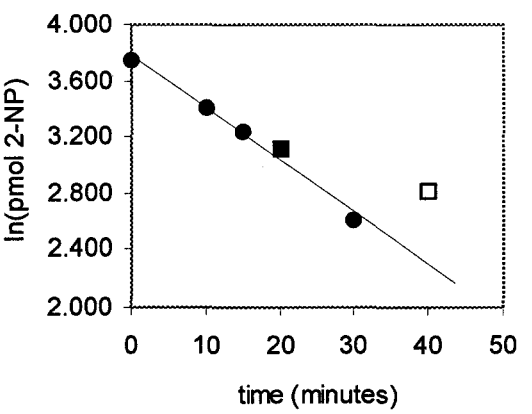

first order rate constant (25°C)	0.00368 min^{-1} (± 7.96%)
first order initial rate (25°C)	497 ± 40 pmol/h/mL culture

2-Nitropyrene.

Error bars represent the estimated error for each data point (20%), where 20% equals the average relative error for 8 sets of duplicate analyses.

■ = Average of 2 duplicate analyses

□ = Point not included in linear regression analysis

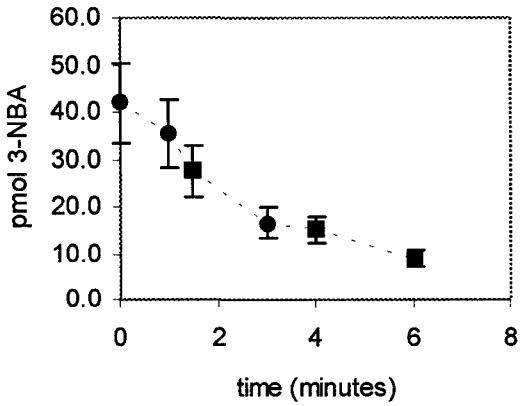

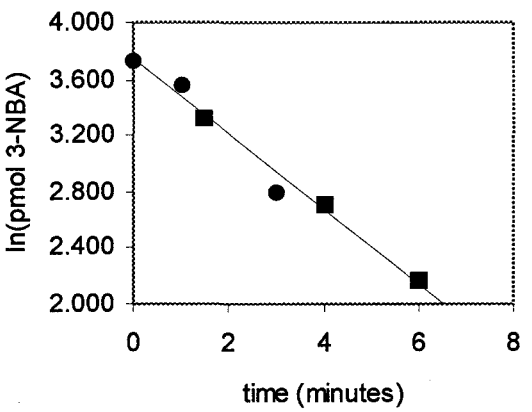

first order rate constant (25°C)	0.266 min^{-1} (± 6.69%)
first order initial rate (25°C)	3600 ± 240 pmol/h/mL culture

3-Nitrobenzanthrone.

Error bars represent the estimated error for each data point (20%), where 20% equals the average relative error for 8 sets of duplicate analyses.

■ = Average of 2 duplicate analyses

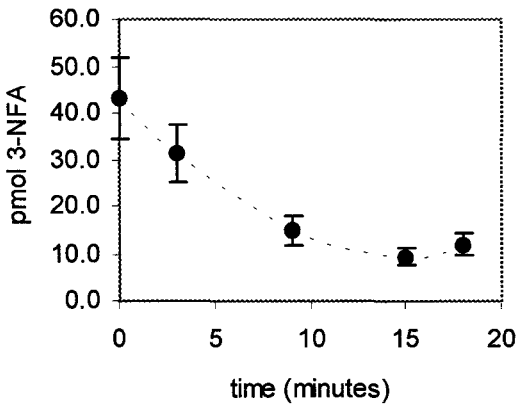

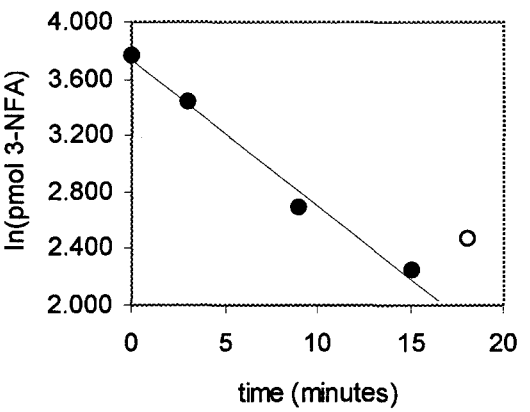

first order rate constant (25°C)	0.103 min^{-1} (± 7.54%)
first order initial rate (25°C)	1390 ± 110 pmol/h/mL culture

3-Nitrofluoranthene.

Error bars represent the estimated error for each data point (20%), where 20% equals the average relative error for 8 sets of duplicate analyses
O = Point not included in linear regression analysis

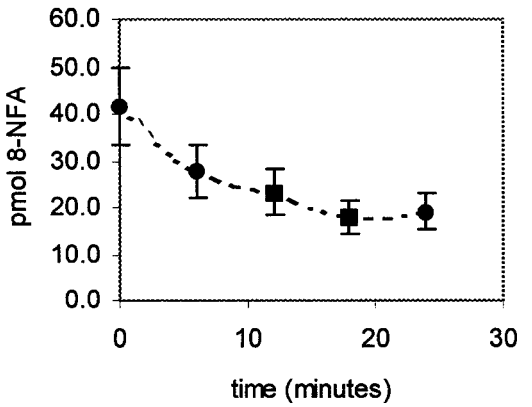

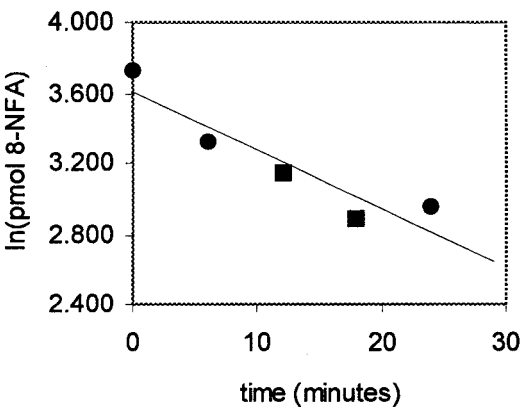

first order rate constant (25°C)	0.0330 min^{-1} (± 22.7%)
first order initial rate (25°C)	446 ± 101 pmol/h/mL culture

8-Nitrofluoranthene.
Error bars represent the estimated error for each data point (20%), where 20% equals the average relative error for 8 sets of duplicate analyses.
■ = Average of 2 duplicate analyses